
Electronic Thesis and Dissertation Repository

9-29-2017 12:00 AM

A Clinico-Pathological Study of the Structural and Functional Changes in the Retina and Optic Nerve Following Diabetic Retinopathy Treatments

Richard Filek, *The University of Western Ontario*

Supervisor: Dr. Cindy Hutnik, *The University of Western Ontario*

Joint Supervisor: Dr. Subrata Chakrabarti, *The University of Western Ontario*

A thesis submitted in partial fulfillment of the requirements for the Doctor of Philosophy degree in Pathology

© Richard Filek 2017

Follow this and additional works at: <https://ir.lib.uwo.ca/etd>



Part of the [Endocrine System Diseases Commons](#), [Endocrinology, Diabetes, and Metabolism Commons](#), [Eye Diseases Commons](#), [Medical Pathology Commons](#), [Ophthalmology Commons](#), [Pathological Conditions, Signs and Symptoms Commons](#), and the [Translational Medical Research Commons](#)

Recommended Citation

Filek, Richard, "A Clinico-Pathological Study of the Structural and Functional Changes in the Retina and Optic Nerve Following Diabetic Retinopathy Treatments" (2017). *Electronic Thesis and Dissertation Repository*. 4939.

<https://ir.lib.uwo.ca/etd/4939>

This Dissertation/Thesis is brought to you for free and open access by Scholarship@Western. It has been accepted for inclusion in Electronic Thesis and Dissertation Repository by an authorized administrator of Scholarship@Western. For more information, please contact wlsadmin@uwo.ca.

Abstract

Diabetic retinopathy (DR) is the result of microvascular changes in the retina due to hyperglycemia which alter the blood-retinal barrier (BRB). The increased permeability of BRB results in the accumulation of extracellular fluid, the development of diabetic macular edema (DME) and capillary occlusion. Capillary occlusion results in retinal ischemia which increases vascular endothelial growth factor (VEGF) levels, increases vascular permeability and results in neovascularization in proliferative diabetic retinopathy (PDR) patients. The treatments clinically used for DR are panretinal photocoagulation (PRP) for PDR and injectable vascular endothelial growth factor inhibitors (anti-VEGFs) for DME.

The safety of PRP and anti-VEGF therapy on the retina and optic nerve was evaluated in treatment-naïve DR patients by undergoing structural (OCT, HRT) and functional (visual field, visual acuity) diagnostic tests over a two year time period. Streptozotocin (STZ)-induced diabetic rats received different doses of intravitreal anti-VEGF injections to analyze the safety of VEGF inhibition on neuronal cells. Retinal cell cultures were exposed to different doses of anti-VEGF to assess metabolic activity, function and toxicity by colorimetric assays.

This study found that patients treated with PRP, despite showing an improvement in peripheral perfusion, had a significant and progressive decline in peripheral vision. There was a discrepancy between the grading of the optic nerves post-PRP by ophthalmologists despite the absence of significant morphological changes. Anti-VEGF treatment was found to be potentially detrimental to the optic

nerve by decreasing retinal nerve fiber layer thickness, increasing cup/disk ratio and cup volume over time. STZ-induced diabetic rats receiving intravitreal anti-VEGF injections had a dose-dependent increase in retinal ganglion cell death. Results from retinal cell cultures suggest that anti-VEGF treatment may be detrimental to the retina by decreasing cellular metabolic activity, and increasing cytotoxicity of retinal cells. Overall, PRP was relatively safe and improved peripheral perfusion but resulted in misdiagnosis of glaucoma based on non-morphological colouration changes of the optic nerve post-PRP. Anti-VEGF treatment appeared to be detrimental to the optic nerve by causing damage to retinal cells. In contrast to current recommendations, it is suggested to monitor both the retina and optic nerve status in patients undergoing frequent injections.

Keywords

Diabetic retinopathy, retina, optic nerve, panretinal photocoagulation (PRP), pascal, iatrogenic, diabetic macular edema (DME), diabetes, anti-VEGF, lucentis, ranibizumab, structural and functional changes, safety, efficacy, ophthalmology

Co-Authorship

Manuscript: Structural and functional changes to the retina and optic nerve following panretinal photocoagulation over a 2-year time period.

Eye (Lond). 2017 Apr 28. doi: 10.1038/eye.2017.66. [Epub ahead of print].

Richard Filek Designed, recruited patients, and conducted experiments.

Philip Hooper Collaborator; recruited patients from his clinic.

Tom Sheidow Collaborator; recruited patients from his clinic.

John Gonder Collaborator; recruited patients from his clinic.

Devesh K Varma Collaborator; graded optic nerve photos.

Lisa Heckler Collaborator; graded optic nerve photos.

William Hodge Collaborator; advised statistical analysis.

Subrata Chakrabarti Supervisor; edited and finalized the manuscript.

Cindy ML Hutnik Supervisor; edited and finalized the manuscript.

Chapters 3-4 contain material from two submitted manuscripts which are co-authored by Richard Filek, Philip Hooper, Tom Sheidow, Subrata Chakrabarti and Cindy ML Hutnik. Richard Filek conducted all experiments.

Acknowledgments

I am extremely grateful to my supervisors Dr. Cindy Hutnik and Dr. Subrata Chakrabarti for giving me the opportunity to carry out my research project, for your support, guidance, patience, and most importantly, your friendship during my graduate studies. Over the past five years, your mentorship has been instrumental in providing me a well-rounded experience consistent with my long-term career goals. You have shaped my growth from a student interested in ophthalmology research to a researcher adapt in basic science, animal, and clinical research. You have encouraged me to not only grow as a researcher but also as an instructor to other students and an independent thinker. For everything you've done for me, I thank you Dr. Hutnik and Dr. Chakrabarti. I am truly indebted to the both of you for this once in a lifetime opportunity.

I would like to thank Dr. Phil Hooper and Dr. Tom Sheidow for your assistance and guidance in starting my graduate career and providing me with the needed foundation for becoming a researcher. You have both walked with me through all stages of this project, and without your consistent, enlightening instructions and support, this thesis could have never matured. I deeply appreciate everything that you have done for me.

I would like to thank Dr. John Gonder, Dr. Devesh Varma and Dr. Lisa Heckler for assisting me in this project. I would like to thank Dr. William Hodge who sparked my interest in ophthalmology research ever since I was a 20 year old student looking for a NSERC supervisor during my third year at Western University. Without you, my passion for research would not have been realized and I would not

have had the chance to meet Dr. Cindy Hutnik, Dr. Phil Hooper and Dr. Tom Sheidow.

I would like to thank the staff, secretaries, and technicians at the Ivey Eye Institute. You have all been instrumental in helping and teaching me so many things like how to perform diagnostic tests, manage patients and gather patient charts.

I would like to thank all members of the Ophthalmology research lab, especially Hong Liu, for your support and patience in teaching me to conduct laboratory tests. I will miss our time spent together in the lab and all the laughter that we have shared. I would like to thank all members of the Chakrabarti lab, especially Francis, for helping teach me animal technical skills.

I would like to thank all members of the Department of Pathology and Laboratory Medicine, the Graduate Education Committee (GEC), and all of my colleagues in the department. It has been a great privilege of mine to be elected by our graduate students to represent their voices in the committee. For the past three years as the student representative, I have come to know the GEC more as a family than a committee. I have a lot of respect and learned so much from each individual in the GEC -- Dr. Chandan Chakraborty, Dr. Zia Khan, Dr. Martin Duennwald, Dr. Mark Darling, Dr. Christopher Howlett, Tracey Koning. It has been a pleasure working with all of you and I hope I get the chance to work with you again in the future.

I would like to thank all of my friends and loved ones for all of your support throughout graduate school. I would like to express a deep gratitude to my dearest

mom and dad who have always stood by me like a pillar in times of need, and to whom I owe my life for their constant love, encouragement, moral support and blessings. You have stood by me in all situations and I thank you for your unwavering love, support and encouragement throughout this journey.

Table of Contents

Abstract	i
Co-Authorship	iii
Acknowledgments	iv
Table of Contents	vii
List of Tables	xi
List of Figures	xii
List of Appendices	xvi
List of Abbreviations	xvii
Chapter 1	1
1 Introduction	1
1.1 Diabetes Mellitus	1
1.2 Epidemiology	7
1.3 Diabetic Complications	9
1.4 Diabetic Retinopathy	12
1.4.1 Retinal Anatomy	12
1.4.2 Epidemiology	27
1.4.3 Pathogenesis	28
1.4.4 Clinical Features of Diabetic Retinopathy	37
1.5 Treatments	52
1.5.1 Panretinal Photocoagulation	54
1.5.2 Anti-VEGF Therapy	60
1.6 Risks	65
1.6.1 Panretinal Photocoagulation	65
1.6.2 Anti-VEGF Therapy	67

1.7 Rationale.....	69
1.8 Hypothesis	70
1.9 Specific Aims	71
1.10 References.....	72
Chapter 2.....	99
2 The structural and functional changes to the retina and optic nerve following panretinal photocoagulation over a 2-year time period¹	99
2.1 Introduction.....	100
2.2 Methods	102
2.2.1 Optical Coherence Tomography	103
2.2.2 Heidelberg Retinal Tomography.....	103
2.2.3 Humphrey Visual Field Analyzer	104
2.2.4 Wide-Field Fluorescein Angiogram and Quantification of Ischemia	104
2.2.5 Optic Nerve Grading	106
2.2.6 Pattern Scan Laser Photocoagulator (Pascal)	106
2.2.7 Statistical Analysis	106
2.3 Results.....	108
2.4 Discussion.....	124
2.5 References	129
Chapter 3.....	135
3 Two-year analysis of structural and functional changes to the retina and optic nerve following anti-VEGF treatments for diabetic macular edema patients	135
3.1 Introduction.....	136
3.2 Methods	138
3.2.1 Optical Coherence Tomography	139
3.2.2 Humphrey Visual Field Analyzer	140

3.2.3	Wide-Field Fluorescein Angiogram and Quantification of Ischemia	140
3.2.4	Optic Nerve Grading	141
3.2.5	Ranibizumab (Lucentis) Injections	142
3.2.6	Statistical Analysis	142
3.3	Results	144
3.4	Discussion	165
3.5	References	171
Chapter 4	182
4	Retinal cell death following anti-VEGF treatment in a diabetic rat model and retinal cell culture	182
4.1	Introduction	183
4.2	Methods	185
4.2.1	Diabetic Animal Model	185
4.2.2	Drug Administration.....	186
4.2.3	TUNEL Assay.....	187
4.2.4	Mixed Retinal Cell Culture.....	188
4.2.5	Dosage.....	188
4.2.6	Immunohistochemistry	189
4.2.7	Colorimetric Assays	191
4.2.8	Statistical Analysis	191
4.3	Results	193
4.3.1	Body weight and blood glucose levels	193
4.3.2	Increasing anti-VEGF concentrations caused more death <i>in vivo</i>	193
4.3.3	No difference in cell death between the clinical dose of ranibizumab and rat anti-VEGF	199
4.3.4	Frequency of injections has no effect on apoptotic cells	199

4.3.5	Verification of mixed retinal cell culture	206
4.3.6	Increasing anti-VEGF concentrations caused cell death <i>in vitro</i> .	206
4.3.7	Increased ranibizumab concentrations result in decreased cellular metabolic activity	209
4.3.8	Increasing ranibizumab concentrations result in increased necrosis	222
4.3.9	Increased apoptosis with increasing ranibizumab concentrations	227
4.3.10	Increased apoptosis and necrosis with rat anti-VEGF concentrations	227
4.4	Discussion	233
4.5	References	239
Chapter 5	245
5	General Discussion, Limitations, and Future Direction	245
5.1	Summary of Discussion	246
5.2	Limitations	254
5.3	Future Direction	256
5.4	References	258
6	Appendices	264
6.1	Approved use of human participants undergoing PRP treatment ..	264
6.2	Approved use of human participants undergoing anti-VEGF treatment	265
6.3	Approved animal use protocol	266
6.4	Copyright permission	267
6.5	Antibodies used for experiments	273
6.6	Curriculum vitae	274

List of Tables

Table 1.1. Global prevalence of diabetes.	8
Table 2.1. Patient demographics.....	109
Table 2.2. Changes in RNFL thickness (μm) over the course of 24 months in the control and PRP laser groups.....	113
Table 3.1. Demographics of patients involved in the study.....	145
Table 3.2. Changes in RNFL thickness (μm) over the course of 24 months in the control and anti-VEGF groups.....	149
Table 4.1. Body weights and serum glucose levels of control and STZ-induced diabetic rats.....	194

List of Figures

Figure 1.1 Pathogenesis of T2DM.....	4
Figure 1.2. Risk factors affecting the development of T2DM	6
Figure 1.3. Sagittal section of the eye	14
Figure 1.4. Wide-field photograph of the normal human fundus.....	16
Figure 1.5. Histology of the retina.....	19
Figure 1.6. Blood-retinal barrier under normal conditions.....	23
Figure 1.7. Schematic of the retinal capillary.....	26
Figure 1.8. Pathologic features of BRB breakdown in a diabetic eye	31
Figure 1.9. Non-proliferative retinopathy	40
Figure 1.10. Diabetic macular edema.....	44
Figure 1.11 Pre-proliferative retinopathy	48
Figure 1.12. Proliferative diabetic retinopathy	51
Figure 1.13. Panretinal photocoagulation	56
Figure 1.14. Effect of panretinal photocoagulation treatment	58
Figure 1.15. Anti-VEGF agents clinically used for DME treatment	62
Figure 2.1 Interval changes in (A) macular thickness, (B) RNFL thickness and (C) mean perfused ratio at baseline, 6, 12, and 24 months later in the control and PRP laser groups.....	111

Figure 2.2. Interval changes in vertical cup/disk ratio measured on the (A) OCT and (B) HRT at baseline, 6, 12, and 24 months later in the control and PRP laser groups	115
Figure 2.3. Interval changes in vertical cup/disk ratio as measured by two masked glaucoma specialists using stereo photographs at baseline, 6, 12, and 24 months later in the (A) PRP laser group and the (B) control group	118
Figure 2.4. Interval changes in mean deviation measured on the (A) Humphrey Visual Field Analyzer and (B) visual acuity at baseline, 6, 12, and 24 months later in the control and PRP laser groups.....	120
Figure 2.5. Interval changes in intraocular pressure at baseline, 6, 12, and 24 months later in the control and PRP laser groups	123
Figure 3.1. Interval changes in (A) macular thickness, (B) RNFL thickness and (C) mean perfused ratio at baseline, 6, 12, and 24 months in the control and anti-VEGF groups	147
Figure 3.2. Interval changes in cup volume measured on the OCT at baseline, 6, 12, and 24 months in the control and anti-VEGF groups.....	151
Figure 3.3. Interval changes in vertical cup/disk ratio measured on the OCT at baseline, 6, 12, and 24 months in the control and anti-VEGF groups.....	153
Figure 3.4. Interval changes in vertical cup/disk ratio measured on the OCT at baseline, 6, 12, and 24 months in participants receiving less than 10 injections and 10 or more injections	156
Figure 3.5. Interval changes in vertical cup/disk ratio measured by two masked glaucoma specialists using stereo photographs at baseline, 6, 12, and 24 months in the (A) anti-VEGF group and the (B) control group	158
Figure 3.6. Interval changes in mean deviation measured on the (A) Humphrey Visual Field Analyzer and (B) visual acuity at baseline, 6, 12, and 24 months in the control and anti-VEGF groups	162

Figure 3.7. Interval changes in intraocular pressure at baseline, 6, 12, and 24 months in the control and anti-VEGF groups.....	164
Figure 4.1. TUNEL staining of control rat retina.....	196
Figure 4.2. TUNEL staining of diabetic rat retina	198
Figure 4.3. Apoptotic death rates following different doses of rat anti-VEGF in control and diabetic rats	201
Figure 4.4. Apoptotic cell death rates between the clinical dose of rat anti-VEGF and ranibizumab in control and diabetic rats	203
Figure 4.5. Effects of frequency of injections on the number of TUNEL-positive cells in control and diabetic rats.....	205
Figure 4.6. Expression of retinal ganglion cell (RGC)-specific markers in the primary rat retinal cell culture	208
Figure 4.7. Morphological effect of different concentrations of ranibizumab on RGCs following 48 hours post treatment.....	211
Figure 4.8. Morphological effect of different concentrations of ranibizumab on RGCs following 72 hours post treatment.....	213
Figure 4.9. Apoptotic cell death upon exposure to different concentrations of ranibizumab following 48 hours post treatment	215
Figure 4.10. Apoptotic cell death upon exposure to different concentrations of ranibizumab following 72 hours post treatment	217
Figure 4.11. Apoptotic cell death of support cells surrounding RGCs.....	219
Figure 4.12. Apoptosis in the INL following TUNEL staining	221
Figure 4.13. Cellular metabolic activity following different concentrations of ranibizumab	224

Figure 4.14. Necrosis following different concentrations of ranibizumab	226
Figure 4.15. Apoptosis following treatments with different concentrations of ranibizumab	230
Figure 4.16. Necrosis and apoptosis following treatments with different concentrations of rat anti-VEGF	232

List of Appendices

6.1	Approved use of human participants undergoing PRP treatment	264
6.2	Approved use of human participants undergoing anti-VEGF treatment.	265
6.3	Approved animal use protocol	266
6.4	Copyright permission	267
6.5	Antibodies used for experiments.....	273
6.6	Curriculum vitae	274

List of Abbreviations

ACVS	Animal Care and Veterinary Services
AMD	Age-related macular degeneration
BCVA	Best-corrected visual acuity
BRB	Blood-retinal barrier
BSA	Bovine serum albumin
C/D	Cup-to-disk ratio
DME	Diabetic macular edema
DR	Diabetic retinopathy
DRS	Diabetic Retinopathy Study
ETDRS	Early Treatment of Diabetic Retinopathy Study
Fab	Antigen binding fragment
FAZ	Foveal avascular zone
FBS	Fetal bovine serum
Fc	Fragment crystallizable region
FcRn	The neonatal Fc receptor for IgG
GC	Ganglion cell
GCL	Ganglion cell layer
GJ	Gap junction

HDL	High density lipoprotein cholesterol
HIF-1	Hypoxia-inducible factor 1
HRT	Heidelberg retinal tomography
iBRB	Inner blood-retinal barrier
INL	Inner nuclear layer
INS	Inner segments
IOP	Intraocular pressure
IPL	Inner plexiform layer
IRMA	Intraretinal microvascular abnormality
IVFA	Intravenous fluorescein angiography
kDa	Kilodalton
LDH	Lactate dehydrogenase
logMAR	Logarithm of the minimum angle of resolution
MD	Mean deviation
MTT	Thiazolyl Blue Tetrazolium Bromide
NBA	Neurobasal A medium
Nd:YAG	Neodymium-doped yttrium aluminum garnet
NFL	Nerve fiber layer
NPDR	Nonproliferative diabetic retinopathy
oBRB	Outer blood-retinal barrier

OCT	Optical coherence tomography
OLM	Outer limiting membrane
ONL	Outer nuclear layer
OPL	Outer plexiform layer
OS	Outer segment
PBS	Phosphate-buffered saline
PCOS	Polycystic ovarian syndrome
PDR	Proliferative diabetic retinopathy
PEDF	Pigment epithelium derived growth factor
PIGF	Placental growth factor
PRP	Panretinal photocoagulation
PVD	Posterior vitreous detachment
RNFL	Retinal nerve fiber layer
RPE	Retinal pigment epithelium
STZ	Streptozotocin
T1DM	Type 1 diabetes
T2DM	Type 2 diabetes
TG	Triglycerides
TUJ-1	Class III β -tubulin
VA	Visual acuity

VEGF Vascular endothelial growth factor

VF Visual field

Chapter 1

1 Introduction

1.1 Diabetes Mellitus

Diabetes mellitus is a chronic metabolic disorder characterized by hyperglycemia¹. Hyperglycemia is a condition in which glucose plasma levels are uncharacteristically high and exceed 7 mmol/L. In diabetics, hyperglycemia results in chronic low grade inflammation induced by inflammatory cytokines, creating persistent damage to host cells². This mechanism also drives insulin resistance and additional complications that are commonly associated with diabetes. Even though hyperglycemia is a common feature of this disorder, the etiology of diabetes can vary. Based on underlying causes, diabetes can be divided into two major categories; type 1 and type 2. Type 1 diabetes (T1DM) is associated with absolute insulin deficiency due to autoimmune destruction of pancreatic beta cells that store and release insulin³. T1DM accounts for approximately 10% of all instances of the disease. These patients require exogenous insulin delivery by injections or insulin pumps to survive due to the inability of their pancreas to synthesize insulin.

The specific etiology of type 2 diabetes (T2DM) is unknown, although autoimmunity is not considered to be a major factor. T2DM accounts for approximately 80-90% of all cases of diabetes⁴. T2DM is primarily caused by a combination of insulin resistance, lack of receptor sensitivity to insulin, and

insulin deficiency. The pancreatic beta cells are still able to secrete insulin but at an insufficient level to overcome insulin resistance⁵. Insulin resistance happens at sites of adipose tissue, skeletal muscle and the liver^{4, 6}. T2DM patients require medications which function to increase insulin release and improve insulin sensitivity to maintain normal blood glucose levels. If hyperglycemia persists and is not controlled in T2DM patients, over time the pancreas continues to compensate by making more insulin, resulting in exhaustion of beta cells leading to functional deterioration, defective insulin secretion and eventual insulin deficiency (**Figure 1.1**). At that stage, T2DM patients require an exogenous insulin supply like T1DM patients⁷.

There are multiple factors that may contribute to the development of diabetes. According to clinical data, the risk of T2DM increases with familial history of diabetes (genetic factors), high blood pressure, ethnicity, metabolic syndrome, dyslipidemia, hypertension, dietary factors, sedentary lifestyle, obesity and age (**Figure 1.2**). T1DM typically occurs in individuals that have familial history of the disease and in genetically susceptible individuals^{5, 8}.

Figure 1.1. Pathogenesis of T2DM. Genetic predisposition and lifestyle factors contribute to insulin resistance. Once resistance develops, to compensate, beta cell hyperplasia attempts to maintain normal blood glucose levels. Eventually, beta cell secretory dysfunction sets in, leading to impaired glucose tolerance and diabetes. Adapted from: Kumar V, Abbas AK, Aster JC, Perkins JA. Robbins basic pathology. Philadelphia, PA: Elsevier; 2018.

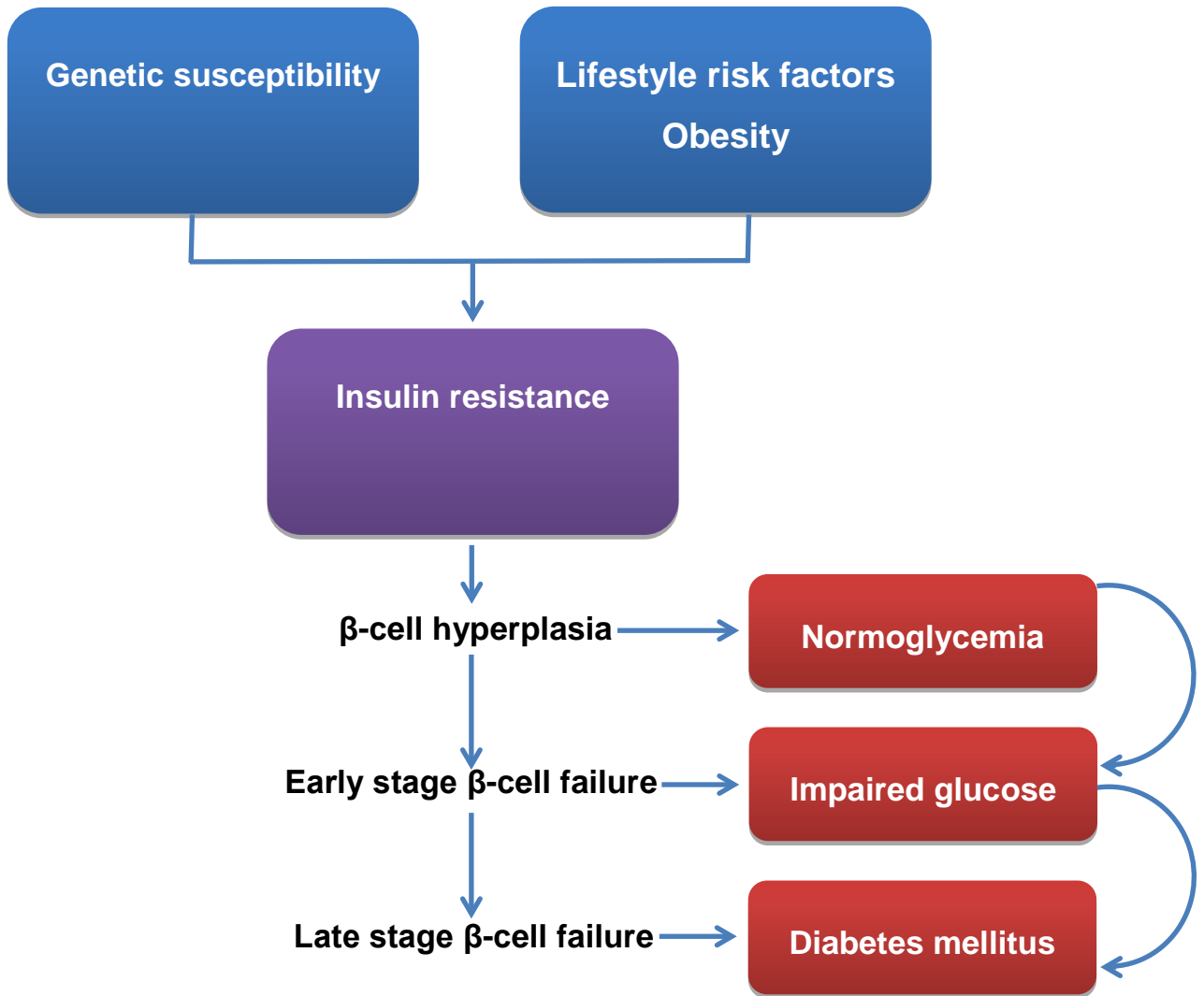
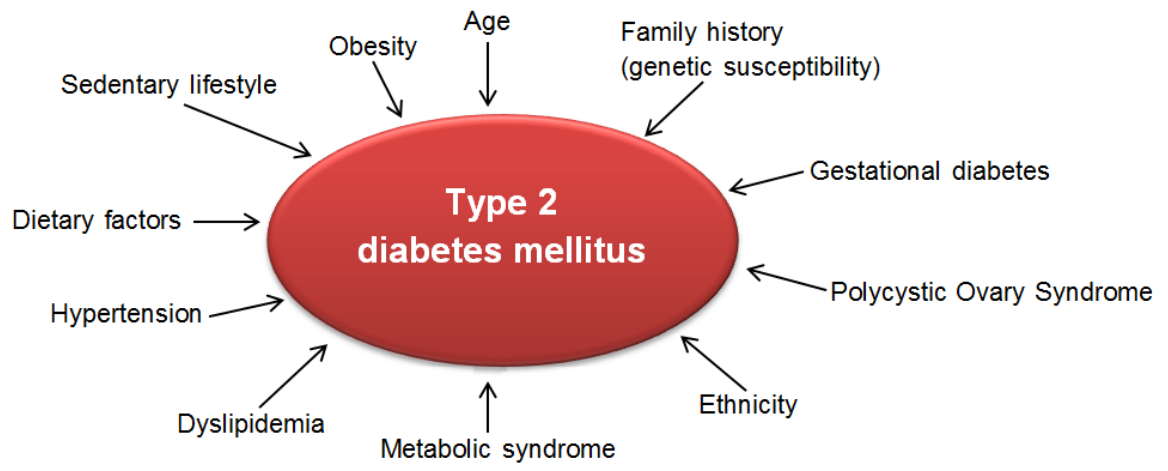


Figure 1.2. Risk factors affecting the development of T2DM. Adapted from:
Holt RIG, Cockram CS, Flyvbjerg A, Goldstein BJ. Textbook of diabetes. 4th ed.
Chichester, West Sussex, UK: Wiley Blackwell; 2010.



1.2 Epidemiology

Diabetes has emerged as a major global health problem, with serious health-related and socioeconomic impacts on individuals and populations alike⁵. Diabetes is the fifth leading cause of death worldwide, claiming 4 million individuals annually. The pandemic growth of the disease is further being driven by improvements in healthcare which has increased life expectancy, shifted demographics, socioeconomics, and lifestyle nutritional patterns⁵. The rates of diabetes have been rapidly rising in middle- and low-income countries where the prevalence of obesity in adults and children has been increasing^{5, 9, 10, 11}. In 2010, the International Diabetes Federation estimated that worldwide, there were 285 million people living with diabetes and that the number would exceed 400 million in the next twenty years¹². In 2014, the World Health Organization ran a global report on diabetes and concluded that the number of people living with diabetes had already reached 422 million, far exceeding the predictions made in 2010 **(Table 1)**¹¹. With the severity of disease complications, co-morbidities and complexity of therapy, the management of diabetes consumes vast resources worldwide⁵.

Table 1.1. Global prevalence of diabetes.

WHO Region	Prevalence (%)		Number (millions)	
	1980	2014	1980	2014
African Region	3.1	7.1	4	25
Region of the Americas	5	8.3	18	62
Eastern Mediterranean Region	5.9	13.7	6	43
European Region	5.3	7.3	33	64
South-East Asia Region	4.1	8.6	17	96
Western Pacific Region	4.4	8.4	29	131
Total*	4.7	8.5	108	442

* Totals include non-Member States

Global report on diabetes. World Health Organization, Geneva, 2016.

1.3 Diabetic Complications

Diabetes can be a debilitating disease that is associated with high morbidity and mortality rates. The prime characteristic of diabetes is abnormal glucose metabolism and other metabolic complications that lead to serious pathological effects that affect practically all body systems⁴. These complications vary among individuals afflicted with diabetes primarily due to differences in the level of glycemic control and underlying pathophysiology⁵. High blood glucose is the primary culprit for the initiation of the damage and the continuation of effects on target tissues and organs¹³. Hyperglycemia induces oxidative stress through the excessive conversion of glucose into pyruvate through glycolysis. The pyruvate is then oxidized in the citric acid cycle to generate high amounts of the electron donors NADH and FADH₂ that feed into the electron transport chain. As the result, the inner mitochondrial membrane voltage gradient increases until a threshold is reached, blocking further electron transfer within complex III. The arrest of electron transport chain being halted leads to coenzyme Q transferring only a single electron to molecular oxygen, generating superoxide. Increased production of superoxide results in cellular toxicity through the activation of five known major pathways involved in diabetic complications: the polyol pathway, intracellular production of advanced glycation end products, expression of the receptor for advanced glycation end products and related activating ligands, the protein kinase C pathway, and the hexosamine pathway^{14, 15}. For most diabetic patients, complications are associated with macrovascular disease in the arteries, microangiopathy, the thickening of basement membranes, diabetic

nephropathy, retinopathy, neuropathy, and other tissues. These complications are observed in both T1DM and T2DM patients^{4, 16}.

Cardiovascular events are the most common complications that occur in patients with T1DM and T2DM. They are involved in as many as 80% of all patient deaths^{4, 17}. The hallmark of this complication is atherosclerosis which is the narrowing of large and medium-sized arteries by fatty plaques. As mentioned previously, in diabetic patients, it is the low-grade inflammation that damages hosts' cells which leads to endothelial dysfunction, alters the microvasculature, accelerates atherosclerosis development and leads to heart disease complications^{2, 18-20}.

Diabetic nephropathy is the leading cause of chronic kidney disease in the world²¹. Small amounts of albumin found in the urine, also known as microalbuminuria, are the earliest manifestations of diabetic nephropathy. Microalbuminuria, due to glomerular leakiness, is caused by hyperglycemia damaging the podocytes of the glomerular filtration barrier and increasing permeability of the capillary wall^{13, 22}. Without treatment, 80% of T1DM and 20-40% of T2DM will progress to definite nephropathy over the course of 10-15 years once symptoms appear. By roughly 20 years post-diagnosis, as glomerular filtration rate progressively decreases, 75% of T1DM and 20% of T2DM afflicted individuals will develop end-stage renal disease and require dialysis or kidney transplantation^{4, 23, 24}.

Diabetic neuropathy may affect the central nervous system, peripheral sensorimotor nerves, and autonomic nervous system. Most commonly the disorder affects the lower extremities, disrupting both motor and sensory functions. Over time, the effects may spread to the upper extremities as well. Diabetic neuropathy may also affect the autonomic nervous system, resulting in bladder and bowel dysfunction, erectile dysfunction, sudden foot drop, wrist drop or cranial nerve palsy^{4, 25}. Diabetic patients tend to be more susceptible to skin infections compared to healthy individuals. Infections of the lower extremities may develop into gangrene and bacteremia. Such infections result in 5% of all diabetic deaths^{4, 26-28}.

1.4 Diabetic Retinopathy

1.4.1 Retinal Anatomy

The retina is a layered structure consisting of photoreceptors and nerve cells lining the inner part of the eye²⁹. The inner layer of retina is in contact with the vitreous body, a gel like substance that fills the space between retina and the lens, and the outer layer is associated with the choroid, a layer of highly vascularized connective tissues (**Figure 1.3**). The retina is not uniformly thick, normally being 0.55 mm at the macula and roughly 0.1 mm at the fovea, the latter being the centre of the macula¹⁷. The blood is supplied to the retina through two different sources. The central retinal artery supplies blood to the inner two-thirds of the retina while the vascular choroid and its choriocapillaris, located posterior to the retina, supply blood to the outer third.

The macula is located near the centre of the retina approximately 4 mm to the temporal side of the optic disk and measures approximately 4 mm in diameter (**Figure 1.4**). Roughly 1.5 mm in diameter, the fovea is responsible for our central vision and is located in the centre of the macula. It is composed entirely of cone photoreceptors which are responsible for our sharp visual acuity and colour vision. Within the fovea is a 0.5 mm diameter foveal avascular zone (FAZ) which is supplied nutrients through the diffusion of blood from the capillaries of the underlying choroid⁵. As a result, there is a depression at the site where FAZ is located which functions to prevent any dispersion or loss of light signal³⁰.

Figure 1.3. Sagittal section of the eye. Internal structure of the eye by OpenStax College [CC BY 3.0 (<http://creativecommons.org/licenses/by/3.0/>)], via Wikimedia Commons.

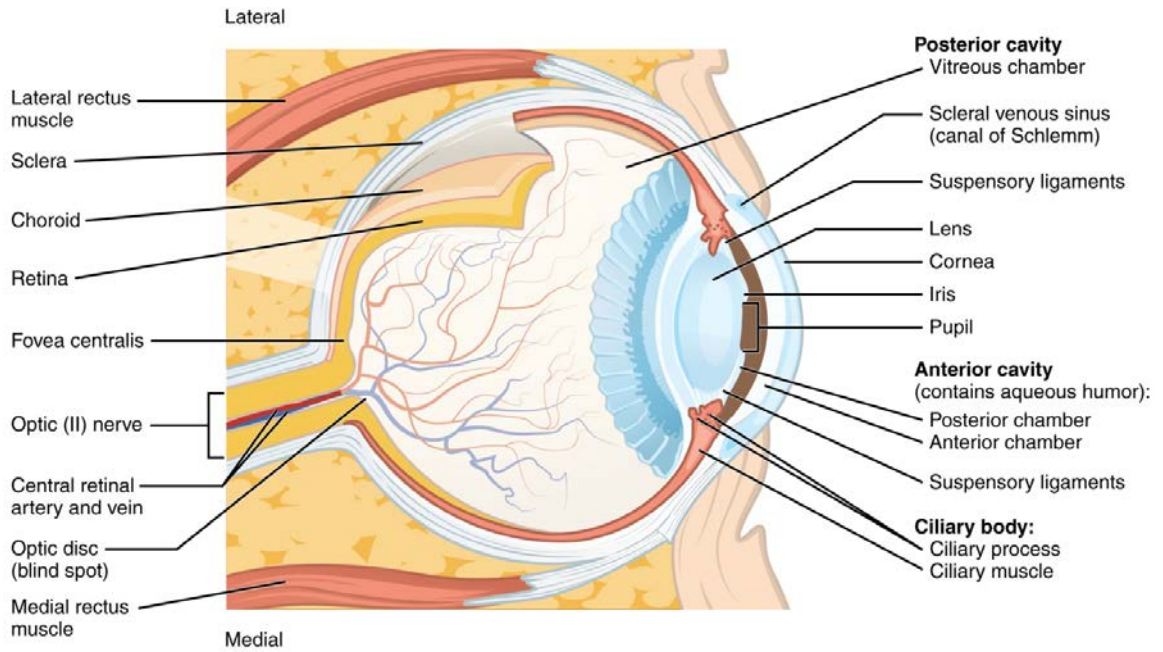
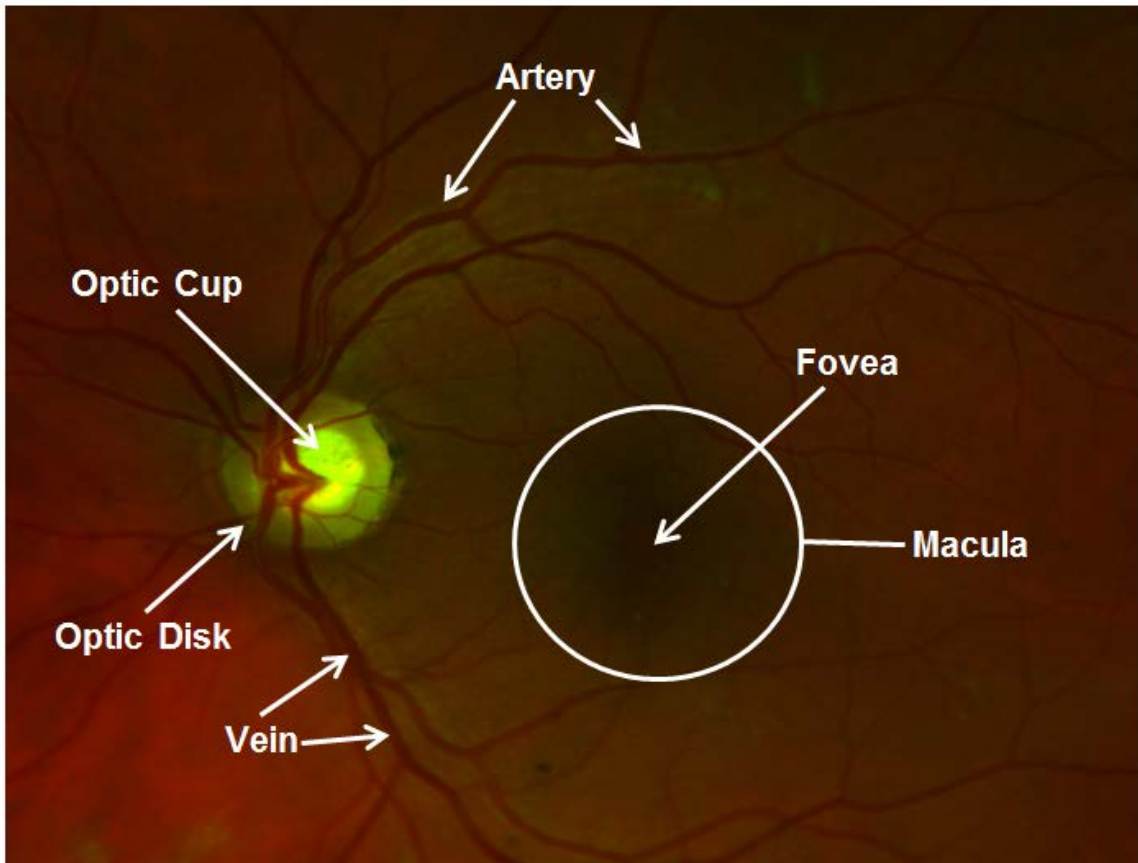


Figure 1.4. Wide-field photograph of the normal human fundus.

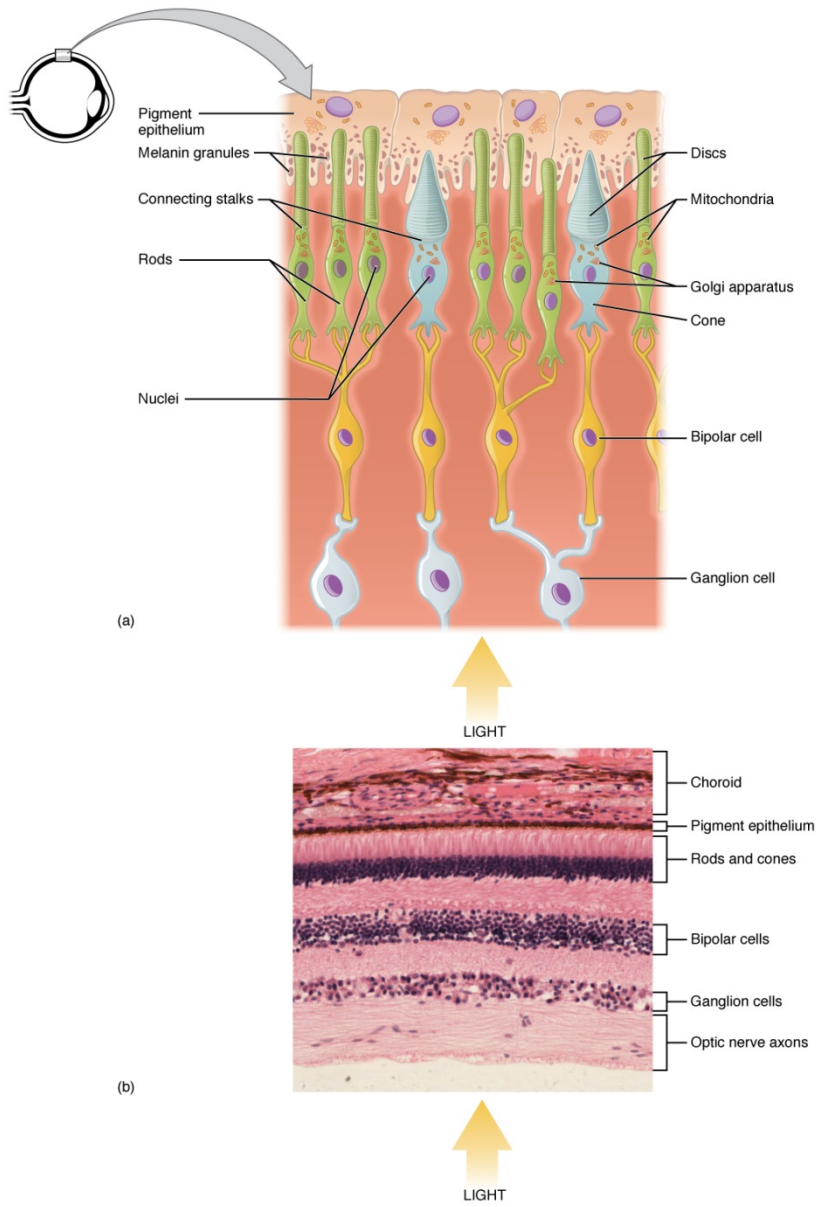


The optic nerve is located 3 mm to the medial side of the macula and is known as the blind spot since there are no retinal layers in this zone³¹. Ganglion cell axons from the neuronal cell layer, located near the inner surface of the retina, puncture through the sclera to form the optic nerve which transmits visual information to the brain. The optic nerve head is roughly 1.8 mm in diameter. Visually, the rim of the optic nerve is known as the disk and it contains nerve fibers from the ganglion cells. The inner section of the rim is the edge of the more whitish coloured cup which does not contain nerve fibers³².

The retina is composed of a “three-neuron system” consisting of photoreceptors, first-, and second-order neurons. In terms of location, inner refers to the layer of cells closest to the vitreous. Outer refers to the layers of cells closest to the sclera, the white outer coat of the eye. Retinal cell nuclei are arranged in specific bands called nuclear layers (**Figure 1.5**). The outer nuclear layer (ONL) is composed of photoreceptor nuclei and lies closest to the vascular choroid and sclera³³. The human eye contains two types of photoreceptors, the rods and cones. Rods sense contrast, brightness and motion while cones are responsible for fine resolution, spatial resolution and colour vision. Photoreceptors absorb light and initiate neuro-electrical impulses. The density of cones increases as you approach the macula, with the fovea having exclusively cones while the periphery of the retina is primarily rod-dominated³¹.

The inner nuclear layer (INL) of the retina is composed of the nuclei of the first-order neurons, the bipolar cells. INL also contains the nuclei of amacrine, horizontal and Muller cells which modulate activity of the ganglion cells³¹.

Figure 1.5. Histology of the retina. (A) Schematic diagram showing the arrangement of the different cell types in the retina. **(B)** Hematoxylin and eosin stained primate retina demonstrating the layered arrangement of the retina. Image by OpenStax College [CC BY 3.0 (<http://creativecommons.org/licenses/by/3.0/>)], via Wikimedia Commons.



Bipolar cells are the dominant cells, with horizontal cell nuclei being found in the outer parts and the amacrine cells found in the inner parts of the INL. Muller cell nuclei are uniformly distributed throughout the INL. Functionally, bipolar cells transmit signals from photoreceptor cells found below the inner layer of the INL to ganglion cells located above the upper layer of INL. Bipolar dendrites synapse with photoreceptors and horizontal cells, while their axons synapse with ganglion and amacrine cells³¹. Horizontal cells have a role in retinal processing and release inhibitory neurotransmitters, primarily GABA, that act on photoreceptor cells. Amacrine cells mostly play an inhibitory role and modulate signals that reach ganglion cells. Amacrine cells may be GABAergic and dopaminergic or can release acetylcholine³¹.

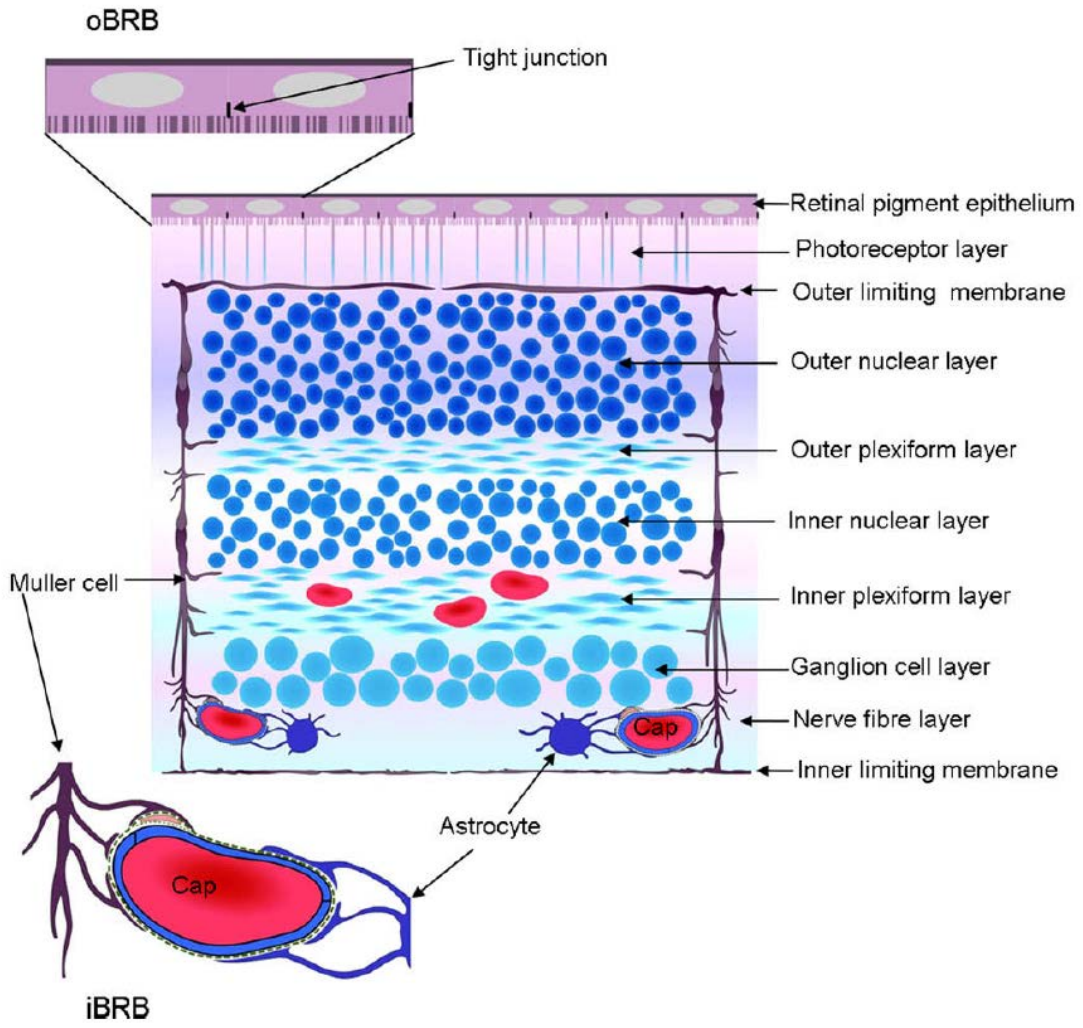
The innermost nuclear layer of the retina is referred to as the ganglion cell layer (GCL) which houses the nuclei of the second-order neurons, the retinal ganglion cells³¹. The GCL is located near the inner surface of the retina between the nerve fiber layer and the inner plexiform layer³¹. The GCL varies in thickness, being the thickest near the fovea and thinnest at the periphery of the retina³³. The axons of the ganglion cells form the nerve fiber layer which is located at the innermost surface of the retina. The bundles of the nerve fibers form the optic nerve which is responsible for transmitting visual information to the brain³¹.

The dense networks of axons and dendrites found in the retina are located within the outer plexiform layer (OPL), located between ONL and INL, and the inner plexiform layer (IPL), located between INL and GCL. The axons of photoreceptors which form synaptic terminals with bipolar cells and horizontal

cells are contained within the OPL. Meanwhile, IPL contains axons of bipolar and amacrine cells, and dendrites of ganglion cells³¹. Glial, astrocytes and oligodendrocytes are located in the GCL and IPL layers of the retina³³. The combination of the neural processing from all of the layers transmits visual information to the brain through the optic nerve³¹.

The blood-retinal barrier (BRB) is comprised of two parts: the endothelial cells of the retinal blood vessels which are connected by tight junctions and the outer retinal pigment epithelial (RPE) cells. The microenvironment of the retina is regulated by BRB which is essential for the structural and functional aspects of the retina³⁴. Under normal conditions, BRB controls molecular and fluid movements between the retina and choroidal vasculature, preventing leakage and other harmful agents from entering the retina. The inner BRB (iBRB) is formed by tight junctions between retinal endothelial cells resting on a basal lamina (**Figure 1.6**)³⁵. They are covered by the processes of astrocytes and Muller cells³⁶. Pericytes are separated from the endothelial cells by the basal lamina and all three cell types play a critical role in maintaining the proper functioning of BRB³⁴. The tight junctions between RPE cells form the outer BRB (oBRB)³⁷. The barrier separates the neural layer of the retina from the choriocapillaris, maintains the cohesion of the neural layer of the retina, facilitates phagocytosis of rods and cones, and transports nutrients from the blood to the outer retina^{31, 34}. In addition, RPE improves image resolution by absorbing light and preventing light from scattering³¹.

Figure 1.6. Blood-retinal barrier under normal conditions. The inner BRB is formed by tight junctions between retinal endothelial cells which are covered by the processes of astrocytes and Muller cells. The tight junctions between RPE cells form the outer BRB (oBRB). Image from: Kaur C, Foulds W, Ling E. Blood-retinal barrier in hypoxic ischaemic conditions: Basic concepts, clinical features and management. *Prog Retin Eye Res* 2008;27(6):622-647.

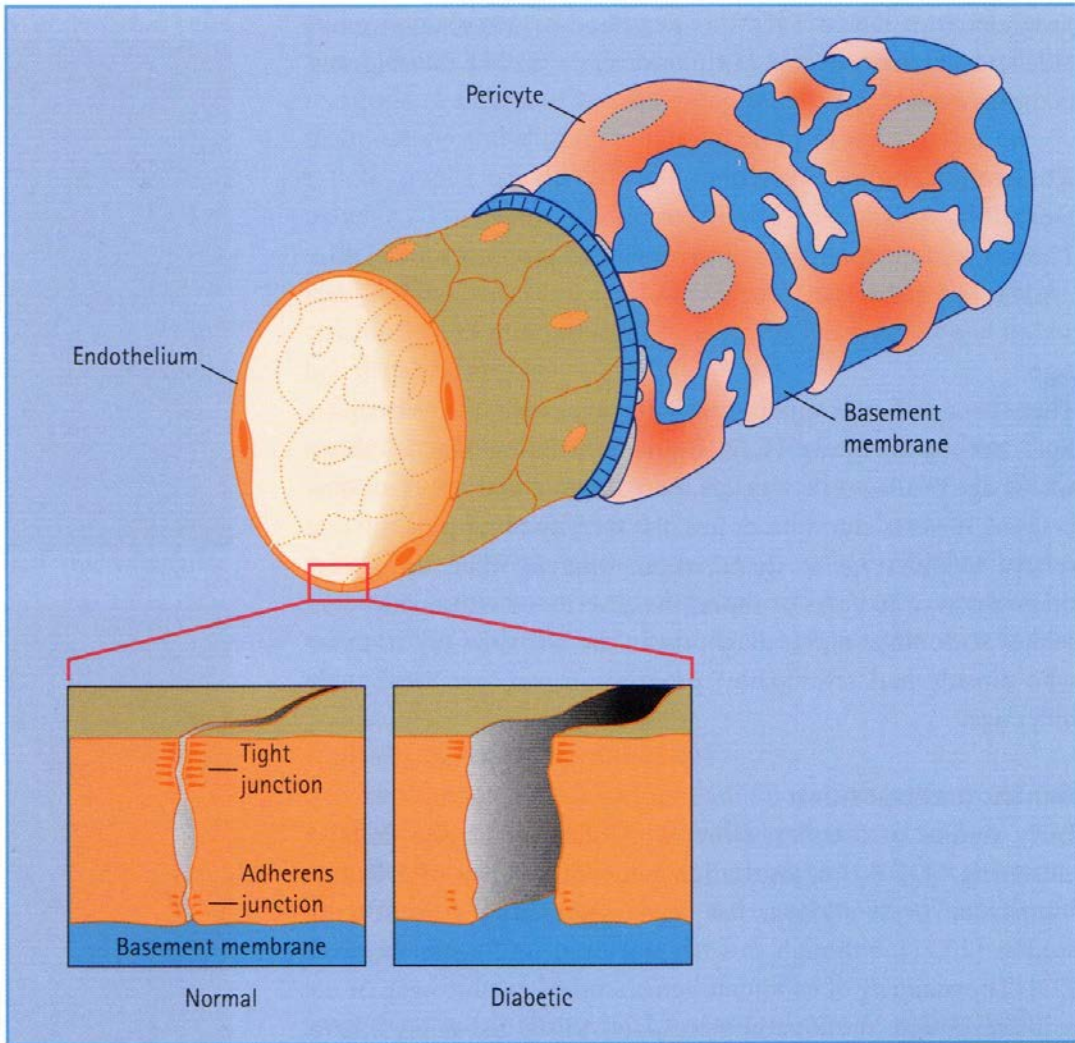


Pericytes, cells that are embedded within the basement membrane of the capillary blood vessels, have numerous roles within the retina (**Figure 1.7**). The ratio of pericytes to endothelial cells is 1:1; more than any other vascular bed³⁸. Pericytes function to regulate vascular tone, support the capillary walls, secrete extracellular material such as fibronectin and are capable of phagocytosis^{38, 39}. Actin, myosin and tropomyosin are all expressed in pericytes, making them capable of contraction and assist in regulation of blood flow within the retinal microcirculation^{39, 40, 41}. Pericytes have also been shown to inhibit proliferation of endothelial cells and angiogenesis⁴².

Muller cells are the supporting glial cells of the retina that are similar in function to oligodendrocytes³¹. Muller cells have an important role in maintaining BRB by supporting neuronal activity, facilitating uptake of nutrients, disposing of wastes, maintaining ion homeostasis, controlling signaling molecules and maintaining extracellular pH^{43, 43, 45, 46}. Muller cells under normal conditions have been found to reduce vascular permeability by secreting pigment epithelium derived growth factor (PEDF). The primary function of PEDF is to antagonize the actions of vascular endothelial growth factor (VEGF) which increases the permeability of BRB.

Astrocytes function to maintain the integrity of retinal vessels and are located in the nerve fiber layer, GCL, IPL and outer INL^{31, 47, 48, 49}. Astrocytes have been shown to modify the morphology of the retinal vascular endothelium by increasing the expression of tight junction protein ZO-1, thus increasing the barrier properties⁵⁰.

Figure 1.7. Schematic of the retinal capillary. An inner layer of retinal endothelial cells is enclosed by a tube of basement membrane, which in turn is surrounded by pericytes. Image from: Holt RIG, Cockram CS, Flyvbjerg A, Goldstein BJ. Textbook of diabetes. 4th ed. Chichester, West Sussex, UK: Wiley Blackwell; 2010.



1.4.2 Epidemiology

DR is the leading cause of blindness amongst working age (20-74 years old) adults with DME being the most common cause of this vision loss^{16, 51}. Approximately 50% of patients with DR will develop DME¹⁶. Presently, millions of people are living with undiagnosed diabetes, and the incidence of T2DM in developed countries is on the rise; even as medicine advances, diabetes remains a major public health concern^{27, 52, 53}. Duration of diabetes is a significant risk factor for developing DR, which is a vascular complication of both T1DM and T2DM²⁶. After 15 years, 90% of T1DM patients develop some form of retinopathy, with half of them progressing to PDR which is characterized by retinal neovascularization^{16, 27}. Retinopathy may be the first clinical manifestation of T2DM in some patients¹⁶. According to the United Kingdom Prospective Diabetes Study, approximately 37% of individuals who were first diagnosed with T2DM patients had already developed retinopathy. Within 15 years of developing diabetes, 60% of patients with T2DM develop some form of retinopathy²⁶. Following the 15 year period, 5-10% of T2DM patients will develop PDR and 10-15% will develop DME. T2DM patients develop much earlier diabetic eye disease compared to T1DM patients as the majority of these patients live with undiagnosed diabetes and start treatment or lifestyle changes very late. Patients that have high-risk PDR, within 5 years have a 60% risk of developing severe vision loss and a 30% risk of moderate vision loss from DME²⁶. Blindness occurs due to DR complications such as vitreous hemorrhages or traction retinal detachments¹⁶.

1.4.3 Pathogenesis

The exact pathogenesis of DR remains unknown, however, the underlying cause of its development is hyperglycemia¹⁷. This is supported by clinical observations of diabetic patients, the duration of their disease relative to the development of DR, retinopathy development in hyperglycemic animal models, and epidemiological and clinical trials showing a strong correlation between glycaemia control and retinopathy development^{17, 53-58}. The exact mechanism by which hyperglycemia leads to retinopathy is unknown¹⁶. The initiation and progression of DR is very complex and relies on several factors that are not yet understood. These factors vary depending on the different stages of DR and the uniqueness of individuals¹⁶. Glucose has a vital role in the disease as it enters the retina by facilitated diffusion, hence a constant high serum glucose will result in high levels of glucose in the retina²⁷. Multiple theories have been proposed on the potential mechanisms that facilitate retinal damage, specifically BRB, as a result of high glucose concentrations in the retina but none of them have been sufficiently supported. The theories propose that high blood glucose levels initiate several biochemical changes and processes, such as aldose reductase converting excess glucose into sorbitol¹⁶. Sorbitol is unable to diffuse out of the retina and, thus, accumulates resulting in damage^{27, 59}. Another theory suggests that high glucose concentrations result in the glycosylation of proteins that play a key role in cellular dysfunction, such as selectively activating the β -isoform of protein kinase C^{60, 61}.

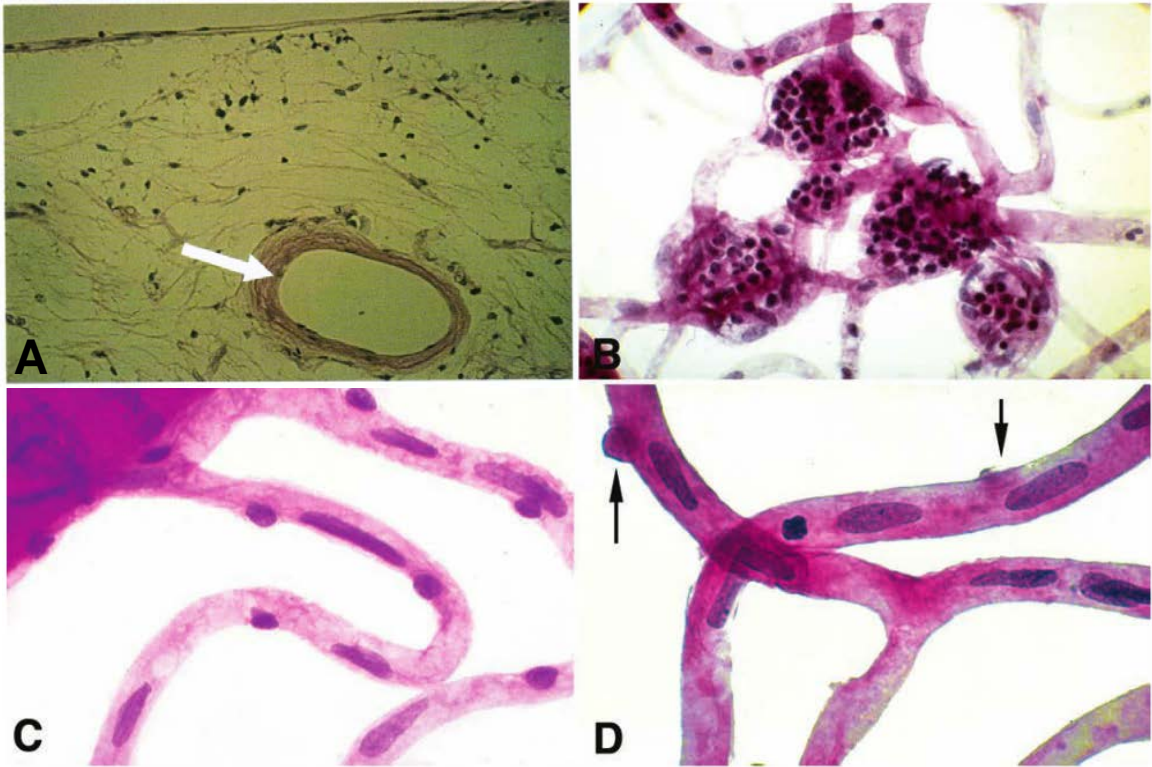
What is absolutely known is that hypoxia, or oxygen deficiency, plays a major role in the breakdown of BRB in a diabetic eye and is present early in the development of DR^{17, 62}. The pathology developing in the microvascular retinal capillaries is responsible for the breakdown of BRB. The first and most well-recognized pathologic feature of BRB is the loss of pericytes with thickening of the capillary basement membrane and microaneurysm development (**Figure 1.8**)^{34, 63, 64}.

During the early stages of DR development, there is a thickening of the capillary basement membrane. Hyperglycemia is directly related to the abnormal production of constituents of the basement membrane, such as fibronectin or collagen, and accumulation of advanced glycation end products. These thicken the basement membrane, increase vascular dysfunction and may possibly occlude retinal capillaries⁶⁵. Rat studies have shown that thickening of the capillary basement membrane may be prevented with aldose reductase inhibitors, but the results have not been consistent and have shown no effect on preventing the progression of DR according to a clinical trial^{17, 66, 67, 68}. The loss of pericytes through apoptosis appears to be initiated by high blood glucose levels. Pericyte loss may potentially have an impact on the formation of microaneurysms^{34, 69, 70}.

Due to capillary closure, oxygen delivery becomes increasingly limited in a diabetic eye, leading to retinal hypoxia. In addition, reduced oxygen delivery is further exacerbated by the higher amounts of glycated hemoglobin in diabetic patients' red blood cells³⁴. Hemoglobin, when exposed to plasma glucose

Figure 1.8. Pathologic features of BRB breakdown in a diabetic eye. (A)

Basement membrane thickening (arrow) in the retinal arteriole. Periodic acid-Schiff stain, magnification x250. Image from: Holt RIG, Cockram CS, Flyvbjerg A, Goldstein BJ. Textbook of diabetes. 4th ed. Chichester, West Sussex, UK: Wiley Blackwell; 2010. **(B)** Diabetic microaneurysms, trypsin retinal digestion. **(C)** Normal retinal capillaries, trypsin retinal digestion. Normal retinal capillaries are composed of approximately equal numbers of endothelial cells and pericytes. The nuclei of the endothelial cells are elongated while the pericytes have small, dark nuclei. The pericytes are embedded in the basement membrane of the capillary wall. **(D)** Retinal capillaries in diabetes mellitus, trypsin retinal digestion. A preferential loss of pericytes occurs in the early stages of diabetic retinopathy, disturbing the normal 1:1 ratio between pericytes and endothelial cells. *Arrows* denote pericyte ghosts in the capillary basement membrane. Diabetic thickening of the basement membrane causes intense staining with PAS stain. Images from: Eagle RC. Eye pathology an atlas and text. Philadelphia (Pennsylvania): Wolters Kluwer; Lippincott Williams & Wilkins; 2011.



through non-enzymatic glycation pathways, forms glycated hemoglobin⁷¹. Non-diabetic patients produce normal levels of glycated hemoglobin. In diabetic patients, if the normal blood glucose levels are not maintained and become elevated, the concentration of glycated hemoglobin increases. The lifespan of the glycated hemoglobin is approximately 3 months which allows it to be used as an approximation of average glucose levels over the last 3 months in diabetic patients. Glycated hemoglobin has a high affinity for oxygen, relative to normal hemoglobin, resulting in decreased oxygen delivery to the retina and contributing to hypoxia³⁴. In an attempt to compensate for oxygen loss, the body increases blood flow to the retina and blood hemoglobin concentrations.

During the early stages of DR, there is vasodilation of blood vessels within the retina due to a combination of hyperglycemia and hypoxia which may further contribute to the breakdown of BRB^{34, 72}. During the later stages, retinal hypoxia is further enhanced by decreased capillary circulation. The reduced circulation is caused by many factors. As the basement membrane thickens, the bore of the vessels affected is reduced, impeding blood flow³⁴. Blood flow is also restricted by abnormal plasma viscosity due to increased levels of fibrinogen in diabetic patients and hemoglobin aggregation^{34, 73, 74, 75}. Previous studies have shown that patients with diabetic retinopathy have abnormal blood viscosity. This increased plasma viscosity is due to elevated levels of fibrinogen and α -2-macroglobulin³⁴. Compared to non-diabetic patients, patients with DR have increased red blood cell aggregation. Plasma viscosity, platelet and red blood cell function, vessel

wall structure, permeability and auto regulatory mechanisms all contribute towards the progression and severity of DR¹⁷.

Capillary closure results in a severe reduction of blood flow to the retina and increased leukocyte adherence to the capillary endothelium^{34, 76}. The resulting tissue hypoxia results in up-regulation of adhesion molecules ICAM-1 and VCAM-1 which are involved in leukocyte adherence^{69, 77, 78, 79}. The aggregation of red blood cells may also be involved in capillary closure⁸⁰. The occlusion of capillaries further drives retinal hypoxia and the up-regulation of vascular permeability and angiogenic factors⁸¹. VEGF and nitric oxide are especially important in increased permeability and vascular dilation of BRB, control of free radicals, inflammatory mediation and hemodynamic alterations which all play a role in the disruption of BRB integrity. Hydrogen peroxide, which is produced from the phagocytosis of retinal components, disrupts tight junctions and causes dysfunction of BRB. Reactive oxygen species, also, indirectly increase vascular permeability of retinal blood vessels by increasing VEGF gene expression in endothelial cells^{34, 82, 83}.

VEGF is an angiogenic growth factor that plays a central role in retinal neovascularization and vascular permeability which results in the development of macular edema^{27, 34, 84, 85}. The development of ischemia in the retina creates hypoxia resulting in increased levels of hypoxia-inducible factor 1 (HIF-1) and increased levels of genes containing HIF-1 binding site in the promoter region, including VEGF²⁷. VEGF is expressed by a wide range of cells including astrocytes, RPE, pericytes, amacrine, Muller and endothelial cells⁸⁶. The exact

mechanism by which VEGF increases vascular permeability is unknown. VEGF binds to VEGFR1 (Flt-1) and VEGFR2 (KDR/Flk-1), both of which are tyrosine kinase receptors and are known to regulate angiogenesis⁸⁷. Activation of the receptors results in disruption of tight junctions of retinal endothelial cells by decreasing the expression of occludin which is important in tight junction stability and barrier function. As a result, the permeability of BRB increases leading to BRB breakdown in DR⁸⁸. The activity of VEGF may be responsible for developing fenestrations in endothelial cells which further increases vascular permeability^{89, 90, 91}. VEGF may also cause rearrangement of inter-endothelial junction-associated proteins such as VE-cadherin and tight junction proteins including ZO-1^{34, 92, 93}. By creating inter-endothelial gaps, endothelial cleavage, and degenerative changes in endothelial basement membranes that affect the structural integrity of the microvessels, VEGF leads to the extravasation of albumin and blood plasma proteins^{34, 84, 94}. According to Starling's Law which describes the relationship between stroke volume and end diastolic volume, the end result of the process is edema formation. Edema is the term used to describe an accumulation of fluid in tissues. The increased permeability, induced by VEGF, leads to osmotically active molecules leaking out into the surrounding tissue followed by water loss. The hydrostatic pressure in the capillaries and vessels increases the flux of water from the vessels to the tissue and results in edema formation⁹⁵.

By increasing permeability, VEGF has also been shown to control inflammatory responses^{34, 85, 96}. As a result of VEGF's pro-inflammatory actions,

ICAM-1 and VCAM-1 expression is increased on the surface of vascular endothelial cells, augmenting the attachment of leukocytes to vascular walls^{34, 78, 97, 98}. The adherence of leukocytes to the vascular endothelium breaks down BRB, further increasing vascular permeability, retinal edema and loss of central vision by causing apoptosis of endothelial cells and blockage of the capillaries^{76, 77, 86, 99, 100, 101}. Inhibition of VEGF and ICAM-1 has been shown to decrease the permeability of BRB^{34, 102}.

The most common manifestation of BRB breakdown is an increase in retinal volume due to increased permeability and accumulation of extracellular fluids in the retina. The fluid accumulation occurs most commonly in macula, creating cystic spaces within and leads to edema. Edema may be spread over an area if there is widespread BRB breakdown in the peripheral retina, or can be restricted to focal areas of macular capillaries³⁴.

During angiogenesis, there is an extensive breakdown of BRB³². Pericytes have been documented to inhibit TGF- β -mediated vascular endothelial cell proliferation. Loss of pericytes, as mentioned previously, creates a loss of this inhibitory effect and may stimulate endothelial cell proliferation and neovascularization³³. New vessel formation on the retina breach through the ILM and proliferate along the interface between the vitreous and the inner surface of the retina. These new blood vessels, which grow in response to VEGF, are highly susceptible to bleeding when a posterior vitreous detachment (PVD) occurs and can result in visual loss due to vitreous hemorrhage^{27, 34}. Furthermore, glial and RPE cells migrate and surround the neovascularization, forming fibrotic scar

tissue. If the vitreous and the scar tissue contract, traction on the retina can occur, resulting in a tractional retinal detachment. If the macula is involved, there is severe loss of vision which can become permanent unless the retina is surgically reattached in a timely matter²⁷.

The up-regulation of VEGF has been implicated in the etiology of macular edema and new vessel formation, as such, it might be expected that both abnormalities would always be present together. However, clinical data suggests otherwise. Macular edema can occur in all stages of DR. Additional factors, apart from the up-regulated VEGF, are likely involved in the etiology of macular edema and PDR in the diabetic eye³⁴.

A previous study has demonstrated that capillary outgrowth from retinal explants was significantly increased when the serum of diabetic patients was added to the media compared to serum from non-diabetic patients. A significantly greater capillary outgrowth occurred when the serum from PDR subjects was added to the media, indicating that circulatory factors play a major role in the development of DR¹⁰³. Over time, as hyperglycemia continues to alter the microenvironment of the retina, the retinal structure deteriorates resulting in vision loss.

1.4.4 Clinical Features of Diabetic Retinopathy

DR can be broadly classified into non-proliferative diabetic retinopathy (NPDR), pre-proliferative retinopathy and proliferative retinopathy (PDR)^{27, 29}. It is crucial that the level of retinopathy is accurately diagnosed and treatment is administered depending on the specific NPDR level, as there is a risk of progression to PDR²⁷. Diabetic maculopathy, described as the presence of macular edema or DME in the macula, can occur at any or all stages of DR.

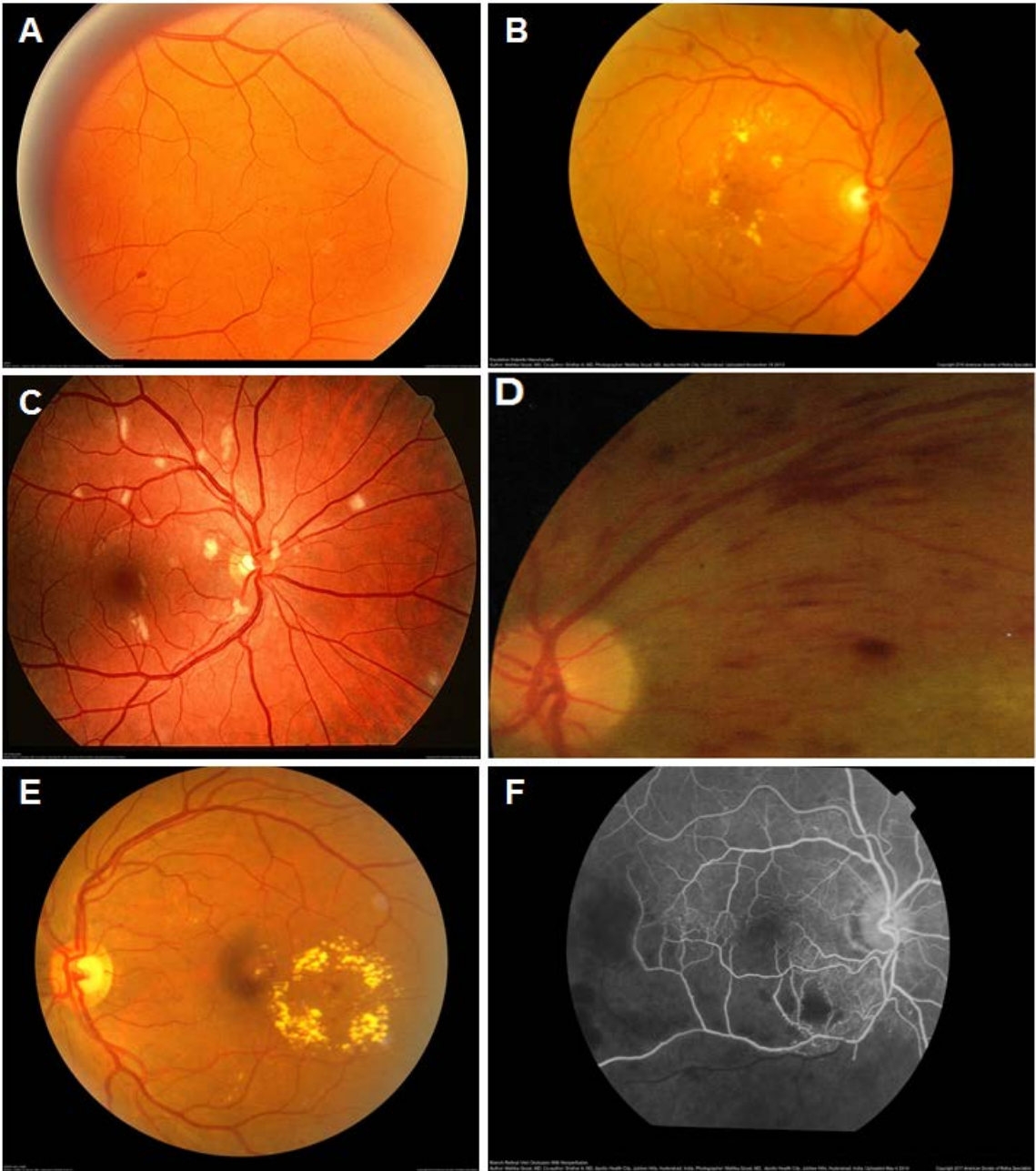
1.4.4.1 Non-proliferative diabetic retinopathy

NPDR is the milder form of retinopathy and can be further subdivided into mild, moderate and severe cases based on the extent of hemorrhages, microaneurysms, hard exudates and cotton wool spots¹⁰⁴. Mild NPDR is marked by at least one microaneurysm and a low number of hemorrhages²⁶. Retinal capillary microaneurysms appear as red dots which form as a result of structural weakness within the capillary wall due to the loss of structurally supportive pericytes. Microaneurysms may also form from fusion of capillary kinks or loops¹⁰⁵. Other clinical features of NPDR are nerve fibre layer and dot blot retinal hemorrhages (**Figure 1.9A**), retinal exudates (**Figure 1.9B**) and “cotton wool spots” (**Figure 1.9C**) which represent localized infarction of the nerve fibre layer.

Retinal hemorrhages can occur either within the retinal substance or superficially amongst the nerve fiber layer (NFL). When present in the NFL, retinal hemorrhages tend to form strips of flame-shaped markings (**Figure 1.9D**). Retinal exudates are lipid residues from damaged capillaries and are yellow in appearance. They may be isolated or found in clusters which often form into circular areas surrounding a cluster of microaneurysms and are referred to as “circinate patches” (**Figure 1.9E**). Exudates are the result of increased vascular permeability allowing fluid and lipoprotein to leak into the surrounding retina. If exudates occur outside of the macula, no treatment is required. Over time, exudates may dissipate by themselves.

“Cotton wool spots”, or soft exudates, indicate regions of retinal ischaemia^{27, 29}. These areas are fluffy and white in appearance representing

Figure 1.9. Non-proliferative retinopathy. (A) View of the superonasal retina showing numerous dot-blot intraretinal hemorrhages. This image was originally published in the Retina Image Bank® website. Henry J. Kaplan and Niloofar Piri. NPDR. Retina Image Bank. 2013;5345. © the American Society of Retina Specialists. **(B)** Exudates in the right macular area. This image was originally published in the Retina Image Bank® website. Mallika Goyal and Sridhar A. Exudative Diabetic Maculopathy. Retina Bank. 2013;11894. © the American Society of Retina Specialists. **(C)** Cotton wool spots. This image was originally published in the Retina Image Bank® website. Henry J. Kaplan and Niloofar Piri. Retinopathy. Retina Bank. 2013;4967. © the American Society of Retina Specialists. **(D)** View of elongated lighter red flame hemorrhages and more oval and darker red blot hemorrhages. Image from: Holt RIG, Cockram CS, Flyvbjerg A, Goldstein BJ. Textbook of diabetes. 4th ed. Chichester, West Sussex, UK: Wiley Blackwell; 2010. **(E)** Photograph of left eye shows circinate (ring pattern) lipid surrounding a leaking microaneurysm inferonasal to the optic nerve. This image was originally published in the Retina Image Bank® website. Jeffrey G. Gross. NPDR with CSME. Retina Bank. 2012;1094. © the American Society of Retina Specialists. **(F)** Fluorescein angiography displaying capillary nonperfusion inferior to the macula. This image was originally published in the Retina Image Bank® website. Mallika Goyal and Sridhar A. DR Nonperfusion. Retina Bank. 2014;17533. © the American Society of Retina Specialists.



microinfarcts developing in the nerve fiber layer of the retina and form from the accumulation of cytoplasm within the nerve axons or axoplasm. The transport system is energy-dependent and relies on the integrity of the retinal capillary bed. If a capillary occlusion occurs and nerve fibers cross the area, transport will fail. However, axoplasmic transport will continue on either side of the occlusion where the capillaries remain intact. As a result, there is an accumulation of deposits at the site of ischemia. An increase in the development and accumulation of cotton wool spots may be indicative that the retinopathy is developing into a more serious type¹⁰⁴.

1.4.4.2 Diabetic Macular Edema

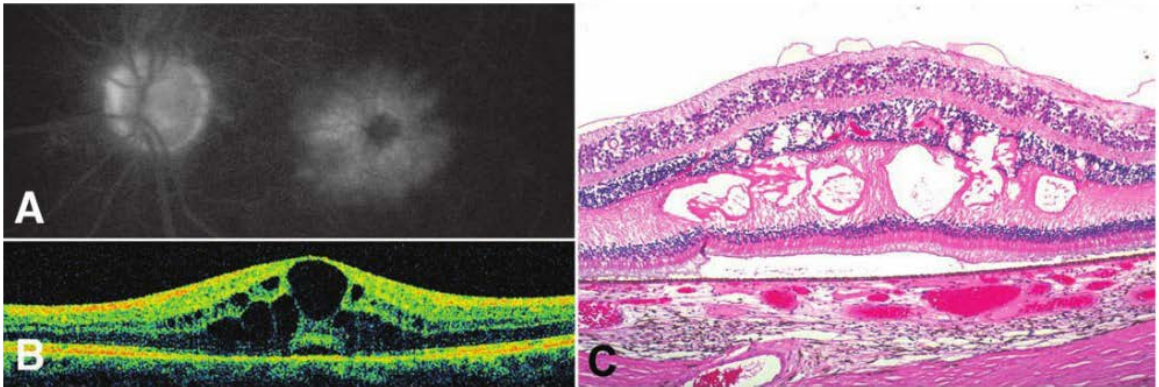
Diabetic macular edema (DME) is the most common cause of vision loss in patients with diabetic retinopathy and can occur at any stage in the overall DR process^{26, 27}. DME is the leading cause of vision loss because T2DM is more prevalent than T1DM and maculopathy is more commonly associated with older T2DM patients. Proliferative retinopathy is more commonly associated with T1DM patients^{29, 106, 107}.

Ischemic maculopathy develops from extensive capillary occlusions within the central retina. The macula is the centre of vision and has very high metabolic activity. If there is inadequate perfusion due to capillary closure, atrophy sets in and visual acuity decreases. The affected macula appears pale, has numerous hemorrhages and microaneurysms with no exudates present. Unfortunately, currently there is no available treatment for ischemic maculopathy.

Diabetic macular edema occurs due to the increased permeability of retinal capillaries due to the breakdown of the BRB and microaneurysms resulting in extracellular fluid and thickening of the retina¹⁷. Fluid filled cystic spaces develop within the retina and at the fovea (**Figure 1.10**). DME can be characterized as either focal or diffuse vascular leakage and is also known as exudative maculopathy due to the plasma lipoproteins which leak out, precipitate and form hard exudates^{27, 29}. This form of maculopathy has greater vision threatening effects the closer it is to the macula and fovea. This hard exudate and macular thickening disrupts the function of the central retina, causing vision

Figure 1.10. Diabetic macular edema. (A) Fluorescein angiogram discloses petalloid pattern of intraretinal cystoid edema in fovea. **(B)** Cross-sectional optical coherence tomography showing clinically significant macular edema with cysts and macular thickening. **(C)** Large cystoid spaces filled with granular proteinaceous fluid are seen in the outer plexiform and inner nuclear layers.

Images from: Eagle RC. Eye pathology an atlas and text. Philadelphia (Pennsylvania): Wolters Kluwer; Lippincott Williams & Wilkins; 2011.

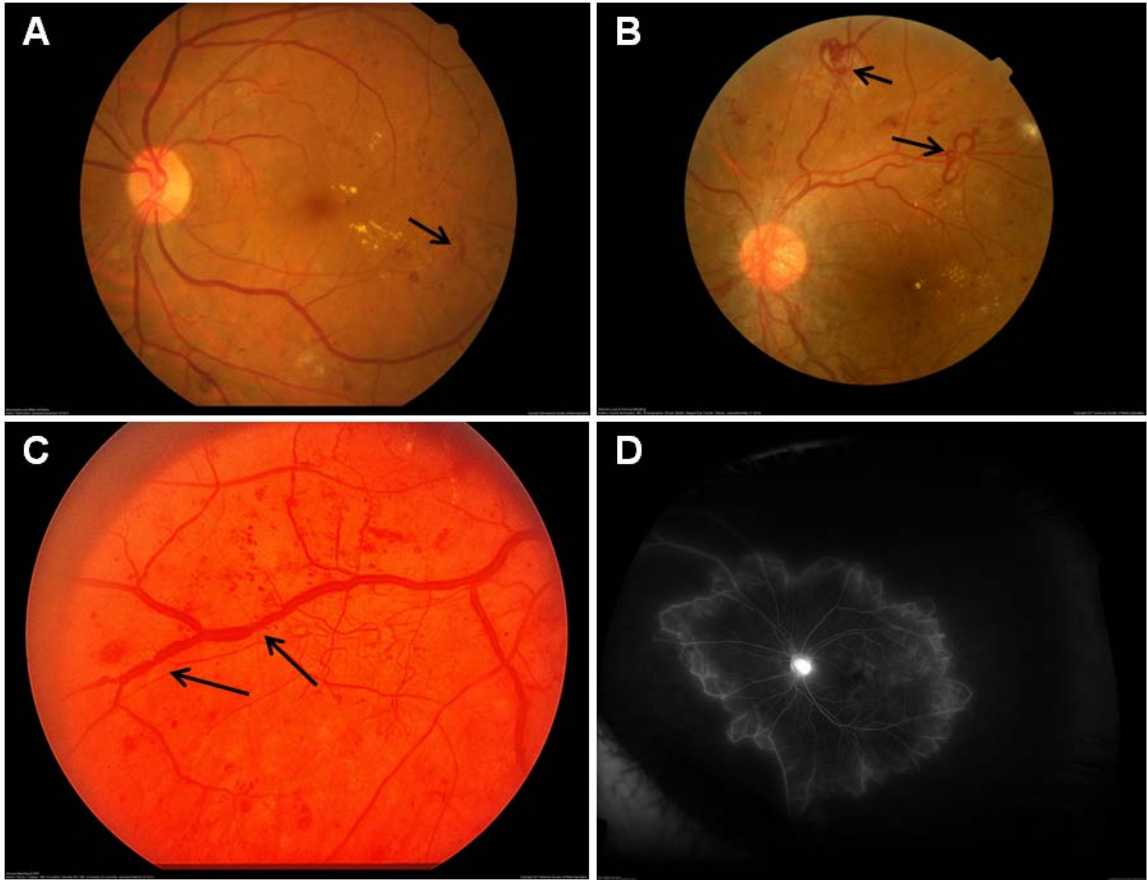


loss. Exudative maculopathy should be treated as early as possible with laser or anti-VEGF injections.

1.4.4.3 Pre-proliferative Retinopathy

In pre-proliferative retinopathy, retinal capillaries continue to close resulting in further ischemia and non-perfusion. Large, blotchy hemorrhages begin to form within the retina. The formation of hemorrhages may be associated with an increased number of cotton wool spots. Intraretinal microvascular abnormality (IRMA), small vascular loops stemming from capillaries or venules, are representative of intraretinal shunt vessels and a form of abnormal vascular development. They may be seen particularly along the edges of regions of capillary occlusions and non-perfusion (**Figure 1.11A**). The retinal vessels may develop venous dilation, reduplication, loops and beading (**Figure 1.11B and C**)^{27, 29}. The occurrence of such changes is indicative that the patient has transitioned into the severe stage of NPDR and is a significant predictor of future progression towards retinal neovascularization and PDR.^{26, 29} Diabetic patients in the pre-proliferative retinopathy stage do not always progress to proliferative retinopathy but the risk is as high as 50% within the year^{107, 108, 109}.

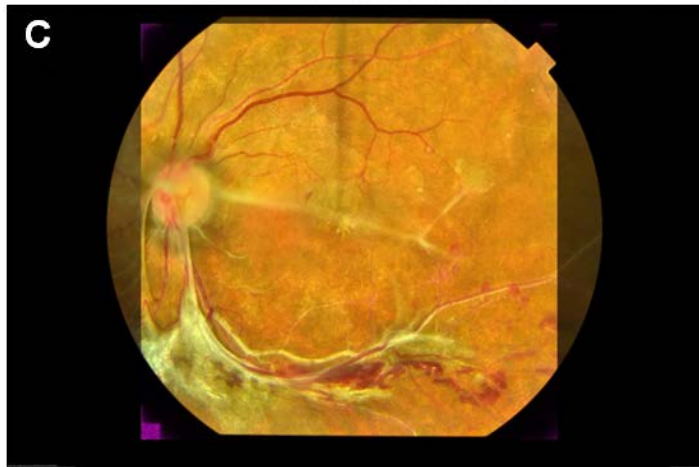
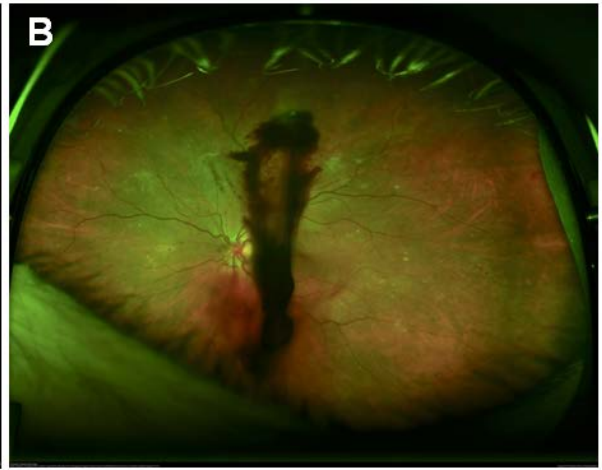
Figure 1.11. Pre-proliferative retinopathy. (A) An example of intraretinal microvascular abnormality (IRMA) in the temporal retina of the left eye (arrow). This image was originally published in the Retina Image Bank® website. Talal Basha. Maculopathy and IRMA Left Retina. Retina Bank. 2013;12528. © the American Society of Retina Specialists. **(B)** Example of venous loops (arrows). This image was originally published in the Retina Image Bank® website. Hamid Ahmadi. Venous Loop & Venous Beading. Retina Bank. 2014;18246. © the American Society of Retina Specialists. **(C)** Venous beading (arrows). This image was originally published in the Retina Image Bank® website. Henry J. Kaplan and Niloofar Piri. Venous Beading & NVE. Retina Bank. 2013;5347. © the American Society of Retina Specialists. **(D)** Fluorescein angiography displaying severe capillary nonperfusion. This image was originally published in the Retina Image Bank® website. Jeffrey S. Heier. Severe Capillary Nonperfusion. Retina Bank. 2013;178. © the American Society of Retina Specialists.



1.4.4.4 Proliferative Diabetic Retinopathy

With increasing retinal capillary bed closure and ischemia, retinal neovascularization may occur. In response to ischemia, vasoproliferative growth factors are secreted to rejuvenate the retinal perfusion, but they typically fail to do so. The new vessels grow on the retinal surface, with the posterior surface of the vitreous acting as a scaffold. At the edge of both perfused and non-perfused retina, neovascularization occurs **(Figure 1.12A)**²⁷. When compared to normal vessels, the new vessels lack endothelial tight junctions, and are therefore very permeable and fragile which may result in bleeding termed a vitreous hemorrhage. If the bleeding is limited, a few floaters might be present which the patient may or may not notice, however if there is extensive bleeding, there can be an abrupt decrease in total vision. These hemorrhages typically develop when the posterior vitreous partially detaches overlying an area of new vessel development **(Figure 1.12B)**. As the neovascularization continues, a fibrous tissue web may accompany the growing new vessels and can eventually undergo contraction over time resulting in a retinal detachment **(Figure 1.12C)**²⁷.

Figure 1.12. Proliferative diabetic retinopathy. (A) Network of blood vessels (arrows) arising from a normal retinal vein represents neovascularization. This image was originally published in the Retina Image Bank® website. Jason S. Calhoun. Neovascularization. Retina Bank. 2013;7786. © the American Society of Retina Specialists. **(B)** Vitreous traction on neovascular tissue in proliferative diabetic retinopathy gives rise to vitreous hemorrhage. This image was originally published in the Retina Image Bank® website. Carmen L Gonzalez. Proliferative Diabetic Retinopathy. Retina Bank. 2013;9750. © the American Society of Retina Specialists. **(C)** Significant fibrovascular proliferation is seen along the major retinal vascular arcades in the left eye of this patient with proliferative diabetic retinopathy. This image was originally published in the Retina Image Bank® website. Daniel Rojas Abatte. Fibrovascular Proliferation. Retina Bank. 2016;26778. © the American Society of Retina Specialists.



1.5 Treatments

Treatments for DR follow the results of Diabetic Retinopathy Study (DRS) and Early Treatment of Diabetic Retinopathy Study (ETDRS)²⁷. Both were landmark trials that set guidelines for the treatment of diabetic retinopathy. The DRS (1972) was established to see if panretinal photocoagulation (PRP) could prevent vision loss in patients with PDR and to assess the safety of the procedure using different lasers¹⁰⁴. The results of that study conclusively showed that PRP significantly reduces serve vision loss in patients with PDR, reducing blindness by 90%^{26, 110-123}. For patients with PDR, DRS showed that the treatment outweighs the risks of laser but recommended that patients with non-proliferative changes should be monitored frequently¹⁰⁴. The ETDRS (1985) was designed to determine the ideal stage of DR to conduct PRP, whether PRP was effective in the treatment of macular edema, and if aspirin was effective in altering the development of DR¹⁰⁴. The results indicated that focal photocoagulation reduced the risk of moderate vision loss by 50% in patients with PDR. ETDRS showed that both early PRP before the development of high-risk PDR and the deferral of treatment until high-risk PDR develops are effective in reducing the risk of severe vision loss. Examining this evidence, it can be concluded that, as the eye approaches the high-risk stage of PDR, PRP should be considered^{26, 124-146}. ETDRS also defined the stages of DR from mild, moderate, severe, very severe NPDR to early, high-risk PDR levels. The classification allows physicians to correlate the level of DR with the risk of progression and the potential outcomes of the treatments²⁷. The definition of mild

to moderate NPDRs is when a patient has an intraretinal hemorrhage in fewer than the four quadrants of the retina (superior, inferior, nasal and temporal), microaneurisms, hard exudates, macular edema and abnormalities in the foveal avascular zone. Moderate to severe NPDR is defined as having mild/moderate intraretinal hemorrhage in four quadrants, having cotton wool spots, venous beading and IRMAs. Severe NPDR is classified as having one of the following: severe intraretinal hemorrhage in four quadrants, venous beading in two quadrants, IRMA in one quadrant. Very severe NPDR is when at least two of the three traits occur: severe intraretinal hemorrhage in four quadrants, venous beading in two quadrants, IRMA in one quadrant. PDR has three of the following: presence of neovessels, location and size of the neovessels, presence of pre-retinal hemorrhage or vitreous hemorrhage¹⁰³. The two treatments used clinically for DR are PRP for PDR and the use of anti-VEGFs for DME.

1.5.1 Panretinal Photocoagulation

PRP is a laser technique employing a visible laser treatment used to destroy select portions of the peripheral retina to reduce oxygen consumption and to restore the balance between oxygen supply and demand⁹⁵. A patient is administered pain numbing medication in the form of proparacaine drops to the eye, the pupil is dilated and a contact lens is placed on the cornea¹⁷. Mild to moderate laser burns that produce a light grey spot on the retina are delivered in a grid-like pattern, sparing the macula and optic nerve, for a total of 1800-2400 burns of 500 µm in diameter delivered over 1-4 treatment sessions (**Figure 1.13A**)^{17, 95}. The laser ray is absorbed by the melanin in the retinal pigment epithelium and causes thermal coagulation of RPE cells and the adjacent photoreceptors (**Figure 1.13B**). Photoreceptors use more oxygen than most cells in the body, and in this oxygen deprived environment, eliminating them is an effective method to reestablish the balance and reduce the oxygen consumption of the retina⁹⁵. The photoreceptors, over time, are replaced by glial cells and oxygen from the vascular choroid can diffuse through the scars in the outer retina to reach the hypoxic inner retina (**Figure 1.14A**). The whole process increases the oxygen tension and improves hypoxia^{95, 147-152}. Since hypoxia is the stimulant for VEGF and neovascularization, the increased oxygen supply results in a stabilization of VEGF production back to normal levels, decreasing endothelial cell proliferation, decreasing permeability and decreasing neovascularization (**Figure 1.14B**). Overall, the treatment reduces the oxygen consumption and the number of photoreceptors in the outer retina by approximately 20%⁹⁵.

Figure 1.13. Panretinal photocoagulation. (A) Ultra-wide field OPTOS photograph taken after panretinal photocoagulation in a patient with proliferative diabetic retinopathy. **(B)** The outer retina and retinal pigment epithelium are photocoagulated and the photoreceptors are absent, whereas the inner retina is relatively intact. Image from: Stefánsson E. The Mechanism of Retinal Photocoagulation – How Does the Laser Work? *European Ophthalmic Review* 2009;02(01):76-79.

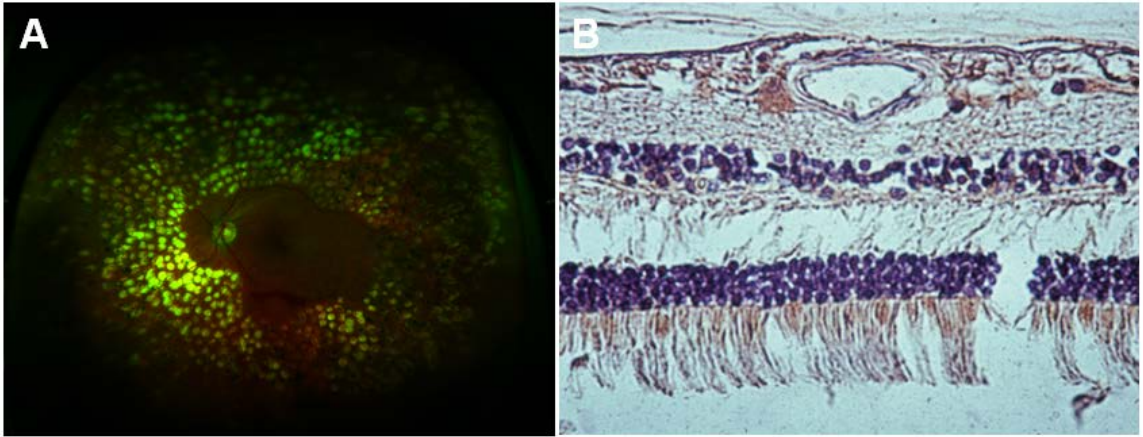
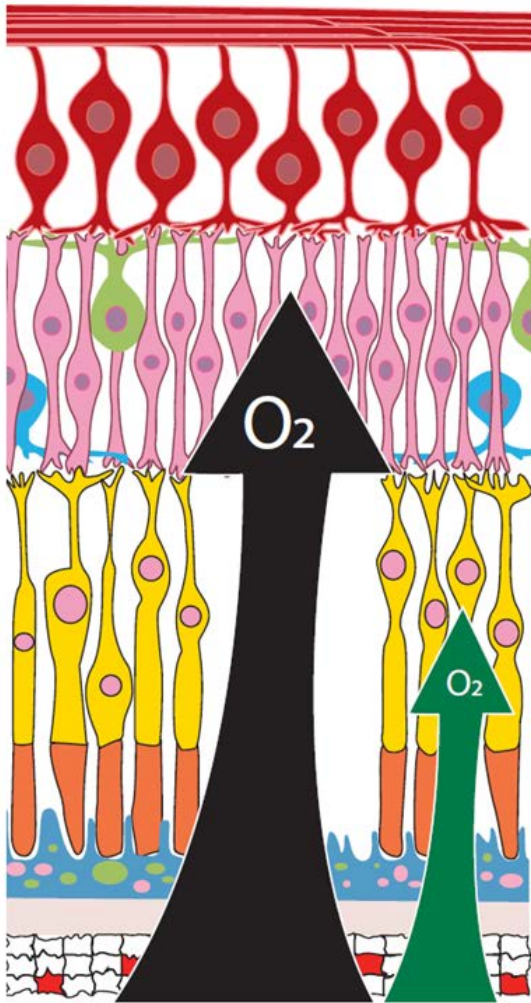
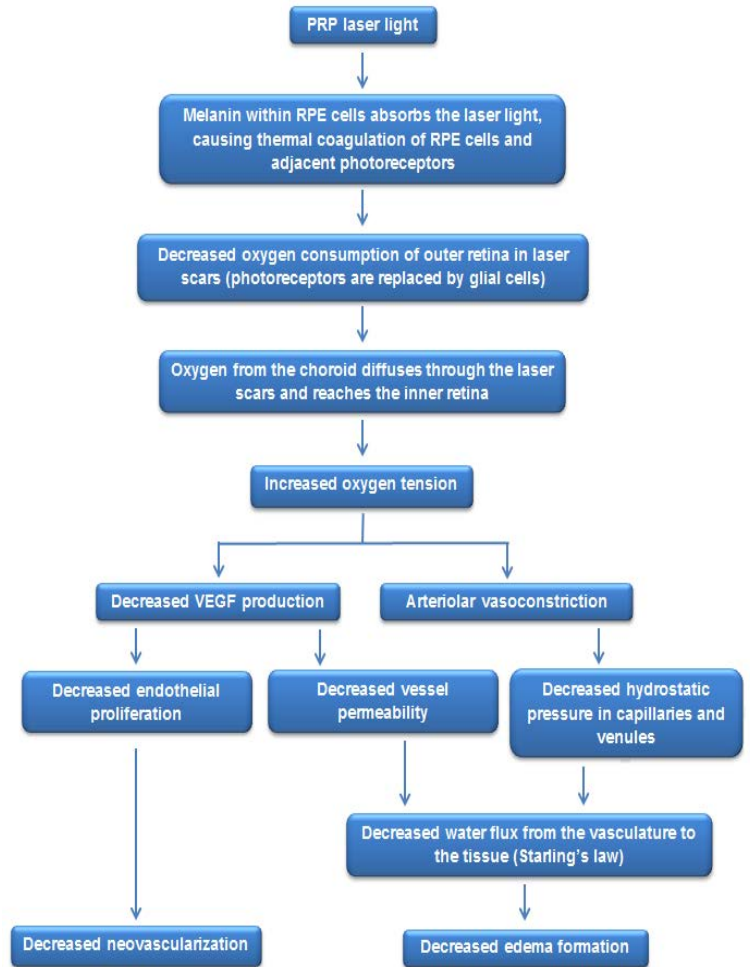


Figure 1.14. Effect of panretinal photocoagulation treatment. (A) The oxygen flux is represented by a black arrow, coming from the choroid and passing through a laser scar into the inner retina. In the laser scar, photoreceptors are replaced by glia and the oxygen consumption is decreased. The oxygen flux from the choroid would normally be consumed by the photoreceptors, indicated by the green arrow. As the oxygen consumption of the glia is less than that of photoreceptors, the oxygen flux reaches the inner retina. **(B)** The schematic flow diagram explains the mechanism by which retinal photocoagulation affects retinal neovascularization and macular edema in diabetic retinopathy and other ischemic retinopathies. RPE = retinal pigment epithelial. Adapted from: Stefánsson E. The Mechanism of Retinal Photocoagulation – How Does the Laser Work? *European Ophthalmic Review* 2009;02(01):76-79.

A



B



Laser can also be administered as a focal treatment for macular edema to ablate leaky microaneurysms around the macula and reduce swelling. This decreases the hydrostatic pressure of capillaries and venules, decreasing water flux from the vasculature to the tissue according to Starling's law and reducing edema formation⁹⁵. Focal laser is administered at a diameter of 100-200 μm to seal the small leaky microaneurysms around the macula¹⁷.

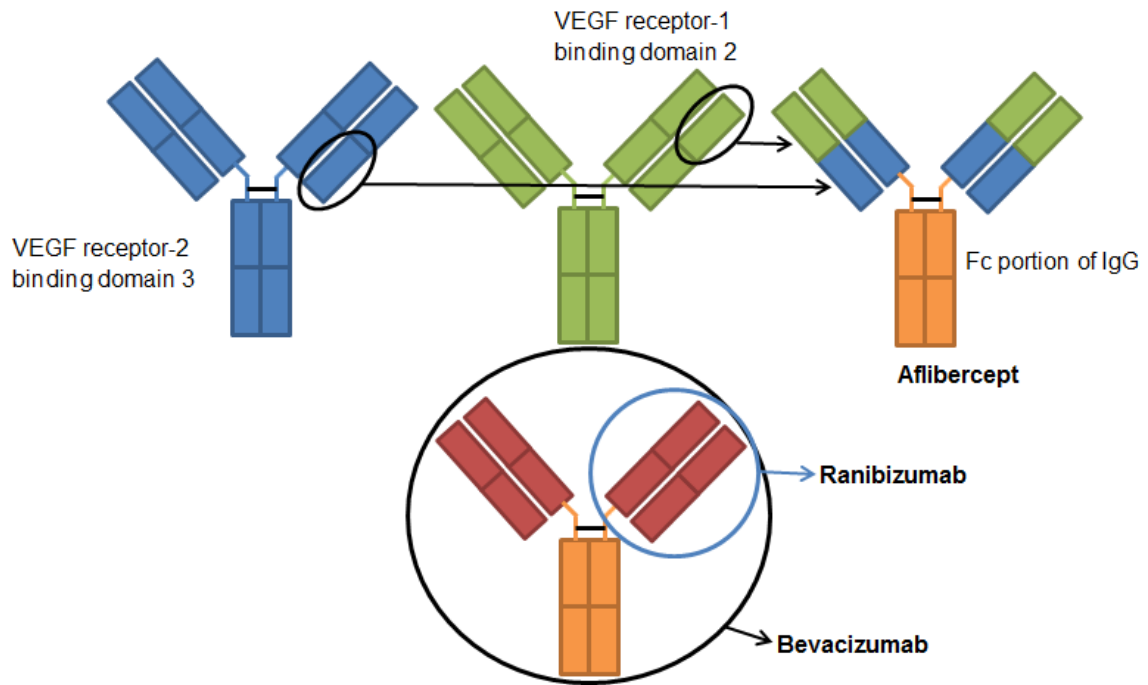
Based on the ETDRS, the current guidelines for diabetic retinopathy from the Royal College of Ophthalmologists state that patients with mild or moderate NPDR do not require treatment but require annual monitoring and are advised to maintain good glycemic control¹⁵³. Patients with severe NPDR require closer monitoring with an assessment every 6 months to detect progression of the disease to PDR. In T2DM patients with very severe NPDR, PRP can be considered if the patient is an older T2DM, monitoring of DR is difficult due to compliance or obscured view of retina, prior cataract surgery and if vision has been lost in one eye. Patients with PDR urgently require PRP to prevent vision loss¹⁰⁴. Since the primary goal of focal laser treatment is to reduce the risk of further vision loss and not to improve vision, treatment with focal laser for patients with macular edema should be considered when the macula is under the risk of being damaged even when vision is 20/20^{26, 27}.

1.5.2 Anti-VEGF Therapy

VEGF is involved in neovascularization, increased vascular permeability and the development of diabetic macular edema. Anti-VEGF treatment has become the gold standard for treating centre-involved diabetic macular edema (edema within the macula)⁵. In humans, VEGF family consists of VEGF-A, -B, -C, -D and placental growth factor (PIGF)¹⁵⁴⁻¹⁵⁶. VEGF-A is the key target in antiangiogenic therapy since it is the major driver of pathological angiogenesis and is involved in increased permeability in DME¹⁵⁴. As a result of alternative splicing and cleavage, VEGF-A is subdivided into several different isoforms^{154, 155}. The VEGF-A isoforms differ in their size and their ability to bind heparin or neuropilins, but are all active as dimers¹⁵⁴.

Over time, new forms of anti-VEGFs have been developed that have increased affinity for VEGF-A as well as an ability to inhibit a broad range of isoforms and other family members of VEGF, thus increasing the anti-angiogenic activity¹⁵⁴. The three VEGF inhibitors used clinically are bevacizumab (Avastin), ranibizumab (Lucentis) and aflibercept (Eylea) (**Figure 1.15**)⁵. Anti-VEGF treatment is administered through a transcleral intravitreal injection in the office setting. The therapy aims to decrease macular swelling through inhibiting the actions of VEGF by preventing the binding of VEGF to its receptor. As the result of inhibition, vascular permeability, endothelial cell proliferation and endothelial cell migration are significantly reduced^{154, 155}.

Figure 1.15. Anti-VEGF agents clinically used for DME treatment. Molecular differences between VEGF inhibitors. Aflibercept is a fusion protein consisting of the key VEGF-binding domains of human VEGF receptors 1 and 2. Bevacizumab is a recombinant, full-length humanized monoclonal antibody and ranibizumab is an affinity-matured antigen-binding fragment (Fab) of the antibody derived from bevacizumab.



Bevacizumab (Avastin) is a recombinant, full-length humanized monoclonal antibody that binds all known isoforms of VEGF-A¹⁵⁴. The drug is approved for the treatment of colorectal cancer but does not have Health Canada approval for intraocular use and is thus used off-label^{154, 157, 158}.

Ranibizumab (Lucentis) was developed for intravitreal administration to treat wet age-related macular degeneration and has subsequently been approved by Health Canada for DME. Ranibizumab (Lucentis) is an affinity-matured antigen-binding fragment (Fab) of the antibody derived from bevacizumab (Avastin)^{5, 154}. Ranibizumab (Lucentis) has approximately 2.5 times greater affinity for VEGF, has been shown to be more effective than Bevacizumab (Avastin) and inhibits all known VEGF-A isoforms^{159, 160}.

Aflibercept (Eylea), also known as VEGF trap, is a human recombinant fusion protein consisting of the key VEGF-binding domains of human VEGF receptors 1 and 2¹⁶⁰. Overall, VEGF trap is the second Ig domain of human VEGFR1 and the third Ig domain of human VEGFR2 expressed as an inline fusion with the constant region (Fc) of human IgG1^{154, 161}. Similar to bevacizumab and ranibizumab, aflibercept (Eylea) binds multiple isoforms of VEGF-A but is also capable of binding to VEGF-B and PlGF which are involved in vascular remodelling^{154, 162}. Aflibercept (Eylea) is a potent drug, binding to VEGF-A with much greater affinity and a faster association rate than ranibizumab (Lucentis) or bevacizumab (Avastin). In 2014, Aflibercept was approved by Health Canada for the use in wet age-related macular degeneration and DME¹⁶³.

In two masked phase 3 clinical trials named RISE and RIDE, monthly injections of ranibizumab with and without laser were compared to the gold standard at the time, focal laser, with findings that visual acuity improved compared to a sham injection over a two year time period¹⁶³. In the RISE study, 44% of patients treated with ranibizumab had an improvement in central vision by 15 letters or more compared to 18% in the control arm. In the RIDE study, 33% of patients intravitreally injected with ranibizumab at a dose of 0.3 mg and 45% of patients at a dose of 0.5 mg gained 15 letters or more, indicating that 0.5 mg should be the clinical dose administered to patients^{163, 164}. Another study, RESTORE, found that a dose of 0.5 mg of ranibizumab administered once a month for 3 months followed by an as-needed treatment thereafter significantly improved visual acuity and reduced macular thickness in patients^{163, 165}. The study helped establish the gold standard for treatment of DME patients in clinic. However, the effects of ranibizumab injections do not last in all patients and many patients require repeated injections to sustain the beneficial effects⁵.

1.6 Risks

1.6.1 Panretinal Photocoagulation

Although laser surgery is often considered painless, when the peripheral retina is being treated, it is common for the patients to experience some discomfort or pain^{26, 166}. To minimize the pain associated with the procedure, patients are given topical anesthetic and Tylenol post-treatment. To further reduce the stress, PRP is often administered in multiple sessions to minimize pain and improve patient experience.

A potential complication of PRP may be the development or digression of edema post-PRP. If the laser is too powerful, the ray may disrupt BRB and fluid can leak from the choroid into the retina. However, BRB is usually restored after 7-10 days¹⁶⁷. To reduce edema, physicians break up PRP treatment into multiple sessions to reduce the number of burns and thus the overall risk¹⁶⁶.

As a result of the treatment, PRP destroys the peripheral photoreceptors of the retina to reduce oxygen consumption, leading to a slight visual field loss. The negative impact is well established and has been documented by numerous studies showing that in the short-term, visual field depression is stable¹⁶⁶.

Some patient's post-PRP may have diminished colour vision. The finding has been reported in ETDRS and it is proposed that it may potentially lead to direct cone destruction¹⁶⁷. In order to reduce the risk of the side effect, laser treatments should be administered in multiple sessions and at minimal duration

and intensity^{166, 167}. Several patients have reported decreased night vision and transient contrast sensitivity post-PRP, although, the degree to which PRP affects either is not fully understood^{166, 168}. Studies have noted that diminished night vision and contrast sensitivity are potential side effects of severe retinopathy. As such, it is difficult to establish whether the effects experienced by the patients are due to the laser treatment or the progression of the disease¹⁶⁸.

Post-laser, choroidal effusions or retinal detachments may occur which may lead to narrowing of the anterior angle, increased IOP or angle-closure glaucoma. This risk is further minimized when treatment is administered in multiple sessions¹⁶⁶.

Post-laser, posterior segment complications, such as a vitreous detachment, may occur. The detachment may be partial or complete and may cause a retinal tear or elevate new vessels causing retinal hemorrhage to develop¹⁶⁷. The application of burns with the laser may cause a formation of epiretinal membrane. An epiretinal membrane is a thin sheet of fibrous tissue that forms over the surface of the macular area of the retina. Surgical procedure is required to treat the complication.

1.6.2 Anti-VEGF Therapy

Since anti-VEGF therapy is administered through an intravitreal injection, the main risk is the development of endophthalmitis, an intraocular infection involving the aqueous and vitreous^{33, 169}. The incidence of developing endophthalmitis is 0.019-1.6%, with the reported rate in recent studies skewing towards the lower incidence rate¹⁶⁹. The most important factor in reducing the risk of endophthalmitis is maintaining sterility through the use of topical antiseptic such as 5% povidone-iodine solution¹⁶⁹. During the injection, it is very important to avoid any contact of the sterile needle with the lashes and eyelids of the patient.

Intraocular inflammation occurs in approximately 1.4-2.9% of patients undergoing intravitreal injections of anti-VEGFs^{169, 170}. As opposed to the infectious endophthalmitis which develops over 2.55 days, acute intraocular inflammation occurs less than 1 day post-injection. Physicians recommend that patients who arrive to the clinic with the symptoms of intraocular inflammation should be treated as potentially being affected with endophthalmitis and administer intravitreal antibiotics^{169, 170}.

There is a 0-0.67% chance of developing a rhegmatogenous retinal detachment after intravitreal injection likely due to the creation of a posterior vitreous detachment or improper needle placement^{169, 171, 172}. Monitoring the technique and using smaller gauge needles is recommended to avoid the retinal detachment.

Intravitreal injections have been documented to cause acute IOP elevation that last several hours^{169, 173, 174}. Numerous theories have been proposed to address the cause of the issue. More prominent theories suggest that IOP elevation may be due to pharmacologic effects of blocking VEGF, an inflammatory mechanism, or impaired/damaged outflow due to repeated injections¹⁷⁵. Topical glaucoma eye drops may be prescribed to lower the acute IOP. Patients with sustained increases in IOP require routine monitoring.

Hemorrhages have been reported in patients post-injection. Subconjunctival hemorrhage or bleeding underneath the conjunctiva of the eye has been reported in roughly 10% of treatments, with patients receiving aspirin having a much higher frequency. In fewer cases, subretinal hemorrhages have also been reported although discontinuing anticoagulants is not advised for the patients due to risk of thromboembolic events^{169, 176-182}.

1.7 Rationale

Over the past decade, there have been increased clinical reports of diabetic patients either post-PRP or treated with anti-VEGFs developing signs of glaucoma and optic neuropathy. The issue has been publicly discussed by Dr. Marianne Edwards in her presentation, "Post-Anti-VEGF injection related glaucoma," at the 2014 Canadian Ophthalmological Society Annual Meeting. With the continued and increased use of intraocular anti-VEGF treatments and PRP being the gold standard treatment used to stabilize and control proliferative disease, numerous questions have been raised. Do these treatments increase the risk of developing glaucoma? What are the long-term effects of these treatments on the optic nerve? None of these questions have been examined in patients with DR nor have the effects of these treatments on retinal perfusion have been assessed. Controlled trials that not only look at visual acuity and central thickness but also retinal and optic structures are greatly needed to substantiate the safety and efficacy of PRP therapy and anti-VEGF drugs.

1.8 Hypothesis

The current study is based on the hypothesis that:

- A) In respect to PRP treatments, PASCAL photocoagulation is a safe and effective panretinal laser treatment that will not cause structural and functional changes in the retina and optic nerve, specifically changes to total retinal thickness, thickness of the nerve fiber layer and optic nerve cupping.

- B) Regarding anti-VEGF treatment, increased exposure to anti-VEGF will result in increased retinal cell death and morphological changes to the optic nerve.

1.9 Specific Aims

PRP Treatment

1. To use structural (OCT, HRT) and functional (visual field, visual acuity) diagnostic systems to monitor the total retinal thickness, nerve fiber layer of the macula, optic nerve and visual field to see if there are any progressive long term changes following the PASCAL laser system.
2. To quantify the amount of ischemia to PRP performed.

Anti-VEGF Treatment

3. To describe the effects of anti-VEGF injections and the frequency of injections on the structural and functional changes to the retina and optic nerve of DR patients with underlying DME using *in vivo* clinical pathological analysis.
4. To evaluate the effect of VEGF inhibition on neuronal cells in a STZ-induced diabetic rat retina by performing intravitreal anti-VEGF injections with different doses.
5. To determine if exposure to different doses of anti-VEGF alter retinal cells metabolic activity and function or induce toxicity by various colorimetric assays.

1.10 References

1. Salsali A, Nathan M. A Review of Types 1 and 2 Diabetes Mellitus and Their Treatment with Insulin. *Am J Ther* 2006;13(4):349-361.
2. Zand H, Morshedzadeh N, Naghashian F. Signaling pathways linking inflammation to insulin resistance. *Diab Met Syndr: Clin Res Rev* 2017;712:1-3.
3. Definition, Classification and Diagnosis of Diabetes, Prediabetes and Metabolic Syndrome. *Can J Diabetes* 2013;37 Suppl: S8-11.
4. Kumar V, Abbas AK, Aster JC, Perkins JA. *Robbins basic pathology*. Philadelphia, PA: Elsevier; 2013.
5. Holt RIG, Cockram CS, Flyvbjerg A, Goldstein BJ. *Textbook of diabetes*. 4th ed. Chichester, West Sussex, UK: Wiley Blackwell; 2010.
6. Björnholm M, Zierath J. Insulin signal transduction in human skeletal muscle: identifying the defects in Type II diabetes. *Biochem Soc Trans* 2005;33(2):354-357.
7. Feinglos MN, Bethel MA. *Type 2 diabetes mellitus: an evidence-based approach to practical management*. Totowa, NJ: Humana Press; 2008.
8. Gavin JR, Alberti KGMM, Davidson MB, DeFronzo RA, Drash A, Gabbe SG et al. Report of the Expert Committee on the Diagnosis and Classification of Diabetes Mellitus. *Diabetes Care* 2003;26:S5-S20.

9. Narayan KMV, Gregg EW, Fagot-Campagna A, Engelgau MM, Vinicor F. Diabetes: a common, growing, serious, costly, and potentially preventable public health problem. *Diabetes Res Clin Pract* 2000;50:S77-S84.
10. Wild S, Roglic G, Green A, Sicree R, King H. Global prevalence of diabetes: estimates for the year 2000 and projections for 2030. *Diabetes Care* 2004;27:1047-1053.
11. Global report on diabetes. World Health Organization, Geneva, 2016.
12. International Diabetes Federation. *Diabetes Atlas*, 4th ed. International Diabetes Federation, 2009. Available from: <http://www.diabetesatlas.org>. Accessed on 4 March, 2017.
13. Xue R, Gui D, Zheng L, Zhai R, Wang F, Wang N. Mechanistic Insight and Management of Diabetic Nephropathy: Recent Progress and Future Perspective. *J Diabetes Res* 2017;2017:1-7.
14. Giacco F, Brownlee M. Oxidative Stress and Diabetic Complications. *Circ Res* 2010;107(9):1058-1070.
15. Brownlee M. Biochemistry and molecular cell biology of diabetic complications. *Nature* 2001;414(6865):813-820.
16. Kennedy L, Idris I, Gazis A. *Problem solving in diabetes*. Oxford: Clinical Publishing; 2006.

17. Porte D, Sherwin RS, Baron A, Ellenberg M, Rifkin H. *Ellenberg & Rifkins diabetes mellitus*. New York: McGraw-Hill, Medical Pub. Division; 2003.
18. Colwell JA, Lopes-Virella M, Halushka PV. Pathogenesis of Atherosclerosis in Diabetes Mellitus. *Diabetes Care* 1981;4(1):121-133.
19. King RJ, Grant PJ. Diabetes and cardiovascular disease: pathophysiology of a life-threatening epidemic. *Herz* 2016;41(3):184-192.
20. Lacerda L, Opie LH, Lecour S. Influence of Tumour Necrosis Factor Alpha on the Outcome of Ischaemic Postconditioning in the Presence of Obesity and Diabetes. *Exp Diabetes Res* 2012;2012:1-10.
21. Stojceva-Taneva O, Otovic NE, Taneva B. Prevalence of Diabetes Mellitus in Patients with Chronic Kidney Disease. *Open Access Maced J Med Sci* 2016;4(1):79.
22. Jarad G, Miner JH. Update on the glomerular filtration barrier. *Curr Opin Nephrol Hypertens* 2009;18(3):226-232.
23. Ludwig S. *Practical diabetes care for Canadian health care professionals*. Toronto, Ontario: Elsevier Canada; 2014.
24. Davidson JK. *Clinical diabetes mellitus a problem oriented approach*. Stuttgart: Thieme; 2000.
25. West KM. *Epidemiology of diabetes and its vascular lesions*. New York: Elsevier; 1978.

26. Joslin EP, Kahn CR. Joslin's diabetes mellitus. Philadelphia: Lippincott Williams & Wilkins; 2005.
27. Sperling MA. Type 1 diabetes: etiology and treatment. Totowa, NJ: Humana Press; 2003.
28. Yanoff M, Duker JS. Ophthalmology. 3rd ed. St. Louis; 2009.
29. Shaw KM. Diabetic complications. S.I.: Wiley; 1996.
30. Riordan-Eva P, Cunningham ET, Vaughan D, Asbury T. Vaughan & Asburys general ophthalmology. 18th ed. New York: McGraw-Hill Medical; 2011.
31. Forrester JV, Dick AD, McMenamin PG, Lee WR. The eye basic sciences in practice. 2nd ed. New York: W.B. Saunders; 2002.
32. Times AE. Glaucoma causes Optic Nerve Cupping (atrophy) and Vision Loss. Glaucoma Information and Glaucoma Risk Factors.
<https://web.archive.org/web/20120708075410/http://www.agingeye.net/glaucoma/glaucomainformation.php>. Accessed March 20, 2017.
33. Eagle RC. Eye pathology an atlas and text. Philadelphia (Pennsylvania): Wolters Kluwer; Lippincott Williams & Wilkins; 2011.
34. Kaur C, Foulds W, Ling E. Blood–retinal barrier in hypoxic ischaemic conditions: Basic concepts, clinical features and management. Prog Retin Eye Res 2008;27(6):622-647.

35. Shakib, M., Cunha-Vaz, J.G. Studies on the permeability of the blood–retinal barrier. IV. Junctional complexes of the retinal vessels and their role on their permeability. *Exp. Eye Res* 1966;5:229-234.
36. Ashton, N. The blood–retinal barrier and vaso-glial relationships in retinal disease. *Trans. Ophthal. Soc. UK* 1965;85:199-230.
37. Cunha-Vaz JG. The blood-retinal barriers. *Doc Ophthalmol* 1976;41(2):287-327.
38. Sims DE. Recent advances in pericyte biology-implications for health and disease. *Can J Cardiol* 1991;7(10):431-443.
39. Shepro D, Morel NM. Pericyte physiology. *FASEB J* 1993;7(11):1031-1038.
40. Wallow IH, Burnside B. Actin filaments in retinal pericytes and endothelial cells. *Invest Ophthalmol Vis Sci* 1980;19(12):1433-1441.
41. Bandopadhyay R, Orte C, Lawrenson JG, Reid AR, De Silva S, Allt G. Contractile proteins in pericytes at the blood–brain and blood–retinal barriers. *J Neurocytol* 2001;30(1):35-44.
42. Hirschi KK, Damore PA. Pericytes in the microvasculature. *Cardiovasc Res* 1996;32(4):687-698.
43. Tout S, Chan-Ling T, Holländer H, Stone J. The role of müller cells in the formation of the blood-retinal barrier. *Neuroscience* 1993;55(1):291-301.

44. Distler C, Dreher Z. Glia Cells of the Monkey Retina—II. Müller Cells. *Vision Res* 1996;36(16):2381-2394.
45. Reichenbach A, Wurm A, Pannicke T, Iandiev I, Wiedemann P, Bringmann A. Müller cells as players in retinal degeneration and edema. *Graefes Arch Clin Exp Ophthalmol* 2007;245(5):627-636.
46. Bringmann A, Skatchkov SN, Pannicke T, et al. Müller glial cells in anuran retina. *Microsc Res Tech* 2000;50(5):384-393.
47. Watanabe T, Raff MC. Retinal astrocytes are immigrants from the optic nerve. *Nature* 1988;332(6167):834-837.
48. Schnitzer J. Retinal astrocytes: their restriction to vascularized parts of the mammalian retina. *Neurosci Lett* 1987;78(1):29-34.
49. Zhang Y, Stone J. Role of astrocytes in the control of developing retinal vessels. *Invest Ophthalmol Vis Sci* 1997;38(9):1653–1666.
50. Gardner TW. Histamine, ZO-1 and increased blood-retinal barrier permeability in diabetic retinopathy. *Trans Am Ophthalmol Soc* 1995;93:583–621.
51. Lechner J, O'Leary OE, Stitt AW. The pathology associated with diabetic retinopathy. *Vision Res*. 2017.
52. Klein R, Klein BEK, Moss SE, Davis MD, DeMets DL. The Wisconsin Epidemiologic Study of Diabetic Retinopathy. II Prevalence and risk of

- diabetic retinopathy when age at diagnosis is less than 30 years. Arch Ophthalmol 1984;102:520-526.
53. Klein R, Klein BE, Moss SE, Davis MD, DeMets DL. The Wisconsin Epidemiologic Study of Diabetic Retinopathy. III Prevalence and risk of diabetic retinopathy when age at diagnosis is less than 30 years. Arch Ophthalmol 1984;102:527-532.
 54. Klein R, Retinopathy in a population-based study. Trans Am Ophthalmol Soc 1992;90:561.
 55. Dobree JH. Simple diabetic retinopathy. Evolution of the lesions and therapeutic considerations. Br J Ophthalmol 1970;54:1.
 56. Engerman RL. Animal models of diabetic retinopathy. Trans Am Acad Ophthalmol Otolaryngol 1976;81:710.
 57. Nelson RG, Wolfe JA, Horton MB. Proliferative retinopathy in Type 2. Incidence and risk factors in Pima Indians. Diabetes 1989;38:435.
 58. Lee ET, Lee VS, Lu M, et al. Development of proliferative retinopathy in Type 2, a follow-up study of American Indians in Oklahoma. Diabetes 1992;41:359.
 59. Gabbay KH. The sorbitol pathway and the complications of diabetes. N Engl J Med 1973;288:831-836.

60. Brownlee M. Glycation and diabetic complications. *Diabetes* 1994;43:836-841.
61. Lee TS, Saltsman KA, Ohashi H, King GL. Activation of protein kinase C by elevation of glucose concentration: proposal for a mechanism in the development of diabetic complications. *Proc Natl Acad Sci USA* 1989;86:5141-5145.
62. Little HL. The role of abnormal hemorrheodynamics in the pathogenesis of diabetic retinopathy. *Trans Am Ophthalmol Soc* 1976;74:574.
63. Cogan DG. Retinal vascular patterns IV. Diabetic retinopathy. *Arch Ophthalmol* 1961;66(3):366-378.
64. Kuwabara T, Cogan DG. Retinal vascular patterns VI. Mural cells of the retinal capillaries. *Arch Ophthalmol* 1963;69(4):492-502.
65. Vlassara H, Brownlee M, Cerami A. Nonenzymatic glycosylation: role in the pathogenesis of diabetic complications. *Clin Chem* 1986;32(10 Suppl):B37-B41.
66. Robison WG JR., Kador PF, Konoshita JH. Retinal capillaries: Basement membrane thickening prevented with aldose reductase inhibitor. *Science* 1983;221:1177.

67. Robison WG JR., Nagata M, Laver N, Hohman TC, Kinoshita JH. Diabetic-like retinopathy in rats prevented with an aldose reductase inhibitor. *Invest Ophthalmol Vis Sci* 1989;30:2285.
68. Sorbinil Retinopathy Trial research Group. A randomized trial of sorbinil, an aldose reductase inhibitor in diabetic retinopathy. *Arch Ophthalmol* 1990;108:1234-1244.
69. Jousseaume AM, Fauser S, Krohne TU, Lemmen KD, Lang GE, Kirchof B. Diabetic retinopathy: Pathophysiology and therapy of hypoxia-induced inflammation. *Ophthalmologie* 2003;100(5):363–370.
70. De Venecia G, Dries M, Engerman R. Chemopathologic correlations in diabetic retinopathy 1. Histology and fluorescein angiography of microaneurysms. *Arch Ophthalmol* 1976;94(10):1766–1773.
71. Peterson KP, Pavlovich JG, Goldstein D, Little R, England J, Peterson CM. What is hemoglobin A1c? An analysis of glycosylated hemoglobins by electrospray ionization mass spectrometry. *Clin Chem* 1998;44(9):1951-1958.
72. Jutte A, Deufrains A, Dietze U. Microcirculation disturbances at the onset of diabetic retinopathy. New therapeutic procedures? *Klin Monatsbl Augenheilkd* 1980;177(1):1-6.

73. Lowe GD, Lowe JM, Drummond MM, Reith S, Wylie J, Belch J, et al. Blood viscosity in young male diabetics with and without retinopathy. *Diabetologia* 1980;18(5):359-363.
74. Melli M, Poggi M, Codeluppi L, Buraldi P, Torlai F, Peduzzi M. Blood viscosity and erythrocyte deformability in diabetic retinopathy. *Ric Clin Lab* 1983;13(Suppl3):371-374.
75. Peduzzi M, Melli M, Fonda S, Codeluppi L, Guerrieri F. Comparative evaluation of blood viscosity in diabetic retinopathy. *Int Ophthalmol* 1984;7(1):15-19.
76. Miyamoto K, Khosrof S, Bursell S-E, et al. Prevention of leukostasis and vascular leakage in streptozotocin-induced diabetic retinopathy via intercellular adhesion molecule-1 inhibition. *Proc Natl Acad Sci USA* 1999;96(19):10836-10841.
77. Jousseaume AM, Murata T, Tsujikawa A, Kirchhof B, Bursell S-E, Adamis AP. Leukocyte-Mediated Endothelial Cell Injury and Death in the Diabetic Retina. *Am J Pathol* 2001;158(1):147-152.
78. Jousseaume AM, Poulaki V, Qin W, Kirchhof B, Mitsuades N, Wiegand SJ, et al. Retinal Vascular Endothelial Growth Factor Induces Intercellular Adhesion Molecule-1 and Endothelial Nitric Oxide Synthase Expression and Initiates Early Diabetic Retinal Leukocyte Adhesion in Vivo. *Am J Pathol* 2002;160(2):501-509.

79. Kim I, Moon S-O, Kim SH, Kim HJ, Koh YS, Koh GY. Vascular Endothelial Growth Factor Expression of Intercellular Adhesion Molecule 1 (ICAM-1), Vascular Cell Adhesion Molecule 1 (VCAM-1), and E-selectin through Nuclear Factor- κ B Activation in Endothelial Cells. *J Biol Chem* 2000;276(10):7614-7620.
80. Bertram B, Wolf S, Kaufhold F, Jung F, Kiesewetter H, Reim M. Rheologic findings in patients with diabetic retinopathy. *Fortschr Ophthalmol* 1991;88(4):321-325.
81. Pe'er J, Shweiki D, Itin A, Hemo I, Gnessin H, Keshet E. Hypoxia-induced expression of vascular endothelial growth factor by retinal cells is a common factor in neovascularizing ocular diseases. *Lab Invest* 1995;72(6):638-645.
82. Kuroki M, Voest EE, Amano S, Beerepoot LV, Takashima S, Tolentino M et al. Reactive oxygen intermediates increase vascular endothelial growth factor expression in vitro and in vivo. *J Clin Invest* 1996;98(7):1667-1675.
83. Chua CC, Hamdy RC, Chua BH. Upregulation of vascular endothelial growth factor by H₂O₂ in rat heart endothelial cells. *Free Radic Biol Med* 1998;25(8):891-897.
84. Dobrogowska DH, Lossinsky AS, Tarnawski M, Vorbrodt AW. Increased blood-brain barrier permeability and endothelial abnormalities induced by vascular endothelial growth factor. *J. Neurocytol* 1998;27(3):163-173.

85. Croll S, Ransohoff RM, Cai N, Zhang Q, Martin FJ, Wei T, et al. VEGF-mediated inflammation precedes angiogenesis in adult brain. *Exp Neurol* 2004;187(2):388-402.
86. Kaur C, Sivakumar V, Foulds WS. Early Response of Neurons and Glial Cells to Hypoxia in the Retina. *Invest Ophthalmol* 2006;47(3):1126-1141.
87. Shibuya M. Vascular endothelial growth factor receptor-1 (VEGFR-1/Flt-1): a dual regulator for angiogenesis. *Angiogenesis* 2006;9(4):225-230.
88. Spoerri PE, Afzal A, Li Calzi S, Shaw LC, Cai J, Pan H et al. Effects of VEGFR-1, VEGFR-2, and IGF-IR hammerhead ribozymes on glucose-mediated tight junction expression in cultured human retinal endothelial cells. *Mol Vis* 2006;12:32-42.
89. Roberts WG, Palade GE. Increased microvascular permeability and endothelial fenestration induced by vascular endothelial growth factor. *J Cell Sci* 1995;108(Pt6): 2369-2379.
90. Roberts WG, Palade GE. Neovasculature induced by vascular endothelial growth factor is fenestrated. *Cancer Res* 1997;57(4):765-772.
91. Esser S, Wolburg K, Wolburg H, Breier G, Kurzchalia T, Risau W. Vascular Endothelial Growth Factor Induces Endothelial Fenestrations In Vitro. *J Cell Biol* 1998;140(4):947-959.

92. Esser S, Lampugnani MG, Corada M, Dejana E, Risau W. Vascular endothelial growth factor induces VE-cadherin tyrosine phosphorylation in endothelial cells. *J Cell Sci* 1998;111(Pt13):1853-1865.
93. Kevil CG, Payne DK, Mire E, Alexander JS. Vascular Permeability Factor/Vascular Endothelial Cell Growth Factor-mediated Permeability Occurs through Disorganization of Endothelial Junctional Proteins. *J Biol Chem* 1998;273(24):15099-15103.
94. Mark KS. Nitric oxide mediates hypoxia-induced changes in paracellular permeability of cerebral microvasculature. *Am J Physiol Heart Circ Physiol* 2003;286(1).
95. Stefánsson E. The Mechanism of Retinal Photocoagulation – How Does the Laser Work? *European Ophthalmic Review* 2009;02(01):76-79.
96. Mayhan WG. VEGF increases permeability of the blood–brain barrier via a nitric oxide synthase/cGMP-dependent pathway. *Am J Physiol* 1999;276(5Pt1):C1148–C1153.
97. Lu M, Perez VL, Ma N, Miyamoto K, Peng HB, Liao JK et al. VEGF increases retinal vascular ICAM-1 expression in vivo. *Invest Ophthalmol Vis Sci* 1999;40(8):1808-1812.
98. Min J-K, Kim Y-M, Kim SW, Kwon M-C, Kong Y-Y, Hwang IK et al. TNF-Related Activation-Induced Cytokine Enhances Leukocyte Adhesiveness: Induction of ICAM-1 and VCAM-1 via TNF Receptor-Associated Factor

- and Protein Kinase C-Dependent NF- B Activation in Endothelial Cells. *J Immunol* 2005;175(1):531-540.
99. Proescholdt MA, Heiss JD, Walbridge S, Mühlhauser J, Capogrossi MC, Oldfield EH et al. Vascular Endothelial Growth Factor (VEGF) Modulates Vascular Permeability and Inflammation in Rat Brain. *J Neuropathol Exp Neurol* 1999;58(6):613-627.
100. Qaum T, Xu T, Jousen AM, Clemens MW, Qin W, Miyamoto K et al. VEGF initiated Blood-retinal barrier breakdown in early diabetes. *Invest Ophthalmol Vis Sci* 2001;42(10):2408-2413.
101. Zhang ZG, Zhang L, Tsang W, Soltanian-Zadeh H, Morris D, Zhang R et al. Correlation of VEGF and Angiopoietin Expression with Disruption of Blood–Brain Barrier and Angiogenesis after Focal Cerebral Ischemia. *J Cereb Blood Flow Metab* 2002;22(4):379-392.
102. Kaur C, Sivakumar V, Yong Z, Lu J, Foulds W, Ling E. Blood–retinal barrier disruption and ultrastructural changes in the hypoxic retina in adult rats: the beneficial effect of melatonin administration. *J Pathol* 2007;212(4):429-439.
103. Kerr, C. An investigative study of endothelial cells and proliferation as related to diabetic retinopathy. PhD Thesis, University of Glasgow, 1986.
104. Royle P, Mistry H, Auguste P, Shyangdan D, Freeman K, Lois N. Pan-retinal photocoagulation and other forms of laser treatment and drug

- therapies for non-proliferative diabetic retinopathy: systematic review and economic evaluation. *Health Technol Assess.* 2015;19(51):1-248.
105. Garner A. Histopathology of diabetic retinopathy in man. *Eye* 1993;7:218-222.
 106. MacCuish AC. Early detection and screening for diabetic retinopathy. *Eye* 1993;7:254-259.
 107. Ulbig MRW, Hamilton AMP. Factors influencing the natural history of diabetic retinopathy. *Eye* 1993;7:242-249.
 108. Miller SM (Ed.). *Vascular retinopathies: the management of diabetic retinopathy.* *Clinical Ophthalmology* 1987;1:238-243.
 109. Cotlier E, Weinreb R. Growth factors in retinal diseases: proliferative vitreo- retinopathy, proliferative diabetic retinopathy, and retinal degeneration. *Survey Ophthalmol* 1992;36:373-384.
 110. The Diabetic Retinopathy Study Research Group. Preliminary report on effects of photocoagulation therapy. *Am J Ophthalmol* 1976;81:383-396.
 111. The Diabetic Retinopathy Study Research Group. Photocoagulation treatment of proliferative diabetic retinopathy: the second report of Diabetic Retinopathy Study findings. *Ophthalmology* 1978;85:82-106.

112. The Diabetic Retinopathy Study Research Group. Four risk factors for severe visual loss in diabetic retinopathy: the third report from Diabetic Retinopathy Study. *Arch Ophthalmol* 1979;97:654-655.
113. The Diabetic Retinopathy Study Research Group. Photocoagulation treatment of proliferative diabetic retinopathy: a short report of long range results. Diabetic Retinopathy Study (DRS) report no. 4. Amsterdam: Excerpta Medica, 1980.
114. Diabetic Retinopathy Study Research Group. Photocoagulation treatment of proliferative diabetic retinopathy: relationship of adverse treatment effects to retinopathy severity: Diabetic Retinopathy Study report no. 5. *Dev Ophthalmol* 1981;2:248-261.
115. Diabetic Retinopathy Study Report Research Group. Report 6: design, methods, and baseline results. *Invest Ophthalmol Vis Sci* 1981;21:149-209.
116. Diabetic Retinopathy Study Research Group. Report 7. A modification of the Airlie House classification of diabetic retinopathy. *Invest Ophthalmol Vis Sci* 1981;21:210-226.
117. The Diabetic Retinopathy Study Research Group. Photocoagulation treatment of proliferative diabetic retinopathy: clinical application of Diabetic Retinopathy Study (DRS) findings, DRS report no. 8. *Ophthalmology* 1981;88:583-600.

118. Diabetic Retinopathy Study Research Group. Report 9: assessing possible late treatment effects in stopping clinical trials early: a case study by F Ederer. MJ Podgor. *Controlled Clin Trials* 1984;5:373-381.
119. Rand Li, Prud'homme GJ, Ederer F, Canner PL, Diabetic Retinopathy Research Group. Factors influencing the development of visual loss in advanced diabetic retinopathy: Diabetic Retinopathy Study report no. 10. *Invest Ophthalmol Vis Sci* 1985;26:983-991.
120. Kaufman SC, Ferris FL III, Swartz M, Diabetic Retinopathy Study Research Group. Intraocular pressure following panretinal photocoagulation for diabetic retinopathy: Diabetic Retinopathy report no. 11. *Arch Ophthalmol* 1987;105:807-809.
121. Ferris FL III, Podgor MJ, Davis MD, the DiabRetinopathy Study Research Group. Macular edema in diabetic retinopathy study patients: Diabetic Retinopathy Study report number 12. *Ophthalmology* 1987;94:754-760.
122. Kaufman SC, Ferris FL III, et al, the DRS Research Group. Factors associated with visual outcome after photocoagulation for diabetic retinopathy: Diabetic Retinopathy Study report #13. *Invest Ophthalmol Vis Sci* 1989;30:233-28.
123. The Diabetic Retinopathy Study Research Group. Indications for photocoagulation treatment of diabetic retinopathy: Diabetic Retinopathy Study report no. 14. *Int Ophthalmol Clin* 1987;27:239-253.

124. Early Treatment Diabetic Retinopathy Study Research Group.
Photocoagulation for diabetic macular edema; Early Treatment Diabetic Retinopathy Study report no. 1. Arch Ophthalmol 1985;103:1796-1806.
125. Early Treatment Diabetic Retinopathy Study Research Group. Treatment techniques and clinical guidelines for photocoagulation of diabetic macular edema: Early Treatment Diabetic Retinopathy Study report no. 2. Ophthalmology 1987;94:761-774.
126. The Early Treatment Diabetic Retinopathy Study Research Group.
Techniques for scatter and local photocoagulation treatment of diabetic retinopathy: Early Treatment Diabetic retinopathy Study report no.3. Int Ophthalmol Clin 1987;27:254-264.
127. The Early Treatment Diabetic Retinopathy Study Research Group.
Photocoagulation for diabetic macular edema: Early Treatment Diabetic Retinopathy Study report no. 4. Int ophthalmol Clin 1987;27:265-272.
128. The Early Treatment Diabetic Retinopathy Study Research Group. Case reports to accompany Early Treatment Diabetic Retinopathy Study reports 3 and 4. Int Ophthalmol Clin 1987;27:273-333.
129. Kinyoun J, Barton F, Fisher M, et al, the ETDRS Research group.
Detection of diabetic macular edema: ophthalmoscopy versus photography-Early treatment Diabetic Retinopathy Study report no. 5. Ophthalmology 1989;96:746-751.

130. Prior MJ, Prout T, Miller D, et al. C-peptide and the classification of diabetes patients in the Early Treatment Diabetic Retinopathy Study. Report no.6. The ETDRS Research Group. Ann Epidemiol 1993;3:9-17.
131. Early Treatment Diabetic Retinopathy Study Research Group. Early Treatment Diabetic Retinopathy Study design and baseline patient characteristics: ETDRS report no.7. Ophthalmology 1991;98(Suppl 5):741-756.
132. Early Treatment Diabetic Retinopathy Study Research Group. Effects of aspirin treatment on diabetic retinopathy: ETDRS report no.8. Ophthalmology 1991;98(Suppl 5):757-765.
133. Early Treatment Diabetic Retinopathy Study Research Group. Early photocoagulation for diabetic retinopathy: ETDRS report no.9. Ophthalmology 1991;98(Suppl 5):766-785.
134. Early Treatment Diabetic Retinopathy Study Research Group. Grading diabetic retinopathy from stereoscopic color fundus photographs-an extension of the modified Airlie House classification: ETDRS report no.10. Ophthalmology 1991;98(Suppl 5):786-806.
135. Early Treatment Diabetic Retinopathy Study Research Group. Classification of diabetic retinopathy from fluorescein angiograms: ETDRS report no. 11. Ophthalmology 1991;98(Suppl 5):807-822.

136. Early Treatment Diabetic Retinopathy Study Research Group. Fundus photographic risk factors for progression of diabetic retinopathy: ETDRS report no.12. Ophthalmology 1991;98(Suppl 5):823-833.
137. Early Treatment Diabetic Retinopathy Study Research Group. Fluorescein angiographic risk factors for progression of diabetic retinopathy: ETDRS report no. 13. Ophthalmology 1991;98(Suppl 5):834-840.
138. Early Treatment Diabetic Retinopathy Study Research Group. Aspirin effects on mortality and morbidity in patients with diabetes mellitus. ETDRS report no. 14. JAMA 1992;268:1292-1300.
139. Early Treatment Diabetic Retinopathy Study Research Group. Aspirin effects on the development of cataracts in patients with diabetes mellitus. ETDRS report no. 16. Arch Ophthalmol 1992;110:339-342.
140. Flynn HW, Chew EY, Simons BD, et al. Early Treatment Diabetic Retinopathy Study Research Group. Pars plana vitrectomy in the early treatment diabetic retinopathy study. ETDRS report no. 17. Ophthalmology 1992;99:1351-1357.
141. Davis MD, Fisher MR, Gangnon RE, et al. Risk factors for high-risk proliferative diabetic retinopathy and severe visual loss: Early Treatment Diabetic Retinopathy Study report #18. Invest Ophthalmol Vis Sci 1998;39:233-252.

142. Early Treatment Diabetic Retinopathy Study Research Group. Focal photocoagulation treatment of diabetic macular edema: relationship of treatment effect to fluorescein angiographic and other retinal characteristics at baseline. ETDRS report no. 19. Arch Ophthalmol 1995;113:1144-1155.
143. Chew EY, Klein ML, Murphy RP, et al. Effects of aspirin on vitreous/preretinal hemorrhage in patients with diabetes mellitus. Early Treatment Diabetic Retinopathy Study report no. 20. Arch Ophthalmol 1995;13:52-55.
144. Chew EY, Klein ML, Ferris FL 3rd, et al. Association of elevated serum lipid levels with retinal hard exudates in diabetic retinopathy. Early Treatment Diabetic Retinopathy Study (ETDRS) report no. 22. Arch Ophthalmol 1996;114:1079-1084.
145. Fong DS, Segal PP, Myers F, et al. Subretinal fibrosis in diabetic macular edema: Early Treatment Diabetic Retinopathy research Group. ETDRS report 23. Arch Ophthalmol 1997;115:873-877.
146. Fong DS, Ferris FL 3rd, Davis MD, et al. Causes of severe visual loss in the early treatment diabetic retinopathy study: ETDRS report no. 24. Early Treatment Diabetic Retinopathy Study Research Group. Am J Ophthalmol 1999;127:137-141.

147. Molnar I, Poitry S, Tsacopoulos M, Gilodi N, Leuenberger PM. Effect of laser photocoagulation on oxygenation of the retina in miniature pigs. *Invest Ophthalmol Vis Sci* 1985;26:1410-1414.
148. Stefánsson E, Hatchell DL, Fisher BL, Sutherland FS, Machemer R. Panretinal photocoagulation and retinal oxygenation in normal and diabetic cats. *Am J Ophthalmol* 1986;101:657-664.
149. Stefansson E, Landers MB III, Wolbarsht ML. Increased retinal oxygen supply following pan-retinal photocoagulation and vitrectomy and lensectomy. *Trans Am Ophthalmol Soc* 1981;79:307-34.
150. Stefánsson E, Machemer R, de Juan E Jr, McCuen BW 2nd, Peterson J. Retinal oxygenation and laser treatment in patients with diabetic retinopathy. *Am J Ophthalmol* 1992;113:36-8.
151. Landers MB III, Stefansson E, Wolbarsht ML. Panretinal photocoagulation and retinal oxygenation. *Retina* 1982;2:167-75.
152. Pournaras CJ. Retinal oxygen distribution. Its role in the physiopathology of vasoproliferative microangiopathies. *Retina* 1995;15:332-47.
153. Hooper P, Boucher MC, Cruess A, Dawson KG, Delpero W, Greve M et al. Canadian Ophthalmological Society evidence-based clinical practice guidelines for the management of diabetic retinopathy. *Can J Ophthalmol* 2012;47(2).

154. Papadopoulos N, Martin J, Ruan Q, Rafique A, Rosconi MP, Shi E et al. Binding and neutralization of vascular endothelial growth factor (VEGF) and related ligands by VEGF Trap, ranibizumab and bevacizumab. *Angiogenesis* 2012;15(2):171-185.
155. Ferrara N, Gerber HP, LeCouter J. The biology of VEGF and its receptors. *Nat Med* 2003;9:669-676.
156. Takahashi H, Shibuya M. The vascular endothelial growth factor (VEGF)/VEGF receptor system and its role under physiological and pathological conditions. *Clin Sci (Lond)* 2005;109(3):227-241.
157. Grothey A, Galanis E. Targeting angiogenesis: progress with anti-VEGF treatment with large molecules. *Nat Rev Clin Oncol* 2009;6(9):507-518.
158. Ferrara N, Hillan KJ, Gerber HP, Novotny W. Discovery and development of bevacizumab, an anti-VEGF antibody for treating cancer. *Nat Rev Drug Discov* 2004;3(5):391-400.
159. Raftery J, Clegg A, Jones J, Tan SC, Lotery A. Ranibizumab (Lucentis) versus bevacizumab (Avastin): modelling cost effectiveness. *Br J Ophthalmol* 2007;91(9):1244-1246.
160. Osaadon P, Fagan XJ, Lifshitz T, Levy J. A review of anti-VEGF agents for proliferative diabetic retinopathy. *Eye (Lond)* 2014;28(5):510-520.

161. Holash J, Davis S, Papadopoulos N, Croll SD, Ho L, Russell M et al. VEGF-Trap: a VEGF blocker with potent antitumor effects. Proc Natl Acad Sci USA 2002;99(17):11393-11398.
162. Rudge JS, Holash J, Hylton D, Russell M, Jiang S, Leidich R et al. VEGF Trap complex formation measures production rates of VEGF, providing a biomarker for predicting efficacious angiogenic blockade. Proc Natl Acad Sci USA 2007;104(47):18363-18370.
163. Boyd SR, Advani A, Altomare F, Stockl F. Retinopathy. Can J Diabetes 2013;37:S137-S141.
164. Nguyen QD, Brown DM, Marcus DM, Boyer DS, Patel S, Feiner L et al. Ranibizumab for diabetic macular edema: results from 2 phase iii randomized trials: RISE and RIDE. Ophthalmology 2012;119(4):789-801.
165. Mitchell P, Bandello F, Schmidt-Erfurth U, Lang GE, Massin P, Schlingemann RO, et al. The RESTORE study: ranibizumab monotherapy or combined with laser versus laser monotherapy for diabetic macular edema. Ophthalmology 2011;118(4):615-625.
166. Deschler EK, Sun JK, Silva PS. Side-Effects and Complications of Laser Treatment in Diabetic Retinal Disease. Semin Ophthalmol 2014;29(5-6):290-300.

167. Side-effects and complications of laser. Side-effects and complications of laser. <http://homepages.abdn.ac.uk/opt065/Lasersideeffects.htm>. Accessed May 7, 2017.
168. Fong DS, Girach A, Boney A. Visual side effects of successful scatter laser photocoagulation surgery for proliferative diabetic retinopathy: A literature review. *Retina* 2007;27(7):816-824.
169. Falavarjani KG, Nguyen QD. Adverse events and complications associated with intravitreal injection of anti-VEGF agents: a review of literature. *Eye (Lond)* 2013;27(7):787-794.
170. Tolentino M. Systemic and ocular safety of intravitreal anti-VEGF therapies for ocular neovascular disease. *Surv Ophthalmol* 2011;56:95-113.
171. Irigoyen C, Ziahosseini K, Morphis G, Stappler T, Heimann H. Endophthalmitis following intravitreal injections. *Graefes Arch Clin Exp Ophthalmol* 2012;250(4):499-505.
172. Meyer CH, Michels S, Rodrigues EB, Hager A, Mennel S, Schmidt JC et al. Incidence of rhegmatogenous retinal detachments after intravitreal antivascular endothelial factor injections. *Acta Ophthalmol* 2011;89:70-75.
173. Bakri SJ, Pulido JS, McCannel CA, Hodge DO, Diehl N, Hillemeier J. Immediate intraocular pressure changes following intravitreal injections of triamcinolone, pegaptanib, and bevacizumab. *Eye* 2009;23(1):181-185.

174. Gismondi M, Salati C, Salvetat ML, Zeppieri M, Brusini P. Short-term effect of intravitreal injection of Ranibizumab (Lucentis) on intraocular pressure. *J Glaucoma* 2009;18(9):658–661.
175. Hoang QV, Mendonca LS, Della Torre KE, Jung JJ, Tsuang AJ, Freund KB. Effect on intraocular pressure in patients receiving unilateral intravitreal anti-vascular endothelial growth factor injections. *Ophthalmology* 2012;119:321-326.
176. Ladas ID, Karagiannis DA, Rouvas AA, Kotsolis AI, Liotsou A, Vergados I. Safety of repeat intravitreal injections of bevacizumab versus ranibizumab: our experience after 2,000 injections. *Retina* 2009;29(3):313-318.
177. Brouzas D, Koutsandrea C, Moschos M, Papadimitriou S, Ladas I, Apostolopoulos M. Massive choroidal hemorrhage after intravitreal administration of bevacizumab (Avastin) for AMD followed by contralateral sympathetic ophthalmia. *Clin Ophthalmol* 2009;3:457-459.
178. Karagiannis DA, Mitropoulos P, Ladas ID. Large subretinal haemorrhage following change from intravitreal bevacizumab to ranibizumab. *Ophthalmologica* 2009;223(4):279-282.
179. Modarres M, Naseripour M, Falavarjani KG, Nikeghbali A, Hashemi M, Parvaresh MM. Intravitreal injection of 2.5 mg vs 1.25 mg bevacizumab (avastin) for treatment of CNV associated with AMD. *Retina* 2009;29:319-324.

180. Loukopoulos V, Meier C, Gerding H. Hemorrhagic complications after intravitreal injections of ranibizumab in patients under coumarin-type anticoagulation. *Klin Monbl Augenheilkd* 2010;227(4):289-291.
181. Mason 3rd JO, Frederick PA, Neimkin MG, White Jr MF, Feist RM, Thomley ML et al. Incidence of hemorrhagic complications after intravitreal bevacizumab (avastin) or ranibizumab (lucentis) injections on systemically anticoagulated patients. *Retina* 2010;30(9):1386-1389.
182. Gordon MS, Cunningham D. Managing patients treated with bevacizumab combination therapy. *Oncology* 2005;69(Suppl3):25-33.

Chapter 2

2 The structural and functional changes to the retina and optic nerve following panretinal photocoagulation over a 2-year time period¹

The chapter addresses specific objectives outlined in aims 1 and 2:

1. To use structural (OCT, HRT) and functional (visual field, visual acuity) diagnostic systems to monitor the total retinal thickness, nerve fiber layer of the macula, optic nerve and visual field to see if there are any progressive long term changes following the PASCAL laser system.
2. To quantify the amount of ischemia to PRP performed.

¹Parts of this work have been published in the following manuscript:

- Filek R, Hooper P, Sheidow T, Gonder J, Varma D, Heckler L, Hodge W, Chakrabarti S, Hutnik CML. Structural and functional changes to the retina and optic nerve following panretinal photocoagulation over a 2-year time period. *Eye (Lond)*. 2017 Apr 28. doi: 10.1038/eye.2017.66. [Epub ahead of print]. Eye applies the *License to Publish* to works. Under section 2 of this license, authors retain ownership of the copyright for their content. No permission is required from the publishers.

2.1 Introduction

Diabetic retinopathy (DR) is the leading cause of blindness among working-aged adults that affects more than 141 million adults worldwide^{1, 2}. Over the past 40 years, epidemiological studies and clinical trials have demonstrated that timely laser photocoagulation treatment can prevent vision loss in DR patients. Panretinal photocoagulation (PRP) has been shown to stabilize and control the proliferative disease and, since the Diabetic Retinopathy Study, has become the gold standard treatment^{3, 4}. Whereas there are reports of PRP resulting in visual field changes, few studies have looked at the impact the procedure has on the optic nerve, especially the long-term effects⁵. The risk of a concurrent diagnosis of treated DR and normal tension glaucoma exists without adequate awareness of the potential impact of PRP on the appearance of the optic nerve head. While PRP has revolutionized how DR patients are managed, the long-term structural and functional effects of PRP on the retina and optic nerve remain to be determined.

Several studies have looked at the short-term effects of PRP on the retina. The Manchester Pascal Study Report 3 expanded on these projects by looking at the short-term effects of Pascal laser on the retinal nerve fiber layer over the course of 12 weeks^{6, 7}. A major limitation of the previous studies has been the relatively short-term evaluation of the effects. Furthermore, despite the evident need, no study has looked at the long-term consequences of the laser treatment

on the retina or established whether the observed changes were due to the laser or progression of diabetes.

The purpose of the following study is to evaluate retinal and optic nerve changes using structural and functional diagnostic tests at 6, 12, and 24 months in DR patients post laser treatment. This is the first comprehensive study to investigate the long-term structural and functional effects of PRP on the retina and optic nerve that involves analysis of macular thickness, the RNFL, mean perfusion, vertical C/D ratio, cup volume, stereo photos, IOP, visual acuity and visual fields.

2.2 Methods

The following was a prospective study conducted at the Ivey Eye Institute, a tertiary care academic center in London, Ontario, Canada. The study complies with Declaration of Helsinki and was approved by Health Sciences Research Ethics Board of Western University. Prospective, treatment-naïve patients over the age of 18 years who had severe non-proliferative and proliferative DR, according to the ETDRS guidelines, and required PRP were recruited into the study. Participants were excluded from the study if they had advanced lens opacity or cataract that could affect diagnostic testing, history of glaucoma or any other disorder of the optic nerve (optic neuropathy, neuritis, uveitis or retinal degeneration), presence of macular edema (central macular thickness $>300\ \mu\text{m}$) and prior retinal treatment (PRP, focal laser or surgery within 6 months of participation). All participants provided informed consent. From this group, eight patients who did not receive laser treatment, as the diabetic retinopathy was at the severe non-proliferative state, were chosen as the control. Participants were evaluated at baseline (pre-laser), 6, 12, and 24 months post-laser. During each study visit, participants underwent optical coherence tomography (OCT), Heidelberg Retinal Tomography (HRT), visual field (VF) and intravenous fluorescein angiography (IVFA) testing as well as a standard ophthalmic exam which included best-corrected Snellen visual acuity (BCVA), intraocular measurement using Goldmann applanation tonometry, and slit lamp examination. Humphrey 24-2 SITA visual field testing was performed with undilated eyes.

2.2.1 Optical Coherence Tomography

Macular thickness, optic disc cube and HD 5 line raster images were obtained using OCT (Cirrus HD-OCT 4000, Carl Zeiss Meditech, Dublin, California). The principles and the protocol have been previously described in detail^{7, 8, 9, 10}. OCT tests were taken at baseline, 6, 12, and 24 months post-laser. Each scan was repeated 3 times to ensure collection of the highest signal strength.

Analysis of the macula were performed using 6 x 6 mm scans with 512 x 128 resolution (128 horizontal scan lines consisting of 512 A-scans). The macular thickness was displayed as 3 concentric circles, with a 1 mm diameter central circular subfield, a 3 mm diameter inner ring, and a 6 mm diameter outer ring. Each ring was divided into superior, inferior, nasal, and temporal quadrants⁷. When performing a scan of the optic nerve, a 3.4 mm ring was centered on the optic nerve and 768 A-scans were performed^{11, 12}. The average RNFL thickness and vertical C/D ratio were measured. To analyze images of the retinal structure, HD 5 line raster was performed. This high-density scan performs 4,096 A-scans in five planes to provide a highly detailed image¹².

2.2.2 Heidelberg Retinal Tomography

Imaging of the optic nerve was performed by Heidelberg Retina Tomograph II. The scanning protocol has been previously described in detail^{13, 14}. Each scan was repeated 3 times to allow for selection of a scan with low

standard deviation. In brief, the optic disc margin contour line was marked at the inner border of the scleral ring by observing disk images. Once the contour line was marked, a standard reference plane was placed 50 μm posterior to the mean retinal height between 350° and 356° along the contour line¹⁵. The area superficial to the reference plane is considered to be the neuroretinal rim while the area deep to the plane is considered to be the cup. HRT software analyzes the shape of the optic nerve and determines, based on the set of stereometric parameters, whether it is within or outside of the normal limits. These parameters were also used to calculate the glaucomatous progression¹⁶.

2.2.3 Humphrey Visual Field Analyzer

Standard Humphrey 24-2 SITA testing algorithm was performed on Humphrey Field Analyzer, model 750i (Zeiss Humphrey Systems, Dublin, CA, USA). In 24-2 SITA testing algorithm, 54 individual points were tested. The threshold values calculated from the individual points were then compared to a normative database for similar aged normal-sighted individuals¹⁷. Data with fixation losses and false negative responses greater than 20% and false positive responses greater than 15% were excluded from the study¹⁶.

2.2.4 Wide-Field Fluorescein Angiogram and Quantification of Ischemia

Angiography was performed on Optos 200 Tx with an intravenous injection of 5 ml of 10% sodium fluorescein¹⁸. Digital stereoscopic photographs

and IVFA images were taken. The best IVFA image, obtained during the arteriovenous phase of each patient, was used to quantify the amount of ischemia. The uncompressed tiff images were transferred from the Optos V2 Vantage Review Software to Adobe software (Adobe Systems, Inc, San Jose, CA) for analysis.

Two graders quantified the amount of ischemia in each patient using the concentric rings method which has been previously described in detail¹⁹. In the method, the innermost circle is first centered on the optic nerve to be sized proportionately and then repositioned to be fovea-centered. The 12 segments in each of the rings were graded as, “perfused,” or “non-perfused,” based upon whether more than 50% of the segment showed either a perfused or non-perfused morphology. The classification of “non-perfused” and “perfused” morphology was taken from the SCORE study. In the control and PRP laser eyes, “non-perfused” was characterized by a darker appearance of the retina and pruned tree appearance (narrowed and difficult to see) of surrounding arterioles. “Perfused” morphology was characterized by its clear ground-glass opacity²⁰. Calculations of the mean perfused ratio were performed using the mean perfusion ratio = area perfused/ (area perfused + non-perfused). Each segment in each of the rings was given a value of either 0 indicating non-perfused or 1 indicating perfused retina.

2.2.5 Optic Nerve Grading

Stereoscopic photographs were taken with Optos 200 Tx at baseline, 6, 12, and 24 months post-laser. Optic nerve photographs were cropped to a size of 4 x 4 mm for grading. Two glaucoma specialists independently graded the C/D ratio of the laser treated eyes and control eyes of diabetic patients not requiring laser. The graders were masked to the type of patients and purpose of the study.

2.2.6 Pattern Scan Laser Photocoagulator (Pascal)

Pascal laser is a semi-automated 532 nm frequency-doubled neodymium-doped yttrium aluminum garnet (Nd:YAG) solid-state laser²¹. The laser was applied in a pattern array using very short pulse durations of 10-20 ms for each burn with typically a higher power compared to conventional photocoagulation (100 mW and 100 ms pulse duration). All patients received PRP with a pulse duration of 20 ms and a spot size of 200 μ m. Power of the laser beam varied between 430 and 600 mW to achieve a mild gray-white burn intensity, which according to the ETDRS guidelines, is a grade 2+ and 3+ burn. Patients received a mean \pm standard deviation of 1720.8 \pm 392.3 laser spots ranging from 1125 to 2125 spots. Between sessions, there was an interval of two to three weeks.

2.2.7 Statistical Analysis

Statistical analysis was performed using GraphPad Prism 5 (GraphPad Software, La Jolla, CA). For statistical analysis, Snellen BCVA measurements

were converted to logarithm of the minimum angle of resolution (logMAR) scores. Unpaired t-test was used to compare the average age and Fisher's exact test was used to compare the percentage of female participants between control and PRP laser groups. Paired t-test was used to compare differences at specified points over time in PRP treated and control groups. Repeated measures ANOVA with Bonferroni's multiple comparison test was used to statistically analyze the interval changes of measurements in PRP laser and control groups at baseline, 6, 12, and 24 months, respectively. ANOVA with Bonferroni method was performed as outlined in J Neter, W Wasserman, and MH Kutner, Applied Linear Statistical Models, 3rd edition, Irwin, 1990. All data was expressed as mean \pm SD and accepted as statistically significant if $p < 0.05$. A correction of $p < 0.017$ was applied for the Bonferroni's multiple comparison test.

To calculate sample size with an overall power of 80%, $p < 0.05$ was used as an acceptable significance level. Using a two-tailed test for a control with an optic nerve of size 0.3 and an atrophy group of size 0.6, both derived from cup/disk ratio, the effect size would be 0.3. Adding the values to the sample size calculation, 16 patients would be needed for an 80% power number. Twenty diabetic patients requiring PRP were recruited into the study but four were removed due to patient compliance. Eight patients were used as diabetic controls not requiring laser. The diabetic control group did not have proliferative disease that developed during the two year study period. They were included to ensure that the observed changes could be correlated with the laser treatments and not due to diabetic disease progression itself.

2.3 Results

A single eye from each of the 16 patients requiring PRP and 8 control patients not requiring PRP, who were recruited between December 20, 2013, to December 27, 2015, were analyzed. The average age of patients was 70.6 ± 8.4 years for the control group and 65.7 ± 12.5 years for the PRP laser group. The control group had 37.5% female participants while the PRP laser group had 25% female participants. The control and PRP laser groups did not significantly differ ($p > 0.05$) in any of these categories (Table 2.1). None of the patients developed diabetic macular edema during the study.

Following laser treatment, the macular thickness (Figure 2.1A) increased by $3.9 \mu\text{M}$ at 6 months ($298.10 \pm 29.02 \mu\text{M}$, $p=0.44$) relative to baseline ($294.20 \pm 24.20 \mu\text{M}$). The macular thickness recovered to $293.30 \pm 20.99 \mu\text{M}$ at 12 months ($p=0.82$) and $291.90 \pm 25.41 \mu\text{M}$ at 24 months ($p=0.74$). Compared to baseline ($276.60 \pm 35.36 \mu\text{M}$), the control group showed no significant change in macular thickness at 6 months ($273.40 \pm 29.22 \mu\text{M}$, $p=0.27$), 12 months ($274.90 \pm 33.48 \mu\text{M}$, $p=0.72$), and 24 months ($272.80 \pm 36.51 \mu\text{M}$, $p=0.31$).

RNFL thickness (Figure 2.1B) increased at 6 months ($86.25 \pm 12.07 \mu\text{M}$, $p=0.14$), 12 months ($85.50 \pm 9.70 \mu\text{M}$, $p=0.29$) and 24 months ($84.38 \pm 13.09 \mu\text{M}$, $p=0.56$) compared to baseline ($82.75 \pm 11.38 \mu\text{M}$). The control group had no significant change in RNFL thickness at 6 months ($74.88 \pm 9.96 \mu\text{M}$, $p=0.51$), 12 months ($74.38 \pm 8.78 \mu\text{M}$, $p=0.93$), and 24 months ($72.75 \pm 9.15 \mu\text{M}$, $p=0.40$) compared to baseline ($74.25 \pm 10.39 \mu\text{M}$). Analyzing each region, there was no

Table 2.1. Patient demographics

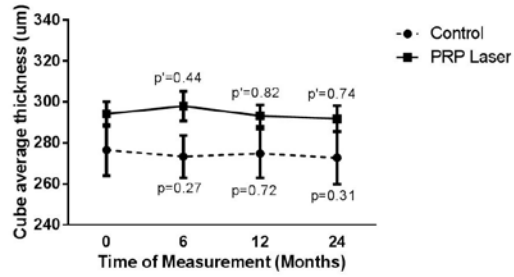
	Control	PRP Laser	P-Value
Number of eyes	8	16	-
Average age (years± SD)	70.6±8.4	65.7±12.5	0.33*
Female Participants (%)	37.5%	25%	0.65†
Mean laser spots ± standard deviation	-	1720.8± 392.3	-

*Unpaired t test

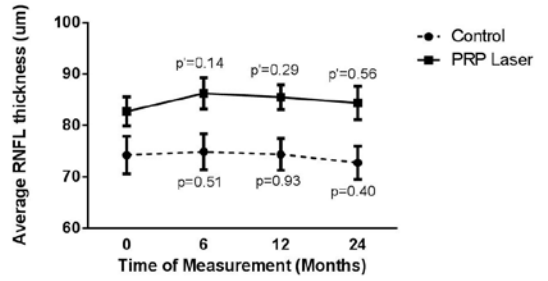
†Fisher's exact test

Figure 2.1. Interval changes in **(A)** macular thickness, **(B)** RNFL thickness and **(C)** mean perfused ratio at baseline, 6, 12, and 24 months later in the control and PRP laser groups. p-value: control group differences between baseline and post-follow-up measurements, paired t-test. p'-value: PRP laser group differences between baseline and post-laser measurements, paired t-test.

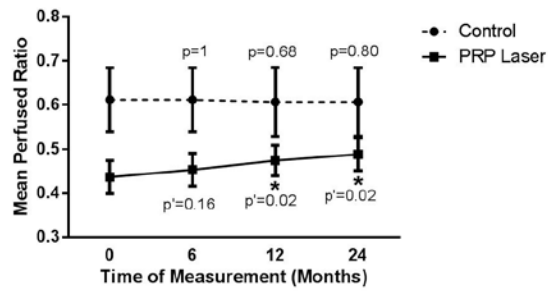
A



B



C



significant difference in thickness in the superior, inferior, temporal and nasal regions of the RNFL for both the control and PRP laser groups ($P \geq 0.18$) (Table 2.2).

The mean perfused ratio showed no significant difference at 6 months (0.45 ± 0.15 , $p=0.16$) but a significant improvement at 12 months (0.47 ± 0.14 , $p=0.02$) and 24 months (0.49 ± 0.15 , $p=0.02$) compared to baseline (0.44 ± 0.15) (Figure 2.1C). There was no significant difference in the control group at 6 months (0.61 ± 0.21 , $p=1.00$), 12 months (0.61 ± 0.22 , $p=0.68$) and 24 months (0.61 ± 0.22 , $p=0.80$) compared to baseline (0.61 ± 0.21).

Analysis of the optic nerve and the associated vertical C/D ratio by OCT (Figure 2.2A) showed a slight increase at 6 months (0.48 ± 0.19 , $p=0.43$), 12 months (0.47 ± 0.20 , $p=0.61$) and 24 months (0.47 ± 0.19 , $p=0.062$) compared to baseline (0.46 ± 0.19). Vertical C/D ratio remained consistent in the control group, being 0.52 ± 0.29 at baseline, 0.54 ± 0.23 at 6 months ($p=0.57$), 0.54 ± 0.24 at 12 months ($p=0.64$) and 0.54 ± 0.27 at 24 months ($p=0.37$).

Analysis of the optic nerve and the corresponding vertical C/D ratio using the HRT (Figure 2.2B) showed an increase at 6 months (0.33 ± 0.30 , $p=0.24$) compared to baseline (0.27 ± 0.26) in the PRP laser group. The ratio remained elevated at 12 months (0.32 ± 0.28 , $p=0.34$) and 24 months (0.31 ± 0.28 , $p=0.44$) post-laser. Vertical C/D ratio showed no significant difference in the control group at 6 months (0.34 ± 0.31 , $p=0.61$), 12 months (0.32 ± 0.30 , $p=0.44$) and 24 months (0.33 ± 0.29 , $p=0.51$) compared to baseline (0.35 ± 0.28).

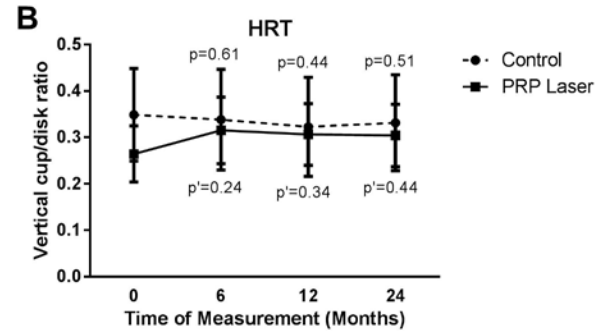
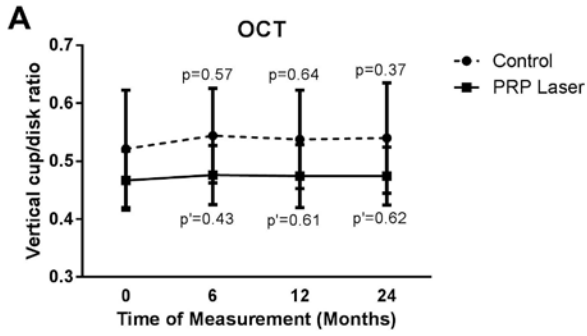
Table 2.2. Changes in RNFL thickness (μm) over the course of 24 months in the control and PRP laser groups.

	Baseline	6 months	12 months	24 months	P-Value*
Average					
Control	74.25 \pm 10.39	74.88 \pm 9.96	74.38 \pm 8.78	72.75 \pm 9.15	0.41
PRP Laser	82.75 \pm 11.38	86.25 \pm 12.07	85.50 \pm 9.70	84.38 \pm 13.09	0.42
Superior					
Control	83.25 \pm 18.38	82.75 \pm 14.96	81.13 \pm 14.93	79.75 \pm 12.83	0.30
PRP Laser	100.00 \pm 18.35	103.38 \pm 17.04	101.75 \pm 17.30	103.25 \pm 23.13	0.78
Inferior					
Control	85.25 \pm 12.52	86.38 \pm 14.14	84.88 \pm 17.63	85.75 \pm 17.65	0.95
PRP Laser	97.19 \pm 19.90	102.38 \pm 18.79	101.56 \pm 15.74	99.13 \pm 21.87	0.48
Temporal					
Control	62.75 \pm 15.15	64.00 \pm 14.31	62.25 \pm 10.73	58.75 \pm 16.42	0.18
PRP Laser	66.38 \pm 12.84	68.56 \pm 11.87	69.13 \pm 10.21	65.19 \pm 11.02	0.21
Nasal					
Control	66.00 \pm 11.41	66.5 \pm 8.65	68.88 \pm 8.11	66.5 \pm 7.05	0.62
PRP Laser	67.44 \pm 8.22	70.56 \pm 9.13	69.44 \pm 10.94	69.75 \pm 14.57	0.66

RNFL = retinal nerve fiber layer

*Repeated Measures ANOVA

Figure 2.2. Interval changes in vertical cup/disk ratio measured on the **(A)** OCT and **(B)** HRT at baseline, 6, 12, and 24 months later in the control and PRP laser groups. p-value: control group differences between baseline and post-follow-up measurements, paired t-test. p'-value: PRP laser group differences between baseline and post-laser measurements, paired t-test.



Two glaucoma specialists were assigned to independently grade the vertical C/D ratio in the same eyes following PRP laser using stereo photographs (Figure 2.3A). Grader 1 indicated at baseline, the mean vertical C/D was 0.44 ± 0.17 and noted an increase at 6 months (0.46 ± 0.17 , $p=0.08$), 12 months (0.46 ± 0.16 , $p=0.15$) and 24 months (0.47 ± 0.16 , $p=0.13$) post-laser. Grader 2 indicated baseline mean vertical C/D ratio of 0.35 ± 0.17 and noted a significant increase at 6 months (0.37 ± 0.18 , $p=0.04$), and 12 months (0.38 ± 0.18 , $p=0.02$) with a further increase at 24 months (0.40 ± 0.19 , $p=0.005$) post-laser. The graders also graded control eyes of diabetic patients not requiring laser treatment. Both grader 1 and 2 found that over 24 months there was no significant difference ($p \geq 0.10$) (Figure 2.3B).

After the laser treatment, visual field tests had an average baseline mean deviation (MD) (Figure 2.4A) in the PRP laser group of -4.39 ± 3.10 dB. Mean MD digressed at 6 months by 1.30 dB (-5.68 ± 5.03 dB, $p=0.24$) and further significantly decreased at 12 months (-5.73 ± 4.07 dB, $p=0.02$) and 24 months (-6.36 ± 3.74 , $p=0.01$) post-laser. Control group showed no significant differences in visual field mean MD at baseline (-8.46 ± 8.83 dB), 6 months (-8.43 ± 6.29 dB, $p=0.98$), 12 months (-7.41 ± 4.78 dB, $p=0.53$) and 24 months (-9.19 ± 6.35 dB, $p=0.64$).

Baseline mean best-corrected visual acuities (Figure 2.4B) were 0.32 ± 0.24 logMAR in the control group and 0.34 ± 0.31 logMAR in the PRP laser group. Visual acuity slightly increased to 0.3 ± 0.29 logMAR at 6 months ($p=0.32$)

Figure 2.3. Interval changes in vertical cup/disk ratio as measured by two masked glaucoma specialists using stereo photographs at baseline, 6, 12, and 24 months later in the **(A)** PRP laser group and the **(B)** control group. p-value: grader 1 differences between baseline and post-laser measurements, paired t-test. p'-value: grader 2 differences between baseline and post-laser measurements, paired t-test.

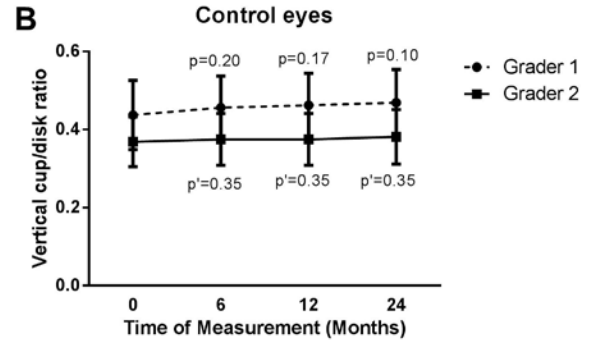
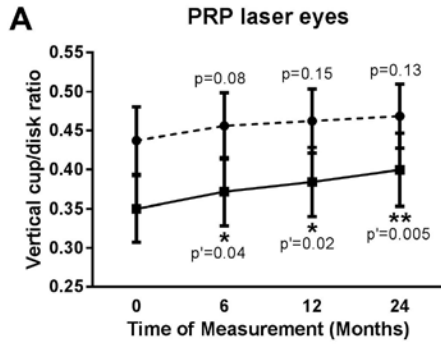
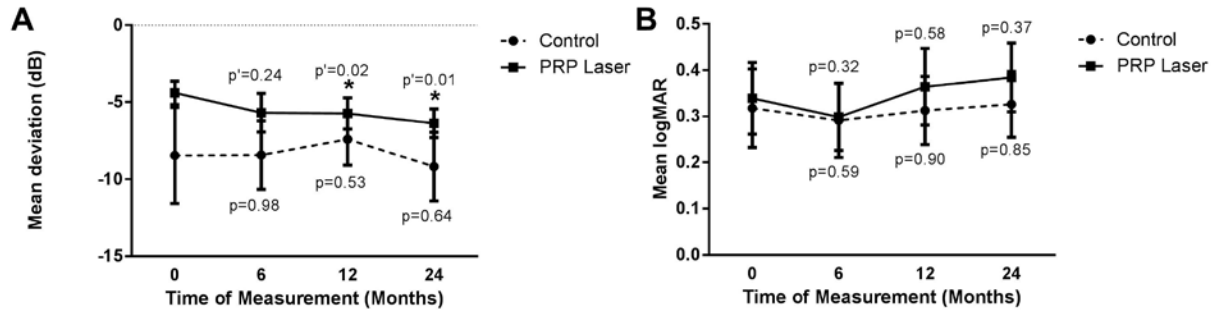


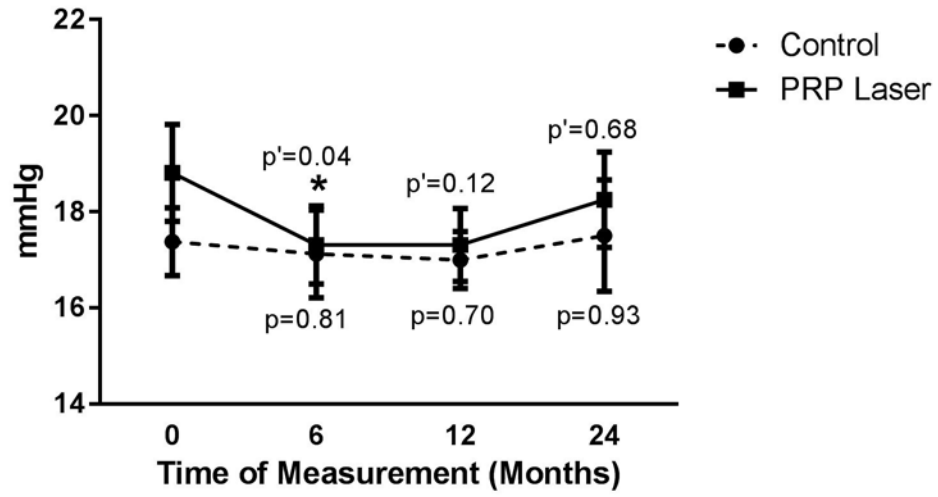
Figure 2.4. Interval changes in mean deviation measured on the **(A)** Humphrey Visual Field Analyzer and **(B)** visual acuity at baseline, 6, 12, and 24 months later in the control and PRP laser groups. p-value: control group differences between baseline and post-follow-up measurements, paired t-test. p'-value: PRP laser group differences between baseline and post-laser measurements, paired t-test.



but gradually decreased to 0.36 ± 0.33 logMAR at 12 months ($p=0.58$) and 0.38 ± 0.30 logMAR at 24 months ($p=0.37$) post-laser. Visual acuity remained consistent in the control group, being 0.32 ± 0.24 logMAR at baseline, 0.29 ± 0.23 logMAR at 6 months ($p=0.59$), 0.31 ± 0.21 logMAR at 12 months ($p=0.90$) and 0.33 ± 0.20 logMAR at 24 months ($p=0.85$). The changes were not statistically significant.

After Pascal photocoagulation, intraocular pressure (IOP) (Figure 2.5) significantly decreased ($p=0.04$) by 1.5 mmHg at 6 months (17.31 ± 3.26 mmHg) compared to baseline (18.81 ± 4.04 mmHg). The pressure remained at 17.31 ± 3.05 mm Hg at 12 months ($p=0.12$) but then increased close to control values (18.25 ± 3.98 mmHg) at 24 months ($p=0.68$). In the control group, IOP remained constant, being 17.38 ± 2.00 mmHg at baseline, 17.13 ± 2.59 mmHg at 6 months ($p=0.81$), 17.00 ± 1.69 mmHg at 12 months ($p=0.70$) and 17.50 ± 3.30 mmHg at 24 months ($p=0.93$). The changes were not statistically significant.

Figure 2.5. Interval changes in intraocular pressure at baseline, 6, 12, and 24 months later in the control and PRP laser groups. mm Hg= millimeter of mercury. p-value: control group differences between baseline and post-follow-up measurements, paired t-test. p'-value: PRP laser group differences between baseline and post-laser measurements, paired t-test.



2.4 Discussion

PRP laser used in this study was Pascal Pattern Scan Laser (OptiMedica, Santa Clara, CA, USA). Compared to conventional photocoagulation lasers which use lower power (100 mW) and longer pulse duration (100 ms), Pascal laser is applied in a pattern array, using very short pulse durations of 10-20 ms for each burn, and typically outputs a higher power. As a result, researchers have suggested that Pascal laser may promote healing while causing less collateral damage compared to conventional photocoagulation lasers²². Despite differences between Pascal laser and conventional argon laser for PRP, past studies have shown that there are no significant differences in the outcomes for patients between the two lasers, showing similar effects on the regression of DR²²⁻²⁵.

The macular and RNFL thickness (Figures 2.1A and B) showed an increase at 6 months and a decrease by 24 months post-laser indicating recovery. Past studies have described similar increases in thickness pre-6 months, likely due to post-laser intraretinal inflammation^{7, 26, 27}. Photocoagulation creates thermal and photochemical damage, resulting in the production of reactive oxygen species (ROS).²⁷ ROS generate an immune response in the retinal tissue by increasing the intraretinal junctional permeability and recruitment of leukocytes^{7, 27-31}. The decrease of the thickness post-6 months suggests that the effects of an inflammatory response persist up to 6 months in the retinal

tissue following laser treatment. Overall, by 24 months, there was no significant change in the macular or RNFL thickness compared to pre-treatment state.

To determine whether the observed changes were due to the laser treatment or diabetes itself, the amount of ischemia was quantified using the mean perfused ratio. The mean perfused ratio was calculated by the concentric rings method utilized by Nicholson et al¹⁹. Compared to the standard ischemic index method wherein the grader draws the ratio of area perfused to the total area graded, the concentric rings method utilizes a set template. It has a perfect agreement with the ischemic index method, a higher inter-grader agreement, and a shorter grading time¹⁹. Using the concentric rings method, it was observed that at 12 and 24 months post laser, PRP laser resulted in a significant increase in the perfusion of the eye while the control eyes showed no change. These results suggest that the changes in ischemia are most likely the result of the laser treatment.

When analyzing the optic nerve, both OCT and HRT testing showed a similar trend. In the vertical C/D ratio on the OCT, there was a slight increase of +0.009 at 6, 12, and 24 months compared to baseline in the PRP laser group. The HRT showed an increase in the vertical C/D ratio by +0.06 post- 6 months. There was a statistically significant decrease in pressure by 1.5 mm Hg at 6 months compared to baseline (18.81 ± 4.04 mm Hg) (Figure 2.5)³². IOP remained lowered before recovering to 18.25 ± 3.98 mm Hg at 24 months.

The current gold standard for analyzing the optic nerve is grading of stereo-photographs by glaucoma specialists. Two glaucoma specialists were assigned to grade over 24 months, whereas grader 2 indicated a significant increase at 6 and 12 months, with a further significant increase at 24 months post-laser. There is a discrepancy between the grading of the optic nerves post-laser treatment by ophthalmologists. This has been shown in other studies of disc analysis and it is apparent that a more objective analysis is needed^{33, 34}. To verify whether the discrepancy is due to the laser treated eyes and not the graders themselves, the graders also assessed control eyes of diabetic patients not requiring laser treatment. When asked to grade the control eyes, both grader 1 and 2 found that over 24 months, there was no significant difference in the C/D ratios. This discrepancy between the graders and OCT/HRT testing data suggests that non-morphological changes in the colour of the optic nerve post-PRP result in a decreased ability to consistently grade nerves for cupping which is important in recognizing the potential for hidden glaucoma.

In addition to the inconsistent clinical grading of the optic nerve post-laser, visual acuity showed a non-significant decline and visual fields showed a progressive significant decline at 12 and 24 months post-laser. It has been shown in a past study done by Hudson et al. that in diabetic macular edema patients, laser photocoagulation results in a perimetric sensitivity loss within 10° of the fovea despite showing visual acuity stabilization³⁵. Visual fields and electroretinography have been performed on diabetic retinopathy patients post-laser treatments and have demonstrated that roughly 40% of the peripheral

retina is destroyed by photocoagulation resulting in visual field defects.⁵ A study by Subush et al. has also documented a mild loss of retinal sensitivity 6 months post-laser treatment³⁶. These past studies have reported the degree of peripheral retina destroyed by photocoagulation; however, none have studied progressive long-term visual field loss over a two year time period^{5, 35, 36}. With the unreliable grading of the optic nerve and further progressive deterioration of visual fields post-laser, it is understandable why some diabetic patients post-PRP are being misdiagnosed as having normal-tension glaucoma despite the likelihood that the presenting symptoms can be attributed to iatrogenic effects of the laser.

One limitation of the current study is that despite meeting the power number calculations for the treatment group, 16 control patients in the study would have been preferred. Although the number of participants for the control group did not meet the limit, the control group did not show any significant difference in any of the testing and showed stable trends. As both glaucoma and the effects of PRP on RNFL and optic disk are often progressive, the idea of extending the follow up period beyond 2 years to increase the ability to discern small, yet progressive changes is enticing. It would be interesting to determine if there are any predictive factors that can indicate which patients who receive PRP will progress and what the rate of that progression will be.

Studies have previously reported short-term visual field changes following PRP but no study has looked at the progressive nature over a two year time period^{5, 36}. The progressive improvement in ischemia following PRP is also a novel finding. Studies have never correlated changes in visual fields with optic

nerve changes post-PRP. For that reason, the current study sought to obtain comprehensive results and conducted analyses of the optic nerve with both structural and functional tests to see if any early changes could be found in the optic nerve post-PRP.

In conclusion, the current study has found that pascal photocoagulation did not cause significant changes to macular or RNFL thickness over the 24 month time period. The morphology of the optic nerve head appeared unchanged following laser treatment as observed on the OCT and HRT diagnostic machines. Despite an improvement in peripheral perfusion, there was a significant progressive decline of peripheral visual field over the study period. Clinical grading of the optic nerve was more unreliable following PRP despite the absence of significant morphological changes as detected by the OCT and HRT diagnostic machines. Additional research is needed to help guide clinicians in making a diagnosis of normal tension glaucoma in diabetic patients who have received PRP.

2.5 References

1. Yau JWY, Rogers SL, Kawasaki R, et al. Global Prevalence and Major Risk Factors of Diabetic Retinopathy. *Diabetes Care* 2012;35(3):556-564.
2. Lee R, Wong TY, Sabanayagam C. Epidemiology of diabetic retinopathy, diabetic macular edema and related vision loss. *Eye and Vision* 2015;2:17.
3. Writing Committee for the Diabetic Retinopathy Clinical Research Network. Panretinal Photocoagulation vs Intravitreal Ranibizumab for Proliferative Diabetic Retinopathy: A Randomized Clinical Trial. *JAMA* 2015;314(20):2137-2146.
4. Photocoagulation treatment of proliferative diabetic retinopathy. Clinical application of Diabetic Retinopathy Study (DRS) findings, DRS Report Number 8. The Diabetic Retinopathy Study Research Group. *Ophthalmology* 1981; 88:583-600.
5. Frank RN. Visual Fields and Electroretinography Following Extensive Photocoagulation. *Arch Ophthalmol* 1975;93(8):591-598.
6. Kim HY, Cho HK. Peripapillary Retinal Nerve Fiber Layer Thickness Change After Panretinal Photocoagulation in Patients With Diabetic Retinopathy. *Korean J Ophthalmol* 2009;23(1):23-26.

7. Muqit MMK, Marcellino GR, Henson DB, Fenerty CH, Stanga PE. Randomized Clinical Trial To Evaluate The Effects Of Pascal Panretinal Photocoagulation On Macular Nerve Fiber Layer. *Retina* 2011;31(8):1699-1707.
8. Fujimoto JG. *Optical Coherence Tomography of Ocular Diseases*. 2nd ed. Thorofare, NJ: Slack Inc;2004:714.
9. Mwanza J-C, Oakley JD, Budenz DL, Anderson DR. Ability of Cirrus HD-OCT Optic Nerve Head Parameters to Discriminate Normal from Glaucomatous Eyes. *Ophthalmology* 2011;118(2).
10. Foo L-L, Perera SA, Cheung CY, et al. Comparison of scanning laser ophthalmoscopy and high-definition optical coherence tomography measurements of optic disc parameters. *Br J Ophthalmol* 2012;96(4):576-580.
11. Meditec CZ. *Stratus OCT User's Manual*. Dublin, CA: Carl Zeiss Meditec; 2003.
12. Vizzeri G, Balasubramanian M, Bowd C, Weinreb RN, Medeiros FA, Zangwill LM. Spectral domain-optical coherence tomography to detect localized retinal nerve fiber layer defects in glaucomatous eyes. *Opt Express* 2009;17(5):4004.
13. Wollstein G, Garway-Heath DF, Hitchings RA. Identification of early glaucoma cases with the scanning laser ophthalmoscope¹¹The authors

have no proprietary interest in the development or marketing of this or a competing instrument. *Ophthalmology* 1998;105(8):1557-1563.

14. Rao HL, Babu GJ, Sekhar GC. Comparison of the Diagnostic Capability of the Heidelberg Retina Tomographs 2 and 3 for Glaucoma in the Indian Population. *Ophthalmology* 2010;117(2):275-281.
15. Rao H, Begum V, Addepalli U, Senthil S, Garudadri C. Optic nerve head parameters of high-definition optical coherence tomography and Heidelberg retina tomogram in perimetric and preperimetric glaucoma. *Indian J Ophthalmol* 2016;64(4):277.
16. Alencar LM, Bowd C, Weinreb RN, Zangwill LM, Sample PA, Medeiros FA. Comparison of HRT-3 Glaucoma Probability Score and Subjective Stereophotograph Assessment for Prediction of Progression in Glaucoma. *Invest Ophthalmol Vis Sci* 2008;49(5):1898.
17. Kummet CM, Zamba KD, Doyle CK, Johnson CA, Wall M. Refinement of Pointwise Linear Regression Criteria for Determining Glaucoma Progression. *Invest Ophthalmol Vis Sci* 2013;54(9):6234.
18. Wessel MM, Aaker GD, Parlitsis G, Cho M, D'amico DJ, Kiss S. Ultra-Wide-Field Angiography Improves The Detection And Classification Of Diabetic Retinopathy. *Retina* 2012;32(4):785-791.

19. Nicholson L, Vazquez-Alfageme C, Ramu J, et al. Validation of Concentric Rings Method as a Topographic Measure of Retinal Nonperfusion in Ultra-Widefield Fluorescein Angiography. *Am J Ophthalmol* 2015;160(6).
20. Blodi BA, Domalpally A, Scott IU, Ip MS, Oden NL, Elledge J, et al. Standard Care vs Corticosteroid for Retinal Vein Occlusion (SCORE) Study system for evaluation of stereoscopic color fundus photographs and fluorescein angiograms: SCORE Study Report 9. *Arch Ophthalmol* 2010;128(9):1140–1145.
21. Sanghvi C, Mclauchlan R, Delgado C, et al. Initial experience with the Pascal photocoagulator: a pilot study of 75 procedures. *Br J Ophthalmol* 2008;92(8):1061-1064.
22. Muqit MMK. In Vivo Laser-Tissue Interactions and Healing Responses From 20- vs 100-Millisecond Pulse Pascal Photocoagulation Burns. *Arch Ophthalmol* 2010;128(4):448.
23. Mahgoub M, M, Macky T, A, The Effect of Laser Panretinal Photocoagulation on Diabetic Macular Edema Using the Pascal® Photocoagulator versus the Conventional Argon Laser Photocoagulator. *Ophthalmologica* 2016;235:137-140.
24. Nagpal M, Marlecha S, Nagpal K. Comparison Of Laser Photocoagulation For Diabetic Retinopathy Using 532-Nm Standard Laser Versus Multispot Pattern Scan Laser. *Retina* 2010;30(3):452-458.

25. Jain A. Effect of Pulse Duration on Size and Character of the Lesion in Retinal Photocoagulation. *Arch Ophthalmol* 2008;126(1):78.
26. Shimura M, Yasuda K, Nakazawa T, Kano T, Ohta S, Tamai M. Quantifying alterations of macular thickness before and after panretinal photocoagulation in patients with severe diabetic retinopathy and good vision. *Ophthalmology* 2003;110(12):2386-2394.
27. Mitsch C, Pemp B, Kriechbaum K, Bolz M, Scholda C, Schmidt-Erfurth U. Retinal Morphometry Changes Measured With Spectral Domain-Optical Coherence Tomography After Pan-Retinal Photocoagulation In Patients With Proliferative Diabetic Retinopathy. *Retina* 2016;36(6):1162-1169.
28. Cui JZ, Wang X-F, Hsu L, Matsubara JA. Inflammation induced by photocoagulation laser is minimized by copper chelators. *Lasers Med Sci* 2008;24(4):653-657.
29. Taguchi H, Ogura Y, Takanashi T, et al. Fluorophotometric detection of intravitreal peroxides after panretinal laser photocoagulation. *Invest Ophthalmol Vis Sci* 1998;39:358–363.
30. Maschio AD. Polymorphonuclear leukocyte adhesion triggers the disorganization of endothelial cell-to-cell adherens junctions. *J Cell Biol* 1996;135(2):497-510.

31. Tsujikawa A, Kiryu J, Dong J, et al. Quantitative Analysis Of Diabetic Macular Edema After Scatter Laser Photocoagulation With The Scanning Retinal Thickness Analyzer. *Retina* 1999;19(1):59-64.
32. Waisbourd M, Ahmed OM, Molineaux J, Gonzalez A, Spaeth GL, Katz LJ. Reversible structural and functional changes after intraocular pressure reduction in patients with glaucoma. *Graefes Arch Clin Exp Ophthalmol* 2016;254(6):1159-1166.
33. Lim MC. Effect of Diabetic Retinopathy and Panretinal Photocoagulation on Retinal Nerve Fiber Layer and Optic Nerve Appearance. *Arch Ophthalmol* 2009;127(7):857-862.
34. Chauhan BC, Burgoyne CF. From Clinical Examination of the Optic Disc to Clinical Assessment of the Optic Nerve Head: A Paradigm Change. *Am J Ophthalmol* 2013;156(2).
35. Hudson C, Flanagan JG, Turner GS, Chen HC, Young LB, Mcleod D. Influence of laser photocoagulation for clinically significant diabetic macular oedema (DMO) on short-wavelength and conventional automated perimetry. *Diabetologia* 1998;41(11):1283-1292.
36. Subash M, Comyn O, Samy A, et al. The Effect of Multispot Laser Panretinal Photocoagulation on Retinal Sensitivity and Driving Eligibility in Patients With Diabetic Retinopathy. *JAMA Ophthalmol* 2016;134(6):666-671.

Chapter 3

3 Two-year analysis of structural and functional changes to the retina and optic nerve following anti-VEGF treatments for diabetic macular edema patients

The chapter addresses specific objectives outlined in aim 3:

3. To describe the effects of anti-VEGF injections and the frequency of injections on the structural and functional changes to the retina and optic nerve of DR patients with underlying DME using *in vivo* clinical pathological analysis.

3.1 Introduction

Diabetic macular edema (DME) is a common complication of diabetic retinopathy (DR). During DR, chronic hyperglycemia results in enhanced production of vascular endothelial growth factors (VEGF), advanced glycation end products, nitric oxide, oxidative stress and inflammation¹. The aforementioned factors disrupt the blood retinal barrier (BRB), increasing permeability, causing interstitial fluid accumulation and the development of DME². Inhibition of these factors can reduce the development of fluid-filled cysts. At the present time, the gold standard, first line of treatments clinically used to treat DME patients are intravitreal anti-VEGF injections³.

Over the past decade, there have been increased clinical reports of diabetic patients receiving anti-VEGFs developing signs of glaucoma and optic neuropathy. Diabetes is a risk factor for the development of glaucoma and the use of anti-VEGFs might augment the risk⁴. Past studies have analyzed the safety of intravitreal anti-VEGF injections in age-related macular degeneration (AMD) but none have examined the effects of the treatments on the optic nerve⁵⁻²⁶. Studies have also reported a sustained increase in intraocular pressures (IOP) following intravitreal injections of anti-VEGFs in AMD patients²⁷⁻³¹. With the continued and increased use of anti-VEGF, numerous questions have been raised in regards to whether they have a role in increasing the risk of developing glaucoma and what are the long-term effects of the IOP spikes^{27, 32}. The results of controlled trials that look at visual acuity and central macular thickness as well

as retinal and optic nerve structures are greatly needed to substantiate the safety and efficacy of anti-VEGF drugs for DR with underlying DME.

The purpose of the following study was to determine whether the use of ranibizumab (Lucentis), an anti-VEGF, results in structural and functional changes to the retina and optic nerve of DR patients with underlying DME over a two year time period. This is the first comprehensive study to investigate the long-term structural and functional effects of anti-VEGF treatments on the retina and optic nerve that involve the analysis of macular thickness, the retinal nerve fiber layer (RNFL), mean perfusion, vertical C/D ratio, cup volume, stereo photos, IOP, visual acuity and visual fields.

3.2 Methods

The prospective study was conducted at the Ivey Eye Institute in London, Ontario, Canada. Ivey Eye Institute is a tertiary care academic center. The study was approved by Health Sciences Research Ethics Board of Western University and complies with the Declaration of Helsinki. Prospective, treatment-naïve diabetic patients with at least one eye having clinically significant diabetic macular edema (central macular thickness $>300\ \mu\text{m}$) according to the ETDRS guidelines and requiring intravitreal anti-VEGF injections were recruited into the study. Participants were over the age of 18 years. Participants were excluded from the study if they had prior intravitreal anti-VEGF injections, advanced lens opacity, cataracts that could affect diagnostic testing, history of glaucoma, any other disorder of the optic nerve (optic neuropathy, neuritis, uveitis or retinal degeneration), presence/development of proliferative disease and prior retinal treatment (PRP, focal laser or surgery within 6 months of participation). All participants provided informed consent. Diabetic patients who did not have clinically significant macular edema and did not require anti-VEGF treatment or other retinal treatments were chosen as control. Participants were evaluated at pre-injection baseline and at 6, 12, and 24 months post-baseline. During each study visit, participants underwent optical coherence tomography (OCT), visual field (VF) and intravenous fluorescein angiography (IVFA) testing as well as a standard ophthalmic exam which included best-corrected Snellen visual acuity (BCVA), intraocular measurement using Goldmann applanation tonometer, and

slip lamp examination. Humphrey 24-2 SITA visual field testing was performed with undilated eyes.

3.2.1 Optical Coherence Tomography

Measurement of the macula and optic nerve through the macular thickness, optic disc cube and HD 5 line raster imaging tests were performed with the optical coherence tomography (Cirrus HD-OCT 4000, Carl Zeiss Meditech, Dublin, California). The principles and protocol have been previously described in detail^{33, 34, 35}. OCT tests were taken at pre-injection baseline and at 6, 12, and 24 months post-baseline. The scan at each time of measurement was repeated 3 times to ensure highest signal strength.

The macula was analyzed by a 6 x 6 mm scan and a resolution of 512 x 128 (128 horizontal scan lines consisting of 512 A-scans). The macular thickness was displayed as 3 concentric circles, the central circular subfield being 1 mm in diameter, the inner ring being 3 mm in diameter and the outer ring being 6 mm in diameter. Each ring was divided into superior, inferior, nasal, and temporal quadrants⁷. When performing a scan of the optic nerve, a 3.4 mm ring was centered on the optic nerve and 768 A-scans were performed^{36, 37}. The average RNFL thickness, vertical C/D ratio, and cup volume were measured. To analyze images of the retinal structure, a HD 5 line raster was performed. This high-density scan does 4,096 A-scans in five planes to provide a high definition image³⁷.

3.2.2 Humphrey Visual Field Analyzer

To measure peripheral visual fields, standard Humphrey 24-2 SITA testing algorithm was performed on Humphrey Field Analyzer, model 750i (Zeiss Humphrey Systems, Dublin, CA, USA). In the 24-2 SITA testing algorithm, 54 individual points are tested. From those points, the threshold values were calculated and compared to a normative database for similar aged normal-sighted individuals^{38, 39}. Participants that had false positive responses greater than 15%, fixation losses and false negative responses greater than 20% were excluded from the study³⁸.

3.2.3 Wide-Field Fluorescein Angiogram and Quantification of Ischemia

Wide-field fluorescein angiography was performed on the Optos 200 Tx with an intravenous injection of 5 ml of 10% sodium fluorescein⁴⁰. Intravenous fluorescein angiography (IVFA) photos and digital stereoscopic photographs were taken. To quantify the amount of ischemia in each patient, the best IVFA image obtained during the arteriovenous phase was used. For analysis, the uncompressed tiff images were transferred from the Optos V2 Vantage Review Software to Adobe software (Adobe Systems, Inc, San Jose, CA).

Two graders that were masked to the study quantified the amount of ischemia in each patient by using the concentric rings method which has been previously described in detail⁴¹. In this method, the innermost circle was first

centered on the optic nerve to be sized proportionately and then repositioned to be fovea-centered. The 12 segments in each of the rings were graded as, “perfused” or “non-perfused” if more than 50% of the segment showed either a perfused or non-perfused morphology. The classification of “non-perfused” and “perfused” morphology was taken from the SCORE study. In the control and anti-VEGF injected eyes, “non-perfused” was characterized by a darker appearance of the retina and pruned tree appearance (narrowed and difficult to see) of surrounding arterioles. “Perfused” morphology was characterized by its clear ground-glass opacity⁴². Calculations of the mean perfused ratio were performed using the mean perfusion ratio = area perfused / (area perfused + non-perfused). Each segment in each of the rings was given a value of either 0 indicating non-perfused or 1 indicating perfused retina.

3.2.4 Optic Nerve Grading

Stereoscopic photographs were taken with Optos 200 Tx at baseline, 6, 12, and 24 months post-baseline injection. Photographs were cropped to a size of 4 x 4 mm for optic nerve grading. Two glaucoma specialists independently graded the cup-to-disk (C/D) ratio of the anti-VEGF injected eyes and control eyes of diabetic patients not requiring injections. The graders were masked to the type of patients and purpose of the study.

3.2.5 Ranibizumab (Lucentis) Injections

During the induction phase, participants received monthly intravitreal injections of ranibizumab (Lucentis, 0.5 mg in 0.05 mL solution for injection; Novartis Pharmaceuticals Canada Inc., Quebec, Canada) for 3 months. Post 3 months, participants received injections on an as needed basis until they were clinically stable based on their OCT tests and clinical assessment. Ranibizumab treatment was reinitiated if BCVA decreased by 5 letters or if central macular thickness became greater than 300 μm .

Patients received injections in clinical rooms. Topical anesthesia was administered and the eye was disinfected with povidone iodine eye drops. An ophthalmic speculum was utilized to retract the eye lid. A 30 gauge needle was used to administer the intravitreal anti-VEGF injection 3.5-4.0 mm posterior to the limbus.

3.2.6 Statistical Analysis

Data was analyzed using GraphPad Prism 5 (GraphPad Software, La Jolla, CA, USA). Snellen best-corrected visual acuity (BCVA) measurements were converted to logarithm of the minimum angle of resolution (logMAR) scores for statistical analysis. To compare the average age of the patients, an unpaired t-test was performed and to compare the percentage of female participants between control and anti-VEGF groups, a fisher's exact test was used. To compare the differences at specified points over time in the anti-VEGF and

control groups, the paired t-test was performed. To statistically analyze the interval changes of measurements in the anti-VEGF and control groups at baseline, 6, 12, and 24 months, respectively, repeated measures ANOVA with a Bonferroni's multiple comparisons test was used. ANOVA with Bonferroni method was performed as outlined in J Neter, W Wasserman, and MH Kutner, Applied Linear Statistical Models, 3rd edition, Irwin, 1990. All data was expressed as mean \pm SD and accepted as statistically significant if $p < 0.05$. A correction of $p < 0.017$ was applied for the Bonferroni's multiple comparison test.

To calculate the sample size with an overall power of 80%, $p < 0.05$ was used as an acceptable significance level. Using a two-tailed test for a control with an optic nerve of size 0.3 and an atrophy group of size 0.6, both derived from cup/disk ratio, the effect size would be 0.3. Adding the values to the sample size calculation, it was calculated that 16 patients would be needed for an 80% power number. Thirty-six diabetic patients requiring anti-VEGF injections were recruited into the study but four were removed due to patient compliance and two for developing proliferative disease and requiring PRP treatment. Twenty-one patients were used as diabetic controls not requiring anti-VEGF injections. The diabetic control group did not have proliferative disease that developed during the two year study period. The control was included to ensure that the observed changes could be correlated with the anti-VEGF treatments and not due to diabetic disease itself.

3.3 Results

A single eye from each of the 30 patients requiring anti-VEGF injections and 21 control patients not requiring anti-VEGF injections, who were recruited between September 11, 2014 and July 23, 2015, was analyzed. The average age of patients was 67.7 ± 7.5 years for the control group and 63.9 ± 6.8 years for the anti-VEGF group. The control group had 33.3% female participants while the anti-VEGF group had 43.3% female participants. The control and anti-VEGF groups did not significantly differ ($p > 0.05$) in any of these categories (Table 3.1). None of the patients developed proliferative diabetic retinopathy during the study. Patients received a mean \pm standard deviation of 9.6 ± 5.3 injections ranging from 4 to 22 injections.

Following anti-VEGF treatment, the macular thickness (Figure 3.1A) significantly decreased by $27.9 \mu\text{M}$ at 6 months ($313.60 \pm 39.87 \mu\text{M}$, $p = 0.0002$) relative to baseline ($341.50 \pm 55.33 \mu\text{M}$). The macular thickness further decreased to $309.80 \pm 33.80 \mu\text{M}$ at 12 months ($p = 0.0001$) and $303.40 \pm 32.16 \mu\text{M}$ at 24 months ($p = 0.0001$). Compared to baseline ($287.70 \pm 29.36 \mu\text{M}$), the control group showed no significant change in macular thickness at 6 months ($286.70 \pm 27.83 \mu\text{M}$, $p = 0.51$), 12 months ($289.40 \pm 31.84 \mu\text{M}$, $p = 0.51$), or 24 months ($288.20 \pm 32.89 \mu\text{M}$, $p = 0.84$).

RNFL thickness (Figure 3.1B) significantly decreased at 6 months ($90.03 \pm 14.40 \mu\text{M}$, $p = 0.0005$), 12 months ($87.97 \pm 12.76 \mu\text{M}$, $p = 0.0001$) and 24 months ($87.47 \pm 11.81 \mu\text{M}$, $p = 0.0001$) compared to baseline ($98.37 \pm 18.89 \mu\text{M}$). The

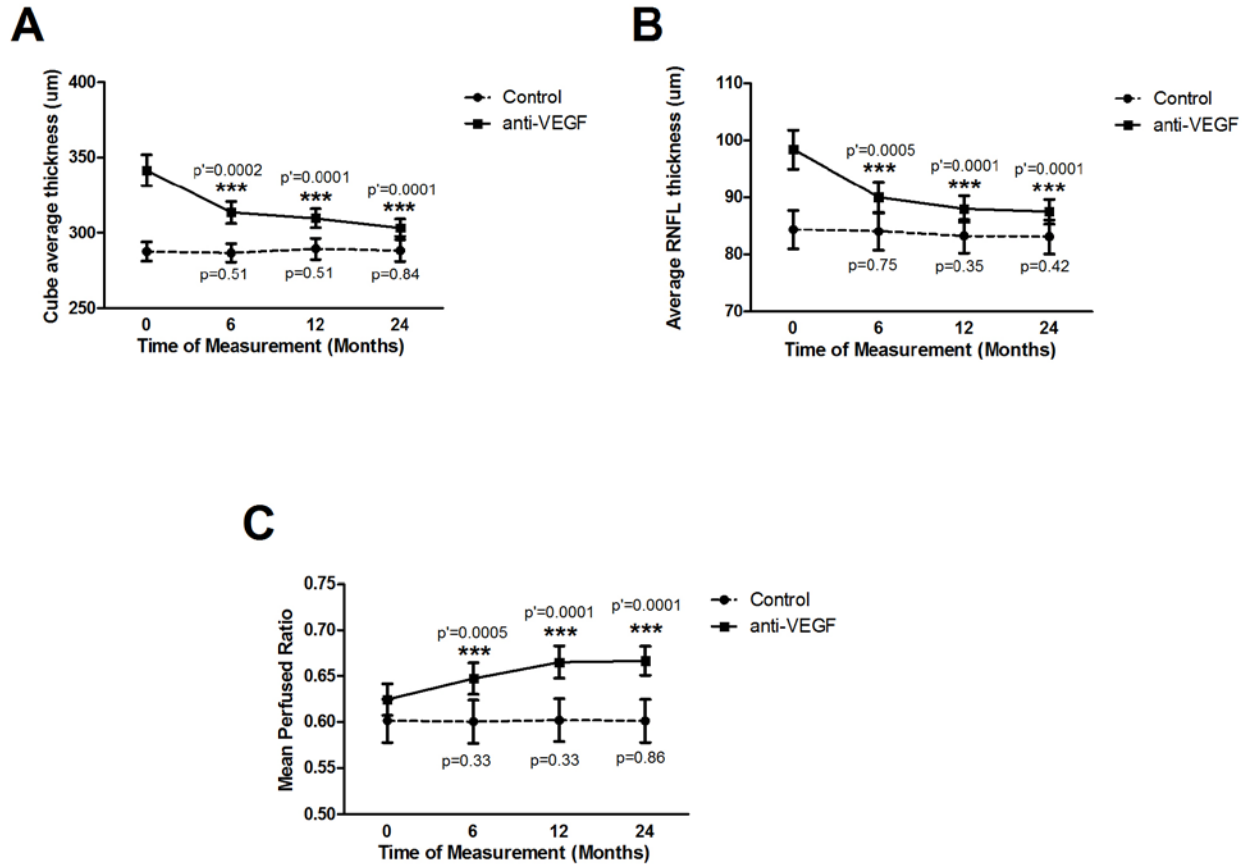
Table 3.1. Demographics of patients involved in the study.

	Control	anti-VEGF	P-Value
Number of eyes	21	30	-
Average age (years± SD)	67.7 ± 7.5	63.9 ± 6.8	0.07*
Female Participants (%)	33.3%	43.3%	0.57†
Mean anti-VEGF injections ± standard deviation	-	9.6 ± 5.3	-

*Unpaired t-test

†Fisher's exact test

Figure 3.1. Interval changes in **(A)** macular thickness, **(B)** RNFL thickness and **(C)** mean perfused ratio at baseline, 6, 12, and 24 months in the control and anti-VEGF groups. p-value: control group differences between baseline and follow-up measurements, paired t-test. p'-value: anti-VEGF group differences between baseline and follow-up measurements, paired t-test.



control group had no significant change in RNFL thickness at 6 months ($84.00 \pm 14.94 \mu\text{M}$, $p=0.75$), 12 months ($83.19 \pm 13.42 \mu\text{M}$, $p=0.35$), or 24 months ($83.10 \pm 13.73 \mu\text{M}$, $p=0.42$) compared to baseline ($84.33 \pm 15.51 \mu\text{M}$). Analyzing each region, there was no significant difference in thickness in the superior, inferior, temporal and nasal regions of the RNFL for the control group but a significant decrease in all regions for the anti-VEGF group ($p < 0.02$) (Table 2).

The mean perfused ratio showed a significant improvement at 6 months (0.65 ± 0.09 , $p=0.0005$), 12 months (0.67 ± 0.10 , $p=0.0001$) and 24 months (0.67 ± 0.09 , $p=0.0001$) compared to baseline (0.62 ± 0.09) for the anti-VEGF group. (Figure 3.1C). There was no significant difference in the control group at 6 months (0.60 ± 0.11 , $p=0.33$), 12 months (0.60 ± 0.11 , $p=0.33$) or 24 months (0.60 ± 0.11 , $p=0.86$) compared to baseline (0.60 ± 0.11).

Analysis of the optic nerve and the associated cup volume by OCT (Figure 3.2) showed a significant increase at 6 (0.094 ± 0.10 , $p=0.02$), 12 (0.096 ± 0.10 , $p=0.007$), and 24 months (0.095 ± 0.10 , $p=0.03$) compared to baseline (0.089 ± 0.1). Cup volume remained consistent and showed no significant difference in the control group at 6 (0.110 ± 0.13 , $p=0.09$), 12 (0.111 ± 0.13 , $p=0.56$), and 24 months (0.116 ± 0.13 , $p=0.86$) compared to baseline (0.115 ± 0.13).

Vertical C/D ratio by OCT (Figure 3.3) showed a significant increase at 6 months (0.42 ± 0.20 , $p=0.0014$), 12 months (0.43 ± 0.19 , $p=0.0009$) and 24 months (0.44 ± 0.18 , $p=0.0009$) compared to baseline (0.39 ± 0.21). Vertical C/D ratio remained consistent in the control group, being 0.47 ± 0.24 at baseline, 0.47

Table 3.2. Changes in RNFL thickness (μm) over the course of 24 months in the control and anti-VEGF groups.

	Baseline	6 months	12 months	24 months	P-Value*
Average					
Control	84.33 \pm 15.51	84.00 \pm 14.94	83.19 \pm 13.42	83.10 \pm 13.73	0.61
anti-VEGF	98.37 \pm 18.89	90.03 \pm 14.40	87.97 \pm 12.76	87.47 \pm 11.81	0.0001
Superior					
Control	99.52 \pm 24.43	99.86 \pm 23.57	97.43 \pm 23.13	96.05 \pm 21.47	0.54
anti-VEGF	113.50 \pm 18.85	109.10 \pm 21.04	107.00 \pm 19.49	104.90 \pm 18.14	0.0001
Inferior					
Control	103.10 \pm 22.61	101.60 \pm 20.94	101.00 \pm 19.45	101.00 \pm 19.28	0.63
anti-VEGF	122.60 \pm 33.94	111.00 \pm 19.89	108.30 \pm 18.29	107.80 \pm 17.80	0.0001
Temporal					
Control	63.05 \pm 12.36	64.81 \pm 11.82	63.57 \pm 11.75	64.43 \pm 14.65	0.64
anti-VEGF	80.07 \pm 25.74	67.07 \pm 14.09	66.20 \pm 13.16	66.83 \pm 14.30	0.0001
Nasal					
Control	71.90 \pm 15.92	69.76 \pm 14.91	70.76 \pm 12.45	69.86 \pm 13.47	0.50
anti-VEGF	77.73 \pm 16.15	73.10 \pm 15.84	70.27 \pm 12.80	69.93 \pm 12.64	0.0001

RNFL = retinal nerve fiber layer

*Repeated Measures ANOVA

Figure 3.2. Interval changes in cup volume measured on the OCT at baseline, 6, 12, and 24 months in the control and anti-VEGF groups. p-value: control group differences between baseline and follow-up measurements, paired t-test. p'-value: anti-VEGF group differences between baseline and follow-up measurements, paired t-test.

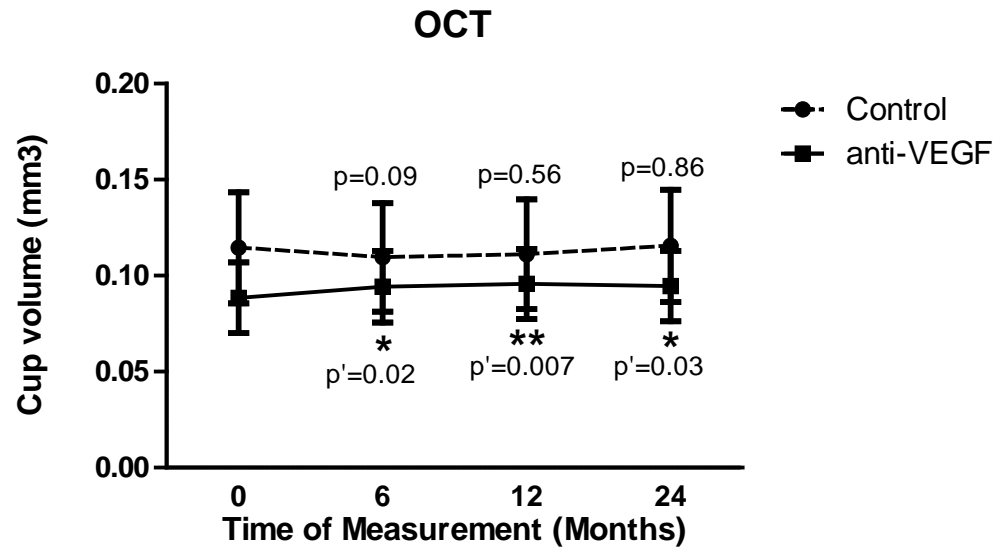
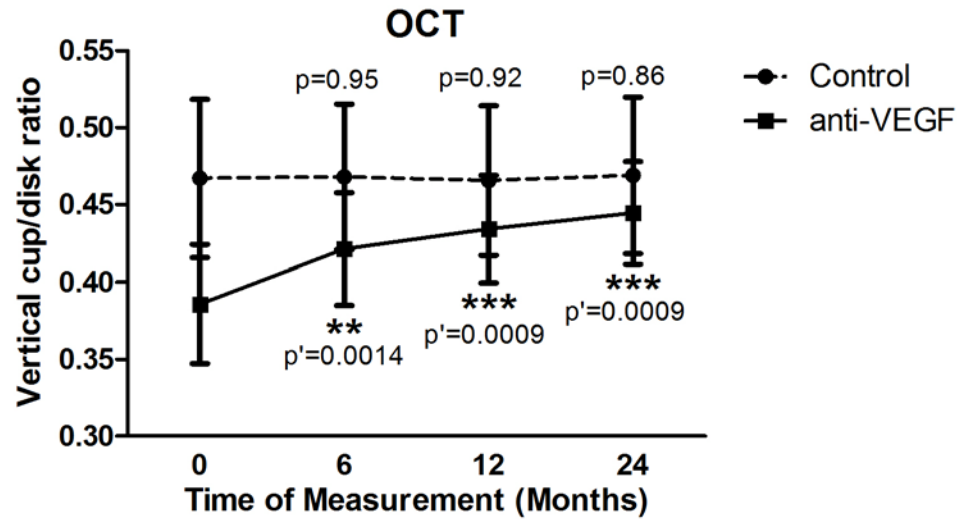


Figure 3.3. Interval changes in vertical cup/disk ratio measured on the OCT at baseline, 6, 12, and 24 months in the control and anti-VEGF groups. p-value: control group differences between baseline and follow-up measurements, paired t-test. p'-value: anti-VEGF group differences between baseline and follow-up measurements, paired t-test.



± 0.22 at 6 months ($p=0.95$), 0.47 ± 0.22 at 12 months ($p=0.92$) and 0.54 ± 0.23 at 24 months ($p=0.86$). When assessing participants receiving less than 10 injections ($n=15$) and those that received 10 or more injections ($n=15$), participants that received 10 or more injections showed a significant increase in the vertical C/D ratio at 6 months (0.48 ± 0.16 , $p=0.03$), 12 months (0.49 ± 0.14 , $p=0.01$) and 24 months (0.50 ± 0.14 , $p=0.002$) compared to baseline (0.44 ± 0.18) (Figure 3.4). Participants that received less than 10 injections showed a non-significant increase in the vertical C/D ratio at 6 months (0.36 ± 0.22 , $p=0.10$), 12 months (0.37 ± 0.22 , $p=0.08$) or 24 months (0.38 ± 0.21 , $p=0.07$) compared to baseline (0.33 ± 0.23).

Two glaucoma specialists were assigned to independently grade the vertical C/D ratios in the same eyes that received anti-VEGF injections using stereo photographs (Figure 3.5A). Both grader 1 and 2 indicated there was a significant increase in the vertical C/D ratio over the course of 2 years. At baseline, the mean vertical C/D was 0.309 ± 0.17 and grader 1 noted an increase at 6 months (0.320 ± 0.16 , $p=0.06$), with a further significant increase at 12 months (0.322 ± 0.17 , $p=0.03$) and 24 months (0.324 ± 0.17 , $p=0.03$). Grader 2 indicated baseline mean vertical C/D ratio of 0.309 ± 0.11 and noted a significant increase at 6 months (0.338 ± 0.11 , $p=0.02$), with a further increase at 12 months (0.353 ± 0.12 , $p=0.005$) and 24 months (0.379 ± 0.14 , $p=0.0006$). The graders also graded control eyes of diabetic patients not requiring anti-VEGF treatment. Both grader 1 and 2 found that over 24 months, there was no significant difference ($p \geq 0.17$) (Figure 3.5B).

Figure 3.4. Interval changes in vertical cup/disk ratio measured on the OCT at baseline, 6, 12, and 24 months in participants receiving less than 10 injections and 10 or more injections. p-value: differences between baseline and follow-up measurements of participants receiving less than 10 injections, paired t-test. p'-value: differences between baseline and follow-up measurements of participants receiving 10 or more injections, paired t-test.

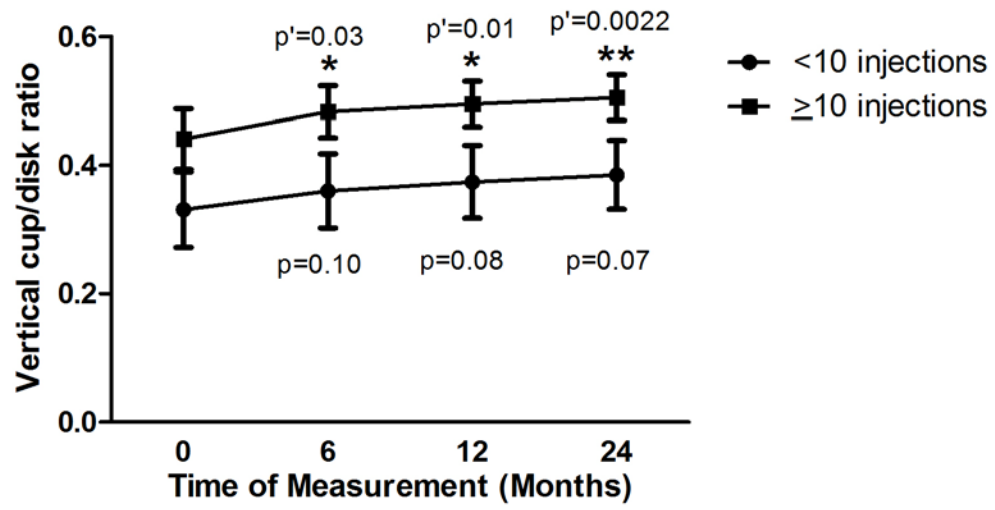
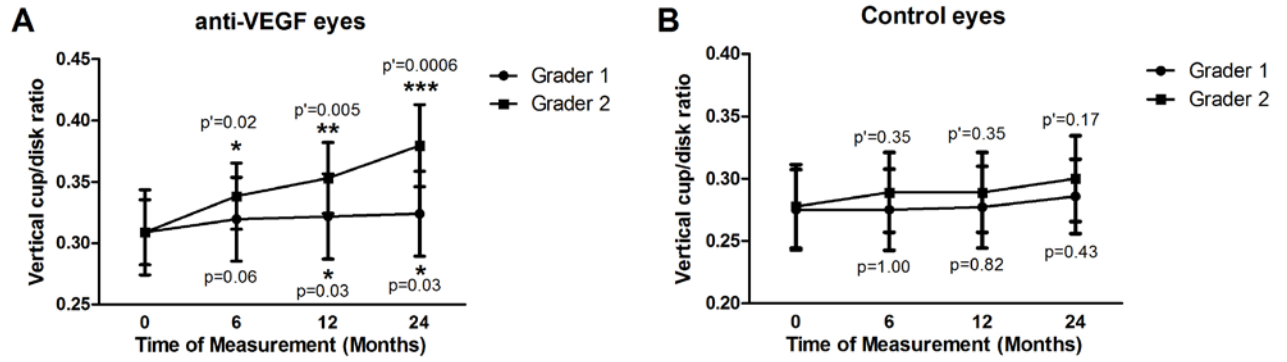


Figure 3.5. Interval changes in vertical cup/disk ratio measured by two masked glaucoma specialists using stereo photographs at baseline, 6, 12, and 24 months in the **(A)** anti-VEGF group and the **(B)** control group. p-value: grader 1 differences between baseline and follow-up measurements, paired t-test. p'-value: grader 2 differences between baseline and follow-up measurements, paired t-test.



Visual field tests had an average baseline mean deviation (MD) (Figure 3.6A) in the anti-VEGF group of -2.37 ± 3.72 dB. Mean deviation improved at 6 months by 0.72 dB (-1.65 ± 4.06 dB, $p=0.052$) but returned to baseline levels by 12 months (-2.40 ± 4.42 dB, $p=0.93$) and worsened by 24 months (-3.01 ± 4.50 , $p=0.10$). The control group showed no significant differences in visual field MD at baseline (-3.85 ± 6.38 dB), 6 months (-3.65 ± 5.52 dB, $p=0.71$), 12 months (-3.76 ± 4.93 dB, $p=0.89$), and 24 months (-4.22 ± 5.60 dB, $p=0.54$). Baseline mean best-corrected visual acuities (Figure 3.6B) were 0.24 ± 0.19 logMAR in the control group and 0.53 ± 0.35 logMAR in the anti-VEGF group. Visual acuity significantly improved to 0.34 ± 0.17 logMAR at 6 months ($p=0.0006$) and maintained this improvement, being 0.34 ± 0.22 logMAR at 12 months ($p=0.0001$) and 0.33 ± 0.15 logMAR at 24 months ($p=0.0006$). Visual acuity remained consistent in the control group, being 0.24 ± 0.19 logMAR at baseline, 0.25 ± 0.19 logMAR at 6 months ($p=0.59$), 0.24 ± 0.19 logMAR at 12 months ($p=0.69$) and 0.25 ± 0.20 logMAR at 24 months ($p=0.45$). The changes were not statistically significant.

In the anti-VEGF group, intraocular pressure (IOP) remained consistent over the two-year time period (Figure 3.7). At baseline, it was 16.57 ± 2.89 mmHg and slightly decreased to 16.53 ± 3.33 mmHg at 6 months ($p=0.96$). At 12 months ($p=0.94$), it was at 16.60 ± 3.09 mmHg and remained constant by 24 months (16.63 ± 3.09 mmHg, $p=0.91$). In the control group, IOP remained constant, being 16.67 ± 2.87 mmHg at baseline, 16.52 ± 3.19 mmHg at 6 months ($p=0.82$), 16.43 ± 2.93 mmHg at 12 months ($p=0.63$) and 16.52 ± 3.67 mmHg at

24 months ($p=0.85$). The changes were not statistically significant.

Figure 3.6. Interval changes in mean deviation measured on the **(A)** Humphrey Visual Field Analyzer and **(B)** visual acuity at baseline, 6, 12, and 24 months in the control and anti-VEGF groups. p-value: control group differences between baseline and follow-up measurements, paired t-test. p'-value: anti-VEGF group differences between baseline and follow-up measurements, paired t-test.

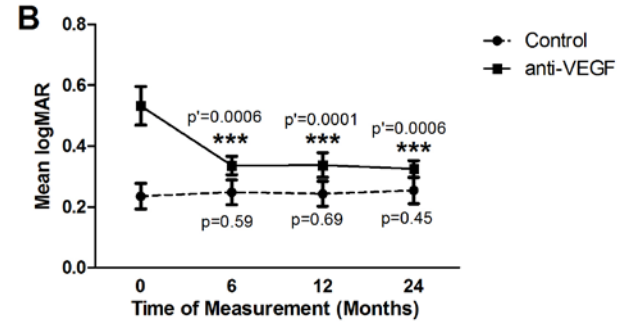
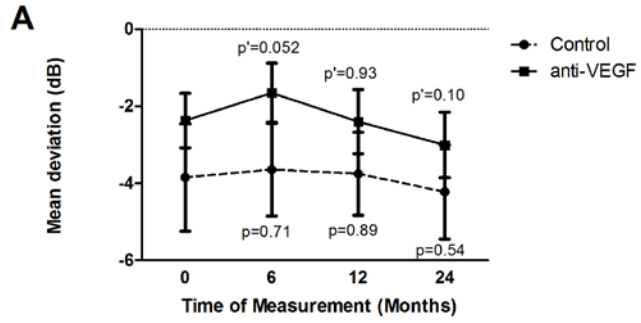
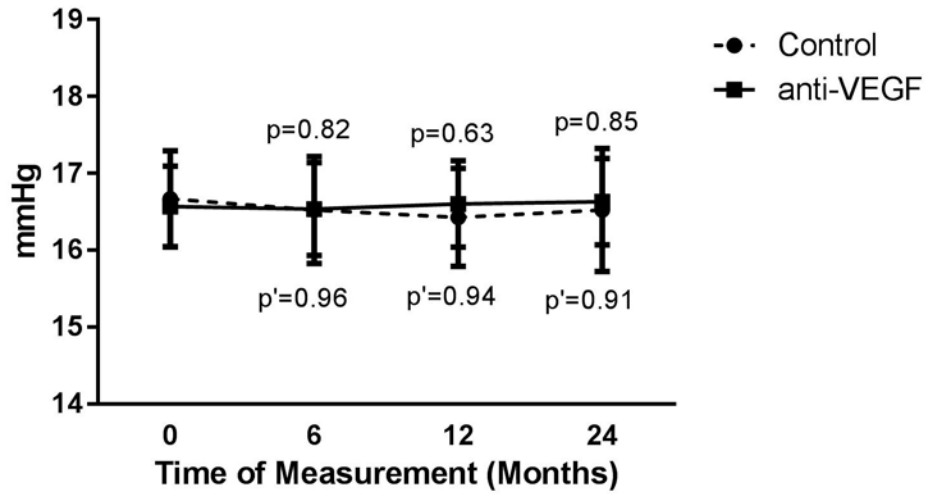


Figure 3.7. Interval changes in intraocular pressure at baseline, 6, 12, and 24 months in the control and anti-VEGF groups. mmHg= millimeter of mercury. p-value: control group differences between baseline and follow-up measurements, paired t-test. p'-value: anti-VEGF group differences between baseline and follow-up measurements, paired t-test.



3.4 Discussion

The 24 month results from the study demonstrate that during anti-VEGF therapy, the macular thickness significantly decreased by 6 months and, while the patients were undergoing therapy, remained lowered over a 24 month time period. Mean BCVA improved by roughly 4 lines of vision at 6 months and the improvement was maintained over a 24 month period of undergoing therapy. The results were expected and coincide with previously published anti-VEGF landmark studies⁴³⁻⁵⁰. The RESTORE study demonstrated that ranibizumab monotherapy alone, or when combined with a laser treatment, is more effective in improving BCVA than only undergoing the laser treatment and, overall, the health-related quality of life is improved⁴⁸. The RISE and RIDE studies have shown that, compared to sham injections, intravitreal injections of ranibizumab (Lucentis) improve BCVA and decrease macular thickness caused by edema⁵⁰. The landmark studies have cemented anti-VEGF therapy as the standard of care for DME treatment. In all instances of anti-VEGF therapy, VEGF is blocked in the diabetic eye, reducing blood vessel proliferation and leakage. If the leakage is centralized within the macula, anti-VEGF therapy reduces macular edema, decreasing the overall macular thickness and in turn improving central vision.

To determine whether anti-VEGF therapy in DME patients results in retinal reperfusion, the amount of ischemia was quantified using the mean perfused ratio. According to the analysis of fluorescein angiography photographs from the RISE and RIDE trials, patients receiving sham injections, as compared to those receiving ranibizumab, had faster progression of retinal nonperfusion⁵¹. The

mean perfused ratio was calculated by the concentric rings method which has been previously utilized by *Nicholson et al*⁴¹. Compared to the standard ischemic index method, wherein the grader draws the ratio of area perfused to the total area graded, the concentric rings method utilizes a set template. The method has a perfect agreement with the ischemic index method, a higher inter-grader agreement, and a short-grading time⁴¹. Using the concentric rings method, there was a significant increase in perfusion of patients in the anti-VEGF group up until 12 months. The increased level of perfusion remained unchanged when measured at 24 months. The control eyes showed no change in perfusion. These results correlate with those of a past study which examined anti-VEGF reperfusion in diabetic retinopathy patients within 5 months of having an injection⁵². That study used standard grading of the reperfusion and quantified using ImageJ software. Roughly 75% of the patient's demonstrated reperfusion⁵². With a higher sample size, longer time-frame, and a different method of analyzing perfusion, our results verify the previous findings. The results suggest that although diabetes remains a contributing factor, the improvement in the degree of ischemia is most likely a result of the anti-VEGF treatment through the stabilization of blood vessels and other unknown mechanisms.

The average RNFL thickness measured from the start of anti-VEGF treatment, significantly decreased over a 24-month time period. Analyzing each quadrant separately, the superior, inferior, temporal, and nasal regions of the RNFL all showed significant decrease over a 24-month time period in patients undergoing anti-VEGF therapy but not in control patients. The greatest observed

change in thickness occurred within the first 6 months. Up until the 6 month period, anti-VEGF treatments are often administered monthly until the patient becomes clinically stable and then receives injections on an as needed basis. A recent study has examined RNFL thickness in diabetic patients in comparison to normal controls. Despite diabetics having a thinner RNFL compared to normal controls, there was no significant reduction of RNFL thickness in both groups over a two-year follow-up period⁵³. Past studies have examined patients affected with age related macular degeneration (AMD). The studies report that patients undergoing long-term anti-VEGF therapy have a decreased retinal ganglion cell layer when compared to the untreated eye but show no change in RNFL thickness^{54, 55}. Due to the nature of the disease, people with diabetes are more sensitive to ocular changes than AMD patients and no other study has examined RNFL or optic nerve in DME patients undergoing anti-VEGF therapy.

The parapapillary RNFL is used as a surrogate measurement of the optic nerve status. When analyzing the optic nerve with OCT, the cup volume significantly increased over a 24-month time period in DME patients undergoing anti-VEGF therapy. The vertical C/D ratio also significantly increased by +0.06 over the time period. This is the first study to analyze the effects of anti-VEGF therapy on the optic nerve. No optic nerve edema was present in any of the patients as visualized by OCT. When assessing participants that received less than 10 anti-VEGF injections and patients that received 10 or more injections, participants that received 10 or more injections showed a significant increase in the vertical C/D ratio by +0.064 over the 24 month time period. Participants that

received less than 10 injections had a non-significant increase of +0.054 in the vertical C/D ratio. There was no significant difference ($p=0.16$) in baseline vertical C/D ratios between the two groups despite participants that had less than 10 injections having a mean baseline vertical C/D ratio of 0.33 ± 0.23 and participants that had 10 or more injections having a mean baseline vertical C/D ratio of 0.44 ± 0.18 .

To eliminate scanning error or results being influenced by the repeatability or reproducibility of the OCT, the vertical C/D ratios were graded by glaucoma specialists using stereo-photographs, which is the current gold standard for analyzing the optic nerve. Two glaucoma specialists, that were masked to the study, were assigned to grade the vertical C/D ratio in the same eyes following anti-VEGF treatment using stereo photographs. Similarly to the OCT results, both grader 1 and 2 indicated that there was a significant vertical C/D ratio increase over 12 months with grader 2 stating a further significant increase at 24 months. Grader 1 indicated there was a +0.02 increase in the vertical C/D ratio whereas, grader 2 indicated there was a +0.07 increase in the vertical C/D ratio over the course of 24 months. Even though there was a discrepancy in the grading method of the optic nerves by the two ophthalmologists, both graders indicated a significant increase in the C/D ratio during anti-VEGF therapy. The discrepancy has been observed in other studies of disc analysis suggesting that a more objective analysis is needed^{56, 57}. To confirm that the observed changes were due to the anti-VEGF therapy and not the graders themselves, the graders also assessed control eyes of diabetic patients not requiring anti-VEGF treatment.

Both grader 1 and 2 have found that over 24 months, there was no significant difference in the C/D ratios. The data combined with OCT results suggests that there are morphological changes that happen to the optic nerve in DME patients under anti-VEGF therapy which are not caused by glaucoma.

Overall, in regards to IOP results, there was no significant difference that occurred in patients over a 24-month treatment time frame. Mean IOP at baseline was 16.57 mmHg and 16.63 mmHg at 24 months. Past studies have shown conflicting results on whether or not long-term anti-VEGF usage results in sustained increase in IOP^{58, 59}. In the current study, that examined DME patients undergoing ranibizumab treatment for 24 months, no sustained increase in IOP was observed. Functionally, looking at the effects of anti-VEGF therapy on peripheral vision, visual field testing showed no significant difference. It is important to note from baseline to 6 months, visual fields slightly improved by 0.72 dB but from 6 months to 24 months, peripheral vision declined by -1.36 dB.

Previous studies have confirmed that structural changes in the retina precede functional changes^{60, 61, 62}. Although this is the longest study of its kind, we feel that analyzing patients over 24-months might not have been sufficient and thus, the time frame has limited the ability to detect more minute changes to the retina. In order to determine whether or not the effects of anti-VEGF therapy, as observed on RNFL, optic disk and ultimately peripheral vision, are indeed progressive and cause optic neuropathy, it would be enticing to extend the follow up period beyond 2 years. The next step would be to conduct a multi-center study analyzing common anti-VEGFs such as ranibizumab, bevacizumab and

aflibercept. While sharing the same basic mechanism, anti-VEGFs all have different molecular characteristics, which cause differences in potency, systemic clearance, and systemic VEGF inhibition^{50, 63}. It would be valuable to determine whether higher affinity anti-VEGFs result in greater changes to the optic nerve as well as if any predictive factors affect the changes to the optic nerve in regards to progress and the rate.

This is the first study to analyze long-term structural and functional changes to the retina and optic nerve in DME patients undergoing anti-VEGF therapy. As such, the current study sought to obtain comprehensive results. The analyses of the optic nerve included both structural and functional tests, and grading of stereo photographs by glaucoma specialists to detect any early changes in the optic nerve in patients starting anti-VEGF treatments.

In conclusion, anti-VEGF therapy may potentially be detrimental to the optic nerve by decreasing RNFL thickness, increasing cup volume and increasing vertical cup/disk ratio over time as measured on OCT and through grading of stereo photographs by glaucoma specialists. Patients that received 10 or more injections had a significant increase in the vertical C/D ratios compared to the patients that received less than 10 injections. Despite an improvement in peripheral perfusion, there was a slight decline of peripheral visual fields from 6 to 24 months in DME patients undergoing anti-VEGF therapy. The results provide a cautionary note to monitor both the retina and optic nerve status in patients undergoing frequent anti-VEGF injections.

3.5 References

1. Kaur C, Foulds W, Ling E. Blood-retinal barrier in hypoxic ischaemic conditions: basic concepts, clinical features and management. *Progress In Retinal And Eye Research* 2008;27(6):622-647.
2. Porte D, Sherwin RS, Baron A, Ellenberg M, Rifkin H. *Ellenberg & Rifkins diabetes mellitus*. New York: McGraw-Hill, Medical Pub. Division; 2003.
3. Holt RIG, Cockram CS, Flyvbjerg A, Goldstein BJ. *Textbook of diabetes*. 4th ed. Chichester, West Sussex, UK: Wiley Blackwell; 2010.
4. Diabetes and Your Eyesight. *Diabetes and Your Eyesight | Glaucoma Research Foundation*. <http://www.glaucoma.org/glaucoma/diabetes-and-your-eyesight.php>. Accessed May 16, 2017.
5. Osaadon P, Fagan XJ, Lifshitz T, Levy J. A review of anti-VEGF agents for proliferative diabetic retinopathy. *Eye (Lond)* 2014;28(5):510-520.
6. Simó R, Hernández C. Intravitreal anti-VEGF for diabetic retinopathy: hopes and fears for a new therapeutic strategy. *Diabetologia* 2008;51(9):1574-1580.
7. Hernández C, Simó R. Strategies for blocking angiogenesis in diabetic retinopathy: from basic science to clinical practice. *Expert Opin Invest Drugs* 2007;16:1209-1226

8. Spaide RF, Fisher YL. Intravitreal bevacizumab (Avastin) treatment of proliferative diabetic retinopathy complicated by vitreous hemorrhage. *Retina* 2006;26:275-278.
9. Oshima Y, Sakaguchi H, Gomi F, Tano Y. Regression of iris neovascularization after intravitreal injection of bevacizumab in patients with proliferative diabetic retinopathy. *Am J Ophthalmol* 2006;142:155-158.
10. Chen E, Park CH (2006) Use of intravitreal bevacizumab as a preoperative adjunct for tractional retinal detachment repair in severe proliferative diabetic retinopathy. *Retina* 2006;26:699-700.
11. Avery RL, Pearlman J, Pieramici DJ, Rabena MD, Castellarin AA, Nasir MAA et al. Intravitreal Bevacizumab (Avastin) in the Treatment of Proliferative Diabetic Retinopathy. *Ophthalmology* 2006;113(10):e1-15.
12. Jorge R, Costa RA, Calucci D, Cintra LP, Scott IU. Intravitreal bevacizumab (Avastin) for persistent new vessels in diabetic retinopathy (IBEPE study). *Retina* 2006;26:1006-1013.
13. Arevalo JF, Wu L, Sanchez JG, Maia M, Saravia MJ, Fernandez CF. Intravitreal bevacizumab (avastin) for proliferative diabetic retinopathy: 6-months follow-up. *Eye (Lond)* 2007;23(1):117-123.

14. Ishikawa K, Honda S, Tsukahara Y, Negi A. Preferable use of intravitreal bevacizumab as a pretreatment of vitrectomy for severe proliferative diabetic retinopathy. *Eye (Lond)* 2007;23(1):108-111.
15. Cunningham ET Jr1, Adamis AP, Altaweel M, Aiello LP, Bressler NM, D'Amico DJ et al. A Phase II randomized double-masked trial of pegaptanib, an anti-vascular endothelial growth factor aptamer, for diabetic macular edema. *Ophthalmology* 2005;112(10):1747-1757
16. Chun DW, Heier JS, Topping TM, Duker JS, Bankert JM. A pilot study of multiple intravitreal injections of ranibizumab in patients with center-involving clinically significant diabetic macular edema. *Ophthalmology* 2006;113:1706-1712.
17. Nguyen QD, Tatlipinar S, Shah SM, Haller JA, Quinlan E, Sung J. Vascular Endothelial Growth Factor Is a Critical Stimulus for Diabetic Macular Edema. *American Journal of Ophthalmology* 2006;142(6):961-969.
18. Haritoglou C, Kook D, Neubauer A, Wolf A, Priglinger S, Strauss R. Intravitreal Bevacizumab (Avastin) Therapy For Persistent Diffuse Diabetic Macular Edema. *Retina* 2006;26(9):999-1005.
19. Arevalo JF1, Fromow-Guerra J, Quiroz-Mercado H, Sanchez JG, Wu L, Maia M et al. Primary intravitreal bevacizumab (Avastin) for diabetic

- macular edema: results from the Pan-American Collaborative Retina Study Group at 6-month follow-up. *Ophthalmology* 2007;114(4):743-750.
20. Diabetic Retinopathy Clinical Research Network¹, Scott IU, Edwards AR, Beck RW, Bressler NM, Chan CK, Elman MJ et al. A Phase II Randomized Clinical Trial of Intravitreal Bevacizumab for Diabetic Macular Edema. *Ophthalmology* 2007;114(10):1860-1867.
 21. Ahmadi H, Ramezani A, Shoeibi N, Bijanzadeh B, Tabatabaei A, Azarmina M et al. Intravitreal bevacizumab with or without triamcinolone for refractory diabetic macular edema; a placebo-controlled, randomized clinical trial. *Graefes Arch Clin Exp Ophthalmol* 2007;246(4):483-489.
 22. Kumar A, Sinha S. Intravitreal bevacizumab (Avastin) treatment of diffuse diabetic macular edema in an Indian population. *Indian J Ophthalmol* 2007;55:451-455.
 23. Gragoudas ES, Adamis AP, Cunningham ET, Feinsod M, Guyer DR. Pegaptamib for neovascular age-related macular degeneration. *N Engl J Med* 2004;351:2805-2816.
 24. Rosenfeld PJ¹, Brown DM, Heier JS, Boyer DS, Kaiser PK, Chung CY et al. Ranibizumab for neovascular age-related macular degeneration. *N Engl J Med* 2006;355(4):1419–1431

25. Brown DM, Kaiser PK, Michels M, Soubrane G, Heier JS, Kim RY et al. Ranibizumab versus verteporfin for neovascular age-related macular degeneration. *N Engl J Med* 2006;355(14):1432-1444.
26. Heier JS, Boyer DS, Ciulla TA, Ferrone PJ, Jumper JM, Gentile RC et al. Ranibizumab Combined With Verteporfin Photodynamic Therapy in Neovascular Age-Related Macular Degeneration. *Arch Ophthalmol* 2006;124(11):1532-1542.
27. Mathalone N, Arodi-Golan A, Sar S, Wolfson Y, Shalem M, Lavi I et al. Sustained elevation of intraocular pressure after intravitreal injections of bevacizumab in eyes with neovascular age-related macular degeneration. *Graefes Arch Clin Exp Ophthalmol* 2012;250(10):1435-1440.
28. Arikan G, Saatci AO, Oner FH. Immediate intraocular pressure rise after intravitreal injection of ranibizumab and two doses of triamcinolone acetonide. *International Journal Of Ophthalmology* 2011;4 (4):402.
29. Good T J, Kimura AE, M Ava N, Kahook MY. Sustained elevation of intraocular pressure after intravitreal injections of anti-VEGF agents. *British Journal Of Ophthalmology* 2011;95 (8):1111-1114.
30. Tseng J, Vance S, Della Torre K, Mendonca L, Cooney M, Klancnik, J. Sustained increased intraocular pressure related to intravitreal antivascular endothelial growth factor therapy for neovascular age-related macular degeneration. *J Glaucoma* 2012;21(4):241-247.

31. Bakri S, Moshfeghi D, Francom S, Rundle A, Reshef D, Lee, P. Intraocular Pressure in Eyes Receiving Monthly Ranibizumab in 2 Pivotal Age-Related Macular Degeneration Clinical Trials. *Ophthalmology* 2014;121(5):1102-1108.
32. Singh R, Kim J. Ocular hypertension following intravitreal anti-vascular endothelial growth factor agents. *Drugs & Aging* 2012;29(12):949-956.
33. Fujimoto JG. *Optical Coherence Tomography of Ocular Diseases*. 2nd ed. Thorofare, NJ: Slack Inc;2004:714.
34. Mwanza J-C, Oakley JD, Budenz DL, Anderson DR. Ability of Cirrus HD-OCT Optic Nerve Head Parameters to Discriminate Normal from Glaucomatous Eyes. *Ophthalmology* 2011;118(2).
35. Foo L-L, Perera SA, Cheung CY, et al. Comparison of scanning laser ophthalmoscopy and high-definition optical coherence tomography measurements of optic disc parameters. *Br J Ophthalmol* 2012;96(4):576-580.
36. Meditec CZ. *Stratus OCT User's Manual*. Dublin, CA: Carl Zeiss Meditec; 2003.
37. Vizzeri G, Balasubramanian M, Bowd C, Weinreb RN, Medeiros FA, Zangwill LM. Spectral domain-optical coherence tomography to detect localized retinal nerve fiber layer defects in glaucomatous eyes. *Opt Express* 2009;17(5):4004.

38. Alencar LM, Bowd C, Weinreb RN, Zangwill LM, Sample PA, Medeiros FA. Comparison of HRT-3 Glaucoma Probability Score and Subjective Stereophotograph Assessment for Prediction of Progression in Glaucoma. *Invest Ophthalmol Vis Sci* 2008;49(5):1898.
39. Kummet CM, Zamba KD, Doyle CK, Johnson CA, Wall M. Refinement of Pointwise Linear Regression Criteria for Determining Glaucoma Progression. *Invest Ophthalmol Vis Sci* 2013;54(9):6234.
40. Wessel MM, Aaker GD, Parlitsis G, Cho M, D'amico DJ, Kiss S. Ultra-Wide-Field Angiography Improves The Detection And Classification Of Diabetic Retinopathy. *Retina* 2012;32(4):785-791.
41. Nicholson L, Vazquez-Alfageme C, Ramu J, et al. Validation of Concentric Rings Method as a Topographic Measure of Retinal Nonperfusion in Ultra-Widefield Fluorescein Angiography. *Am J Ophthalmol* 2015;160(6).
42. Blodi BA, Domalpally A, Scott IU, Ip MS, Oden NL, Elledge J, et al. Standard Care vs Corticosteroid for Retinal Vein Occlusion (SCORE) Study system for evaluation of stereoscopic color fundus photographs and fluorescein angiograms: SCORE Study Report 9. *Arch Ophthalmol* 2010;128(9):1140-1145.
43. Nguyen QD, Shah SM, Heier JS, Do DV, Lim J, Boyer D et al. Primary End Point (Six Months) Results of the Ranibizumab for Edema of the

- mAcula in Diabetes (READ-2) Study. *Ophthalmology* 2009;116(11):2175-2181.
44. Nguyen QD, Shah SM, Khwaja AA, Channa R, Hatef E, Do DV et al. Two-Year Outcomes of the Ranibizumab for Edema of the mAcula in Diabetes (READ-2) Study. *Ophthalmology* 2010;117(11):2146-2151.
45. Do DV, Nguyen QD, Khwaja AA, Channa R, Sepah YJ, Sophie R et al. Ranibizumab for Edema of the Macula in Diabetes Study. *JAMA Ophthalmol* 2013;131(2):139-145.
46. Do DV, Sepah YJ, Boyer D, Callanan D, Gallemore R, Bennett M et al. Month-6 primary outcomes of the READ-3 study (Ranibizumab for Edema of the mAcula in Diabetes—Protocol 3 with high dose). *Eye (Lond)* 2015;29(12):1538-1544.
47. Massin P, Bandello F, Garweg JG, Hansen LL, Harding SP, Larsen M et al. Safety and Efficacy of Ranibizumab in Diabetic Macular Edema (RESOLVE Study): A 12-month, randomized, controlled, double-masked, multicenter phase II study. *Diabetes Care* 2010;33(11):2399-2405.
48. Mitchell P1, Bandello F, Schmidt-Erfurth U, Lang GE, Massin P, Schlingemann RO et al. The RESTORE study: ranibizumab monotherapy or combined with laser versus laser monotherapy for diabetic macular edema. *Ophthalmology* 2011;118(4):615-625.

49. Ishibashi T, Li X, Koh A, Lai TY, Lee FL, Lee WK et al. The REVEAL Study: Ranibizumab Monotherapy or Combined with Laser versus Laser Monotherapy in Asian Patients with Diabetic Macular Edema. *Ophthalmology* 2015;122(7):1402-1415.
50. Brown DM, Nguyen QD, Marcus DM, Boyer DS, Patel S, Feiner L et al. Long- term Outcomes of Ranibizumab Therapy for Diabetic Macular Edema: The 36-Month Results from Two Phase III Trials. *Ophthalmology* 2013;120(10):2013- 2022.
51. Campochiaro PA, Wykoff CC, Shapiro H, Rubio RG, Ehrlich JS. Neutralization of Vascular Endothelial Growth Factor Slows Progression of Retinal Nonperfusion in Patients with Diabetic Macular Edema. *Ophthalmology*. 2014;121(9):1783-1789.
52. Levin A, Rusu I, Orlin A, Gupta M, Coombs P, Damico D et al. Retinal reperfusion in diabetic retinopathy following treatment with anti-VEGF intravitreal injections. *Clin Ophthalmol* 2017;11:193-200.
53. Takis A, Alonistiotis D, Ioannou N, Kontou E, Mitsopoulou M, Papaconstantinou D. Follow-up of the retinal nerve fiber layer thickness of diabetic patients type 2, as a predisposing factor for glaucoma compared to normal subjects. *Clin Ophthalmol* 2017;11:1135-1141.
54. Beck M, Munk MR, Ebnetter A, Wolf S, Zinkernagel MS. Retinal Ganglion Cell Layer Change in Patients Treated With Anti–Vascular Endothelial

- Growth Factor for Neovascular Age-related Macular Degeneration. *Am J Ophthalmol* 2016;167:10-17.
55. Saleh R, Karpe A, Zinkernagel MS, Munk MR. Inner retinal layer change in glaucoma patients receiving anti-VEGF for neovascular age related macular degeneration. *Graefes Arch Clin Exp Ophthalmol* 2017;255(4):817-824.
56. Lim MC. Effect of Diabetic Retinopathy and Panretinal Photocoagulation on Retinal Nerve Fiber Layer and Optic Nerve Appearance. *Arch Ophthalmol* 2009;127(7):857-862.
57. Chauhan BC, Burgoyne CF. From Clinical Examination of the Optic Disc to Clinical Assessment of the Optic Nerve Head: A Paradigm Change. *Am J Ophthalmol* 2013;156(2).
58. Hariprasad S, Nariani A, Williams B. Long-term effect of anti-vascular endothelial growth factor injections on intraocular pressure. *Indian J Ophthalmol* 2016;64(9):643.
59. Baek SU, Park IW, Suh W. Long-term intraocular pressure changes after intravitreal injection of bevacizumab. *Cutan Ocul Toxicol* 2016;35(4):310-314.
60. Kragstrup TW, Kjaer M, Mackey AL. Structural, biochemical, cellular, and functional changes in skeletal muscle extracellular matrix with aging. *Scand J Med Sci Sports* 2011;21(6):749-757.

61. Greenstein VC, Duncker T, Holopigian K, Carr RE, Greenberg JP, Tsang SH et al. Structural And Functional Changes Associated With Normal And Abnormal Fundus Autofluorescence In Patients With Retinitis Pigmentosa. *Retina* 2012;32(2):349-357.
62. Ismael ZF, El-Shazly AAE-F, Farweez YA, Osman MMM. Relationship between functional and structural retinal changes in myopic eyes. *Clin Exp Optom* 2017.
63. Chakravarthy U, Harding SP, Rogers CA, Downes SM, Lotery AJ, Wordsworth S. Ranibizumab versus Bevacizumab to Treat Neovascular Age-related Macular Degeneration. *Ophthalmology* 2012;119(7):1399-1411.

Chapter 4

4 Retinal cell death following anti-VEGF treatment in a diabetic rat model and retinal cell culture

The chapter addresses specific objectives outlined in aims 4 and 5:

4. To evaluate the effect of VEGF inhibition on neuronal cells in a STZ-induced diabetic rat retina by performing intravitreal anti-VEGF injections with different doses.
5. To determine if exposure to different doses of anti-VEGF alter retinal cells metabolic activity and function or induce toxicity by various colorimetric assays.

4.1 Introduction

Diabetic retinopathy (DR) is the result of microvascular retinal changes caused by hyperglycemia which alter the blood-retinal barrier (BRB). In DR, hyperglycemia results in enhanced production of vascular endothelial growth factors (VEGF), advanced glycated end products, nitric oxide, oxidative stress and inflammation within the eye¹. The factors increase the permeability of BRB, resulting in accumulation of extracellular fluid within the retina and the development of diabetic macular edema (DME). If the leakage is centralized within the macula, the condition may lead to significant loss of central visual function and acuity.

Inhibition of these unregulated factors can reduce the developing leakage, so the gold standard treatment for DME is intravitreal anti-VEGF injections². Intravitreal anti-VEGF injections inhibit the action of VEGF, decreasing permeability, leakage, and proliferation of blood vessels. While excess VEGF is harmful, past studies have found that VEGF is involved in neuroprotection by protecting retinal cells against the damaging insults of hypoxia, glutamate excitotoxicity and deprivation of serum³⁻¹⁰.

Over the past decade, there have been increased clinical reports of diabetic patients on anti-VEGF therapy developing signs of glaucoma and optic neuropathy. Diabetes is already a risk factor for the development of glaucoma and the use of anti-VEGFs might augment the risk¹¹. In addition to this, our past research has demonstrated that over 24 months, DME patients undergoing anti-

VEGF therapy have decreased retinal nerve fiber layer (RNFL) thickness, increased cup volume, increased vertical cup/disk (C/D) ratio that is dependent on number of injections and show deterioration of peripheral vision. There is an uncertainty in regards to whether eliminating the neuroprotective role of VEGF through anti-VEGF therapy causes optic neuropathy and death of retinal cells. With newer, higher affinity anti-VEGFs being introduced into the market, the question remains whether or not neuronal cells in the diabetic retina may be further affected by the treatment.

The purpose of the following study is to examine whether increased exposure to anti-VEGFs will result in increased retinal cell death. First, the effects of VEGF inhibition on neuronal cells in a streptozotocin (STZ)-induced diabetic rat retina will be evaluated by performing intravitreal anti-VEGF injections of different doses. Second, we will determine whether the exposure to different doses of anti-VEGF alters retinal cells metabolic activity or induces toxicity by various colorimetric assays.

4.2 Methods

4.2.1 Diabetic Animal Model

Experimental protocols were approved by Animal Use Committee of Western University. Animals were approved by Animal Care and Veterinary Services (ACVS) of Western University and complied with the NIH Guide for the Care and Use of Laboratory Animals (NIH publication no. 80-23, revised in 1996). Animal care adhered to the Guiding Principles in the Care and Use of Animals.

Male Sprague-Dawley rats (250-300 grams, 7-8 weeks old) were obtained from Charles River (Charles River Canada Ltd., Saint-Constant, Quebec, Canada). Diabetes was induced in 25 randomly selected rats by a single intraperitoneal injection of streptozotocin (STZ) (Sigma-Aldrich, St. Louis, MO, 65mg/kg in citrate buffer at a pH of 5.6)¹². The remaining 25 rats were designated as control and were injected with an identical volume of citrate buffer^{13, 14}. Three days following STZ injection, the blood glucose levels for each rat were measured on an automated OneTouch Ultra glucometer (LifeScan Inc., Milpitas, California, USA). A blood glucose reading of >20 mmol/L was considered diabetic and the rat was used for further experimentation. To prevent ketoacidosis, diabetic rats were injected with an insulin implant (2 U/d, Linshin Canada Inc., Toronto, Ontario, Canada) that released small doses of insulin. For the duration of 5 months, diabetic rats were routinely monitored through body weight measurements and monitoring of blood glucose levels. The control and diabetic groups were comprised of five animals for each experimental procedure.

4.2.2 Drug Administration

After 5 months, rats received intravitreal injections. For each intravitreal injection, rats were anesthetized with 4% isoflurane during the induction phase and 3% for maintenance level. Prior to the injection, the eye was disinfected with topical povidone iodine eye drops. A 30 gauge needle was used to administer the intravitreal injection to the inferior temporal quadrant, posterior to the limbus. For each rat, the right eye was the test eye and the left eye was the control, injected with saline. With 25 control rats and 25 STZ-induced diabetic rats, each group had a n=5 consisting of 5 rats receiving 1 unit of 0.3375 mg/mL (final concentration in the eye being 0.0625 mg/mL, which is half the clinical dose) injection, 5 rats receiving 1 unit 0.675 mg/mL (final concentration being 0.125 mg/mL, clinical dose) injection, and 5 rats receiving 1 unit 1.35 mg/mL (final concentration being 0.25 mg/mL-double the clinical dose) injection of rat anti-VEGF (AF564; R&D Systems, Minneapolis, MN, USA). Five rats also received 1 unit of Ranibizumab (Lucentis, 0.5 mg in 0.05 mL solution for injection; Novartis Pharmaceuticals Canada Inc., Quebec, Canada) at 0.675 mg/mL (final concentration being 0.125 mg/mL-clinical dose). These injections were performed once a week for 3 weeks to simulate the injection frequency of human patients receiving injections once a month for the duration of 3 months. The remaining 5 rats received an injection of 1 unit 0.675 mg/mL (final concentration being 0.125 mg/mL-clinical dose) only once to analyze the effects of frequency of injections. The needle remained in the eye for 3-4 seconds before being drawn out to avoid reflux. Once finished, the isoflurane was shut off and the rat was

maintained on oxygen until fully recovered. At week 4, rats were euthanized in a carbon dioxide gas chamber, eyes were enucleated, fixed in 4% paraformaldehyde for 24 hours and placed in 70% ethanol for paraffin embedding.

4.2.3 TUNEL Assay

Following paraffin-processing, the eye tissues were sectioned to a thickness of 4 μm along the sagittal plane of the eye and transferred to positively-charged, transparent microscope slides (VWR, Radnor, PA). The slides were stored in -80°C until staining. To evaluate tissue integrity, efficacy of tissue preservation and to determine optic nerve location, every tenth slide was stained with Hematoxylin and Eosin according to standard protocol.

TUNEL Assay was performed to evaluate apoptotic cells. The sections were dewaxed and stained using the TUNEL method according to the manufacturer's protocol (In Situ Cell Death Detection Kit, Fluorescein; Ref. 11684795910 Roche Applied Science, Indianapolis, Indiana, USA). In the assay, the enzyme terminal deoxynucleotidyl transferase catalyzes the reaction that labels the sites of DNA breaks with deoxyuridine. Slides were counterstained with 1 μM DAPI for 10 minutes at room temperature to identify nuclei and washed with phosphate-buffered saline (PBS) before being put under cover glass. Sections were imaged with a Zeiss LSM 510 META confocal microscope equipped with an AxioCam MR3 (Carl Zeiss Canada, North York, Ontario, Canada). To quantify the number of TUNEL-positive cells in the retina for the

control and diabetic rats, cell bodies were counted in each layer by two graders. The graders were masked to the type of animal and purpose of the study.

4.2.4 Mixed Retinal Cell Culture

Eyes from 1 week old Sprague-Dawley rats were enucleated en bloc, and placed in CO₂-independent medium supplemented with 0.1% antibiotic-antimycotic (Ref. 15240096 Thermo Fisher Scientific, Waltham, Massachusetts, USA) and 4mM L-glutamine. Eyes were dissected and retinas were extracted within 1 hour of enucleation. Retinal cells were washed with Hank's Balanced Salt Solution supplemented with 1% penicillin, placed in a 0.2% papain activated solution, and incubated in a 37°C water bath for 20 minutes with gentle stirring every 5 minutes. Digestion was stopped with the addition of 0.5 µL of DNase1 (114 U/µL) and 1mL of warm Neurobasal A medium (NBA) supplemented with 2% fetal bovine serum (FBS), 0.5 mM L-glutamine, and 2% B-27 (Ref. 17504044 Thermo Fisher Scientific, Waltham, Massachusetts, USA). Retinal cells were dissociated by trituration in NBA and the suspension was centrifuged at 68 xg for 4 minutes. The cell pellet was resuspended in fresh NBA. The cells were seeded at 5×10^5 cells per well onto 24-well plates containing 12-mm glass cover slips precoated sequentially with poly-D-lysine (2µg/cm² for 2 hours at 37°C) and laminin (1µg/cm² overnight at 37°C). Cells were maintained at 37°C in a 5% CO₂ incubator.

4.2.5 Dosage

NBA was refreshed two days after plating. On the fourth day of cultivation, the medium was removed from the mixed retinal cell cultures and replaced with

medium containing ranibizumab (Lucentis, Novartis Pharmaceuticals Canada Inc., Quebec, Canada) diluted down to clinical relevant concentrations (0.125 mg/mL) as well as half the clinical dose (0.0625 mg/mL) and double the clinical dose (0.25 mg/mL). Control wells contained only medium and no anti-VEGF (0 mg/mL). In another subset of experiments, mixed retinal cell cultures were also exposed to medium containing rat anti-VEGF (AF564; R&D Systems, Minneapolis, MN, USA) diluted down to the same concentrations. The cells were exposed to these concentrations for 48 or 72 hours at 37°C in a 5% CO₂ incubator.

4.2.6 Immunohistochemistry

Following 48 or 72 hours of exposure to anti-VEGF, the cells were fixed with 100% methanol for 5 minutes at -20°C for Thy 1.1 labelling. The cells were incubated for 1 hour at room temperature with 1% bovine serum albumin (BSA), 10% normal goat serum, and 0.3M glycine in 0.1% PBS-Tween as per the manufacturer's protocol. This increased the permeability of the cells and blocked non-specific protein-protein interactions. The cells were incubated for one hour at room temperature with a mouse anti-rat primary antibody against CD90/Thy 1.1 (1:200; ab225; Abcam, Toronto, Ontario, Canada) followed by a goat anti-mouse IgG secondary antibody conjugated to Alexa Fluor 488 (1:1000; Life Technologies Inc., Burlington, Ontario, Canada) at room temperature in the dark for 1 hour.

For double-labeling studies, cells were blocked in a blocking buffer consisting of 1X PBS, 5% normal goat serum, and 0.3% Triton X-100 for 1 hour

in room temperature as per the manufacturer's protocol. Primary and secondary antibodies were prepared in an antibody dilution buffer consisting of 1X PBS, 1% BSA, and 0.3% Triton X-100. The cells were incubated overnight at 4°C with a chicken anti-rat primary antibody Class III β -Tubulin antibody (1:400; TUJ-1; ab107216; Abcam, Toronto, Ontario, Canada), rabbit anti-rat primary Brn3a antibody (1:100; ab81213; Abcam, Toronto, Ontario, Canada), or rabbit anti-rat primary cleaved caspase-3 antibody (1:400; Asp175; Cell Signaling Technology Inc., Boston, Massachusetts, USA). After washing with PBS, cells were incubated for one hour in the dark with goat anti-chicken IgG secondary antibody, Texas Red (1:1000; Life Technologies Inc., Burlington, Ontario, Canada), and goat anti-rabbit IgG secondary antibody conjugated to Alexa Fluor 488 (1:1000; Life Technologies Inc., Burlington, Ontario, Canada). Cells were counterstained with 1 μ M DAPI for 10 minutes at room temperature to identify nuclei, washed with PBS, and mounted with Fluoromount G (Electron Microscopy Sciences, Hatfield, PA) on positively charged slides (VWR, Radnor, PA). Antibody concentrations were individually optimized to achieve optimal fluorescence with minimal background staining. Images were taken using a Zeiss Axio Imager.Z1 fluorescent microscope (Carl Zeiss Canada, Toronto, ON, Canada) equipped with an AxioCam MR3 (Carl Zeiss Canada).

Negative controls were utilized for every round of slide staining to eliminate suspicion of non-specific secondary antigen binding. For single-staining optimization experiments using anti-CD90/Thy 1.1, one slide was exposed to the appropriate secondary antibody in absence of its respective primary antibody.

For dual-staining experiments using both anti-TUJ-1 and anti-Brn3a or anti-cleaved caspase-3, one slide served as a control for each of the following conditions: TUJ-1 secondary antibody alone in absence of primary, Brn3a or cleaved caspase-3 secondary antibody alone in absence of primary, and both TUJ-1 and Brn3a or cleaved caspase-3 secondary antibodies in the absence of either primary antibody.

4.2.7 Colorimetric Assays

After 48 or 72 hours of treatment with the different doses of anti-VEGF, three colorimetric assays were performed; MTT (Thiazolyl Blue Tetrazolium Bromide) assay (M2128-1G; Sigma-Aldrich, St. Louis, Missouri, USA), lactate dehydrogenase (LDH) assay (11644793001; Roche Life Science, Laval, Quebec, Canada), and the cell death detection ELISA assay (11544675001; Roche Life Science, Laval, Quebec, Canada). The colorimetric assays were performed as per the manufacturers' instructions. The MTT assay assessed cellular metabolic activity of the experimental cells to the control. The LDH and cell death detection ELISA assays were used to evaluate cytotoxicity of the experimental cells to the control cells by examining cell death through necrosis in the LDH assay and cell death through apoptosis in the ELISA assay. Protein concentrations (23225; Pierce™ BCA Protein Assay Kit, Thermo Fisher Scientific, Waltham, Massachusetts, USA) were measured for each sample to normalize the absorption data of the LDH and cell death detection ELISA assays.

4.2.8 Statistical Analysis

Statistically analysis was performed using one-way ANOVA with a

Bonferroni's multiple comparison test and an unpaired t-test on the GraphPad Prism 5 software (GraphPad Software, La Jolla, CA). ANOVA with Bonferroni method was performed as outlined in J Neter, W Wasserman, and MH Kutner, Applied Linear Statistical Models, 3rd edition, Irwin, 1990. All data was expressed as mean \pm SD and accepted as statistically significant if $p < 0.05$. A correction of $p < 0.017$ was applied for the Bonferroni's multiple comparison test.

4.3 Results

4.3.1 Body weight and blood glucose levels

The body weight and blood glucose levels of the control and STZ-induced diabetic male Sprague-Dawley rats were monitored (Table 4.1). Five months post STZ injection, diabetic rats had a significant decrease in their body weight and a significant increase in the blood glucose levels compared to the non-diabetic control rats. The changes indicate that diabetic dysmetabolism was established and verifies that a diabetic rat model was used.

4.3.2 Increasing anti-VEGF concentrations caused more death *in vivo*

To determine whether different doses of anti-VEGF result in increased apoptotic cells in the retina, sagittal eye sections of control rats and STZ-induced diabetic rats underwent TUNEL staining. Imaging under a fluorescent microscope revealed that as the concentration of anti-VEGF increased, more apoptotic cells were present in both the control (Figure 4.1) and STZ-induced diabetic rats (Figure 4.2). Apoptotic cells were localized to the ganglion cell layer (GCL) and the inner nuclear layer (INL). When quantifying the number of TUNEL-positive cells in the retina of the control rats, untreated control (0 mg/mL) had a baseline number of 0.64 ± 1.29 apoptotic cells. At half the clinical dose (0.0625 mg/mL), the number increased to 1.60 ± 1.82 apoptotic cells, at the clinical dose (0.125 mg/mL) to 2.40 ± 2.07 apoptotic cells, and at double the clinical dose (0.25 mg/mL) the number significantly increased ($p=0.0004$) to 4.40 ± 0.89 apoptotic cells

Table 4.1. Body weights and serum glucose levels of control and STZ-induced diabetic rats.

Parameter	Control	STZ-induced diabetic rats	P-Value
Body Weight (g)			
Start	240.4	245.5	0.09*
Finish	481.9	417.3	0.0001*
Blood Glucose (mmol/L)	5.8	17.8	0.0001*

*Unpaired t-test

Figure 4.1. TUNEL staining of control rat retina. TUNEL staining performed in control rats showed increased apoptotic cells in the ganglion cell layer following different doses of anti-VEGF injections compared with untreated retina from the control group. Blue represents DAPI-stained nuclei and green represents TUNEL staining. Magnification x40. n=5 for each group. Scale bar: 50 μ m.

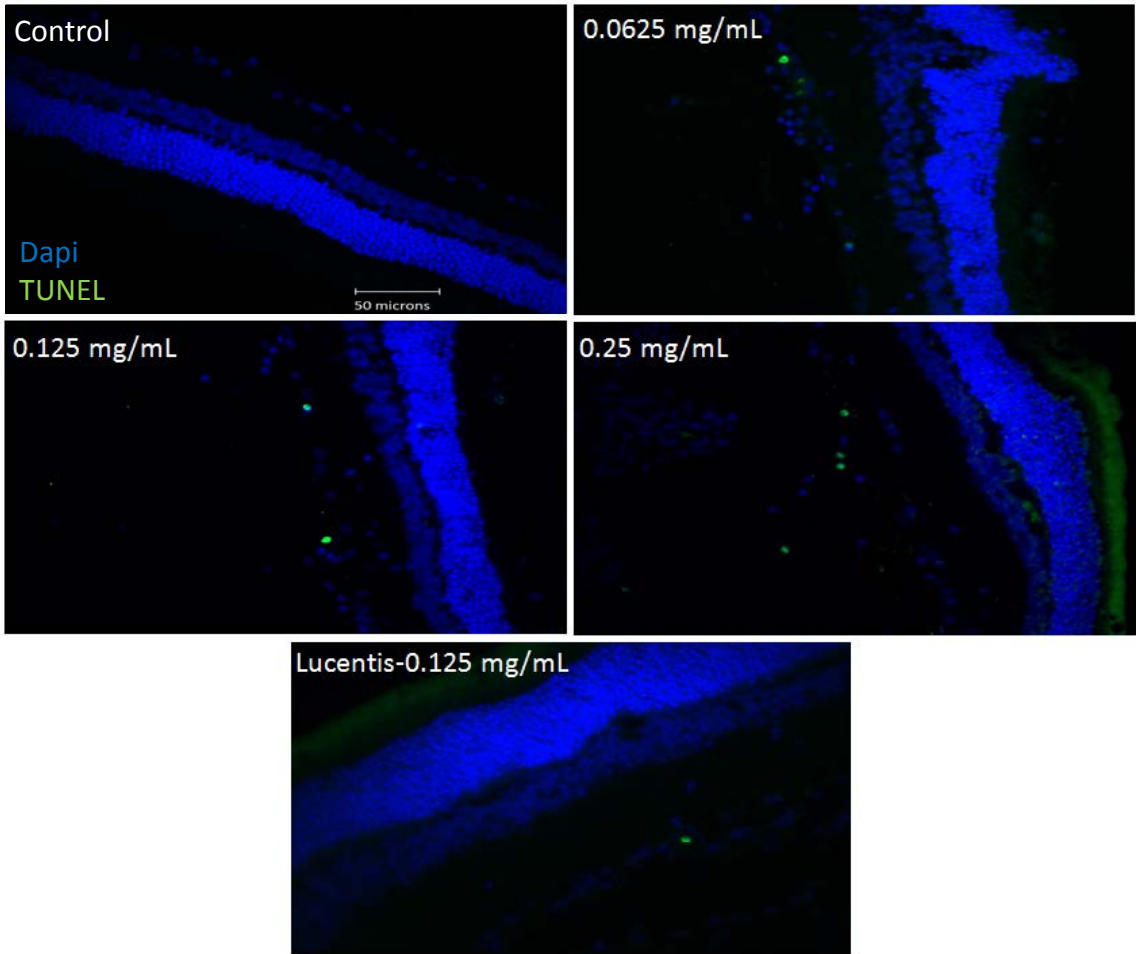
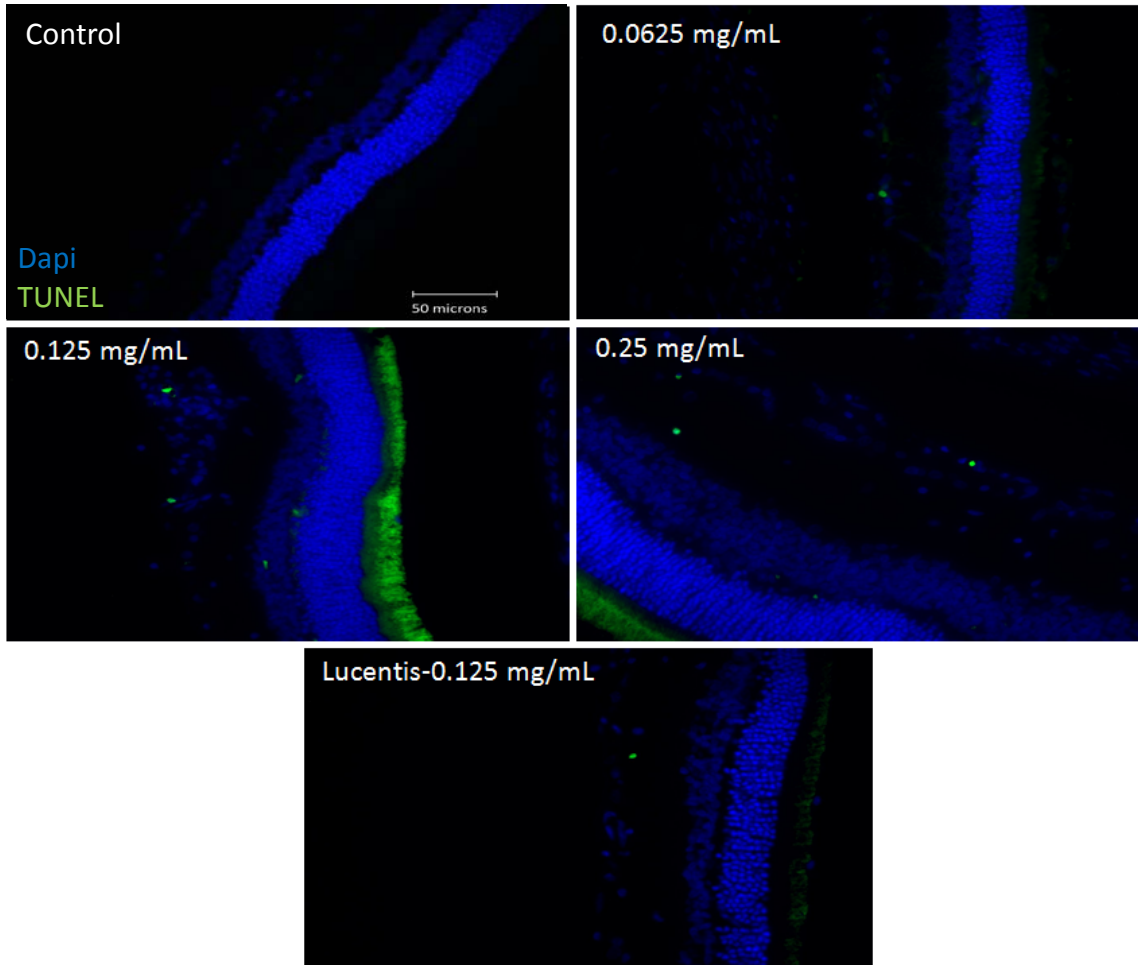


Figure 4.2. TUNEL staining of diabetic rat retina. TUNEL staining performed in STZ-induced diabetic rats showed increased apoptotic cells in the ganglion cell layer following different doses of anti-VEGF injections compared with untreated retina from the diabetic control group. Blue represents DAPI-stained nuclei and green represents TUNEL staining. Magnification x40. n=5 for each group. Scale bar: 50 μ m.



compared to the control (Figure 4.3A). For the STZ-induced diabetic rats, control had a baseline number of 0.46 ± 1.06 apoptotic cells. The number significantly increased at half the clinical dose to 2.60 ± 1.34 ($p=0.01$), 4.5 ± 3.32 at the clinical dose ($p=0.02$), and 6.8 ± 2.95 ($p=0.03$) at double the clinical dose (Figure 4.3B).

4.3.3 No difference in cell death between the clinical dose of ranibizumab and rat anti-VEGF

In control rats when comparing the clinical dose of ranibizumab (Lucentis-0.125 mg/mL) to the clinical dose of rat anti-VEGF (0.125 mg/mL) in regards to the amount of apoptotic cells, both were not significantly different from one another despite rat-anti-VEGF showing higher numbers of apoptotic cells (2.40 ± 2.07 cells) compared to ranibizumab (1.25 ± 0.96 cells) and untreated control (0.64 ± 1.29 cells) (Figure 4.4A). Similarly, in the diabetic rats, ranibizumab (2.00 ± 1.23) and rat anti-VEGF (4.5 ± 3.32) were also not significant to each other but both had significantly increased ($p<0.03$) apoptotic cells compared to untreated diabetic control (Figure 4.4B).

4.3.4 Frequency of injections has no effect on apoptotic cells

The frequency of injections did not have a significant effect on the number of apoptotic cells. In the control rats, single versus triple injections of the clinical dose of rat-anti-VEGF showed no significant difference ($p=0.79$). Single injections resulted in 2.00 ± 2.16 apoptotic cells while 3 injections resulted in 2.4 ± 2.074 apoptotic cells. Control rats injected with anti-VEGF had no significant difference ($p>0.36$) when compared to untreated control (0.64 ± 1.29 cells)

Figure 4.3. Apoptotic death rates following different doses of rat anti-VEGF in control and diabetic rats. The number of TUNEL-positive cells in the GCL was significantly greater at double the clinical dose (0.25 mg/mL) in the control rats (**A**) and significantly greater at half the clinical (0.0625 mg/mL), clinical (0.125 mg/mL), and double the clinical dose (0.25 mg/mL) in the diabetic rats (**B**) compared to untreated controls. Data are expressed as means \pm SD. n=5 for each group. *p < 0.03, ***p=0.0004 compared with controls.

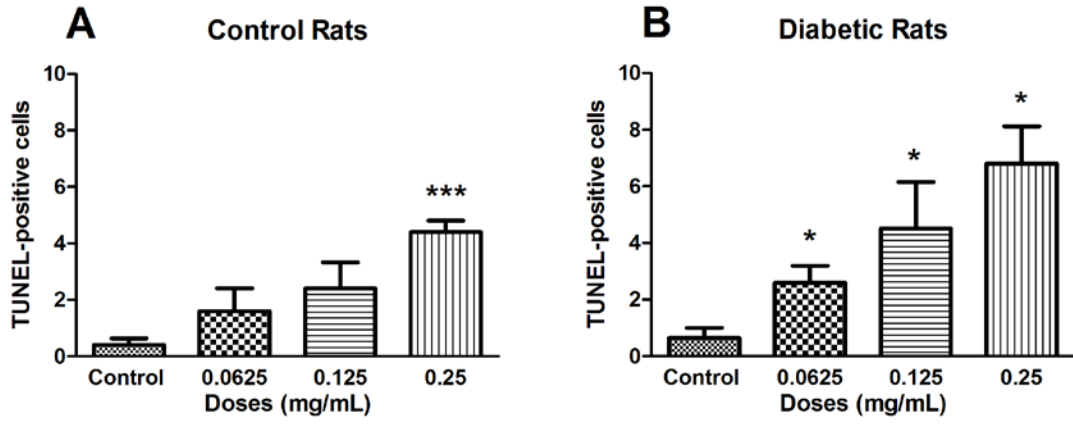


Figure 4.4. Apoptotic cell death rates between the clinical dose of rat anti-VEGF and ranibizumab in control and diabetic rats. Comparing the clinical dose of ranibizumab (Lucentis-0.125 mg/mL) to the clinical dose of rat anti-VEGF (0.125 mg/mL) in control (**A**) and diabetic (**B**) rats, neither was significant to each other regarding the number of TUNEL-positive cells. Compared to the untreated control in the control rats (**A**), the number of TUNEL-positive cells was not significantly greater at the clinical dose of ranibizumab and rat anti-VEGF but in the diabetic rats (**B**), both the clinical dose of ranibizumab and rat anti-VEGF had significantly increased numbers of TUNEL-positive cells compared to untreated diabetic control. Data are expressed as means \pm SD. n=5 for each group. *p < 0.03, compared with controls.

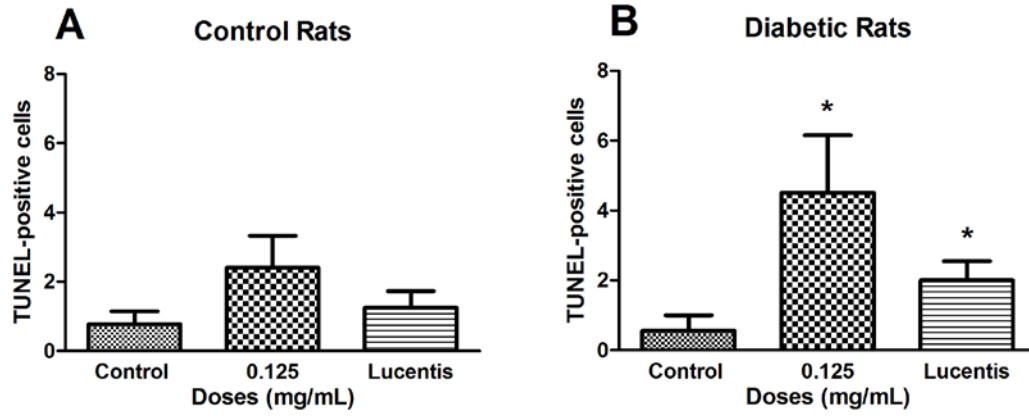
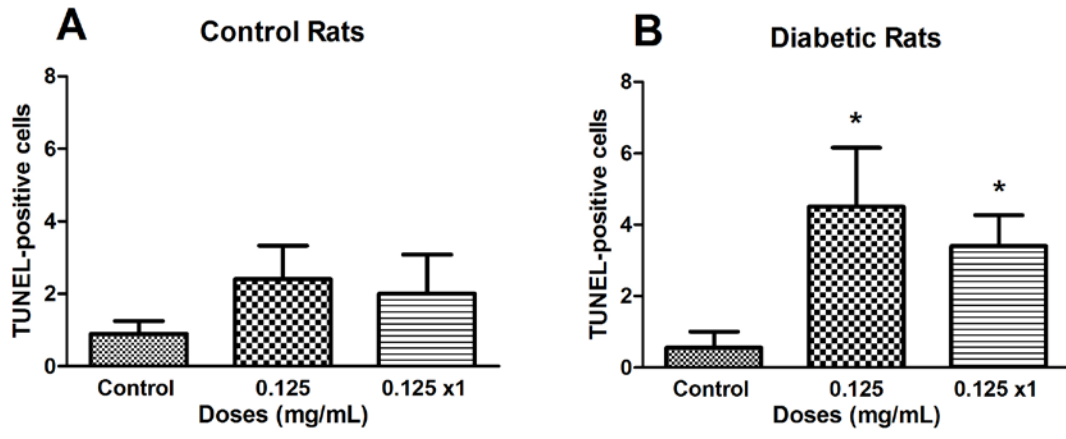


Figure 4.5. Effects of frequency of injections on the number of TUNEL-positive cells in control and diabetic rats. Injecting the clinical dose of rat-anti-VEGF once versus three times showed no significant difference between each other for both the control (**A**) and diabetic (**B**) rats. Injecting once versus three times in the control rats (**A**) had no significant difference when compared to untreated control. In the diabetic rats (**B**), injecting once or 3 times both showed significantly increased TUNEL-positive cells compared to untreated diabetic controls. Data are expressed as means \pm SD. n=5 for each group. *p < 0.03, compared with controls.



(Figure 4.5A). In the diabetic rats, a single injection of the clinical dose (3.40 ± 1.95 cells) had no significant differences from a dose consisting of 3 injections despite having more apoptotic cells (4.50 ± 3.32 cells). A single dose injection as compared to 3 injections both had significantly increased ($p < 0.03$) number of apoptotic cells relative to untreated diabetic control (Figure 4.5B).

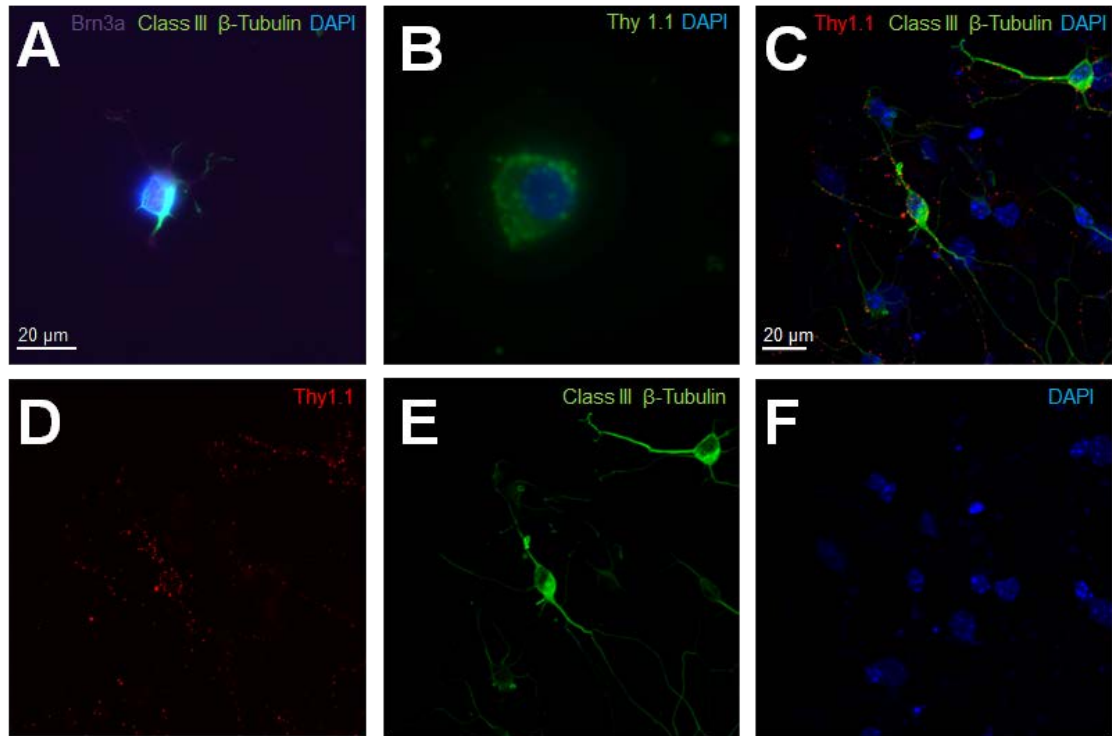
4.3.5 Verification of mixed retinal cell culture

The mixed retinal cell cultures were stained for Class III β -Tubulin, a known neuronal marker, with BRN3A and Thy 1.1 which are both retinal ganglion cell (RGC)-enriched markers. Cells were imaged at 60x magnification. Alexa Fluor 488 green emissions corresponded with staining for Class III β -Tubulin, suggesting that retinal neuronal cells were present in the mixed retinal cell culture. The expression of Brn3a and Thy 1.1 was indicative of the mixed retinal cell culture containing RGC's. Initial immunofluorescence of primary rat retinal cell cultures showed positive expression of Brn3a, Class III β -Tubulin (Figure 4.6A) and Thy1.1 (Figure 4.6B). Confocal triple immunofluorescence indicated the co-staining of Thy1.1 (Figure 4.6D), Class III β -Tubulin (Figure 4.6E), and nuclear DAPI (Figure 4.6F) in cells at day 3 of culture (merged image in Figure 4.6C). The RGCs in culture showed dendritic outgrowth and elongation with axonal processes frequently contacting each other.

4.3.6 Increasing anti-VEGF concentrations caused cell death *in vitro*

Examining RGC's under different concentrations of ranibizumab using immunocytochemistry, as the anti-VEGF concentration increased, the

Figure 4.6. Expression of retinal ganglion cell (RGC)-specific markers in the primary rat retinal cell culture. A-B: Immunofluorescence of primary rat retinal cell culture at day 1 of culture showed positive expression of Brn3a, Class III β -Tubulin (**A**) and Thy1.1 (**B**). Confocal triple immunofluorescence showed the co-staining of Thy1.1 (**D**), Class III β -Tubulin (**E**), and nuclear DAPI (**F**) in cells at day 3 of culture (**merged image in C**). The RGCs in culture showed dendritic outgrowth and elongation with axonal processes frequently contacting each other. **A-B** Magnification x80. **C-F** Magnification x60. Scale bars: 20 μ m.



morphology of the RGC's changed as well (Figures 4.7 and 4.8). Visually, as the anti-VEGF concentration increased, the number of RGC's decreased, fewer contacts between RGC's were observed and fewer dendritic and axonal outgrowths were detected. The observations were conducted at both 48 (Figure 4.7) and 72 (Figure 4.8) hours.

Immunostaining of cleaved caspase-3 in the mixed retinal cell culture under different ranibizumab concentrations showed increased apoptotic cell death in half the clinical (0.0625 mg/mL), clinical (0.125 mg/mL), and double (0.25 mg/mL) the clinical doses compared to untreated control (0 mg/mL). The observations were made at both 48 (Fig 4.9) and 72 (Fig 4.10) hours.

Double-labeling studies of Class III β -Tubulin and cleaved caspase-3 indicated that at double the clinical dose (0.25 mg/mL) RGC's began to die from apoptosis. At half the clinical (0.0625 mg/mL), clinical (0.125 mg/mL), and double (0.25 mg/ml) the clinical doses, the surrounding supporting cells were dying through apoptosis in the mixed retinal cell culture (Figure 4.11). This was also observed in the TUNEL analysis of retinal sections, since death was observed in the INL as well for both the control and diabetic rats (Figure 4.12).

4.3.7 Increased ranibizumab concentrations result in decreased cellular metabolic activity

At 48 hours, as ranibizumab concentrations increased, cellular metabolic activity decreased as measured using the MTT assay. Cellular metabolic activity

Figure 4.7. Morphological effect of different concentrations of ranibizumab on RGCs following 48 hours post treatment. RGCs were stained for nuclei (blue) and Class III β -tubulin (red). Immunofluorescence of RGCs under different concentrations of ranibizumab for 48 hours showed that as the concentration increased, the morphology of the RGC's changed. As the concentration went from untreated control to double the clinical dose (0.25 mg/mL), the number of RGC's decreased, had fewer contacts between each other, and had fewer dendritic outgrowths. Magnification x60. Scale bar: 20 μ m.

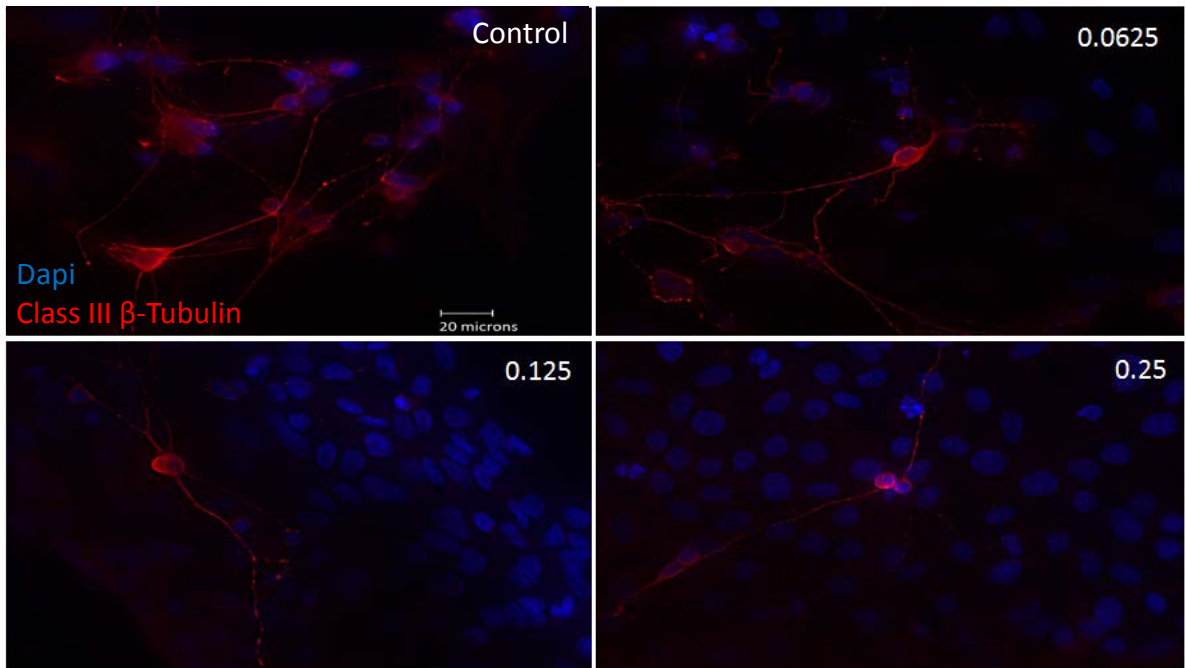


Figure 4.8. Morphological effect of different concentrations of ranibizumab on RGCs following 72 hours post treatment. RGCs were stained for nuclei (blue) and Class III β -tubulin (red). Immunofluorescence of RGCs under different concentrations of ranibizumab for 72 hours showed that as the concentration increased, the morphology of the RGC's continued to change. As the concentration went from untreated control to double the clinical dose (0.25 mg/mL), the amount of RGC's showed a further decrease in number, had fewer contacts between each other and had fewer dendritic outgrowths. Magnification x60. Scale bar: 20 μ m.

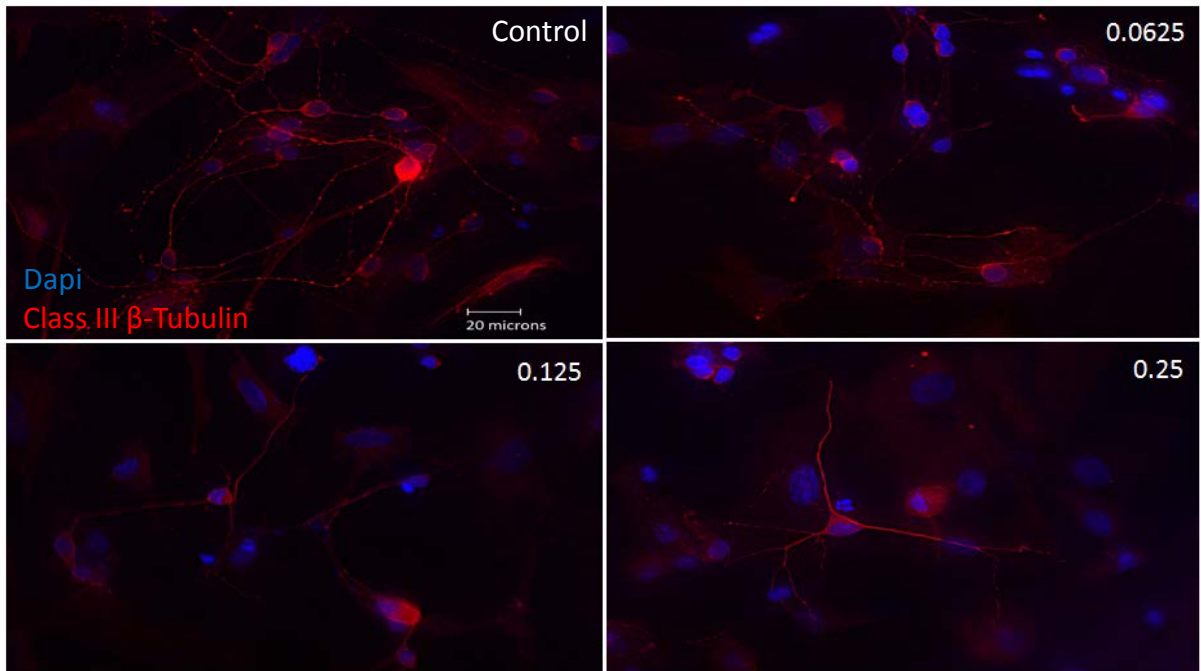


Figure 4.9. Apoptotic cell death upon exposure to different concentrations of ranibizumab following 48 hours post treatment. Immunofluorescence staining for cleaved caspase-3 (green) and nuclei (blue) in the mixed retinal cell culture under different ranibizumab concentrations for 48 hours showed that there was an increase in apoptotic cell death in half the clinical (0.0625 mg/mL), clinical (0.125 mg/mL) and double (0.25 mg/mL) the clinical doses compared to untreated control (0 mg/mL). Magnification x20. Scale bar: 50 μ m.

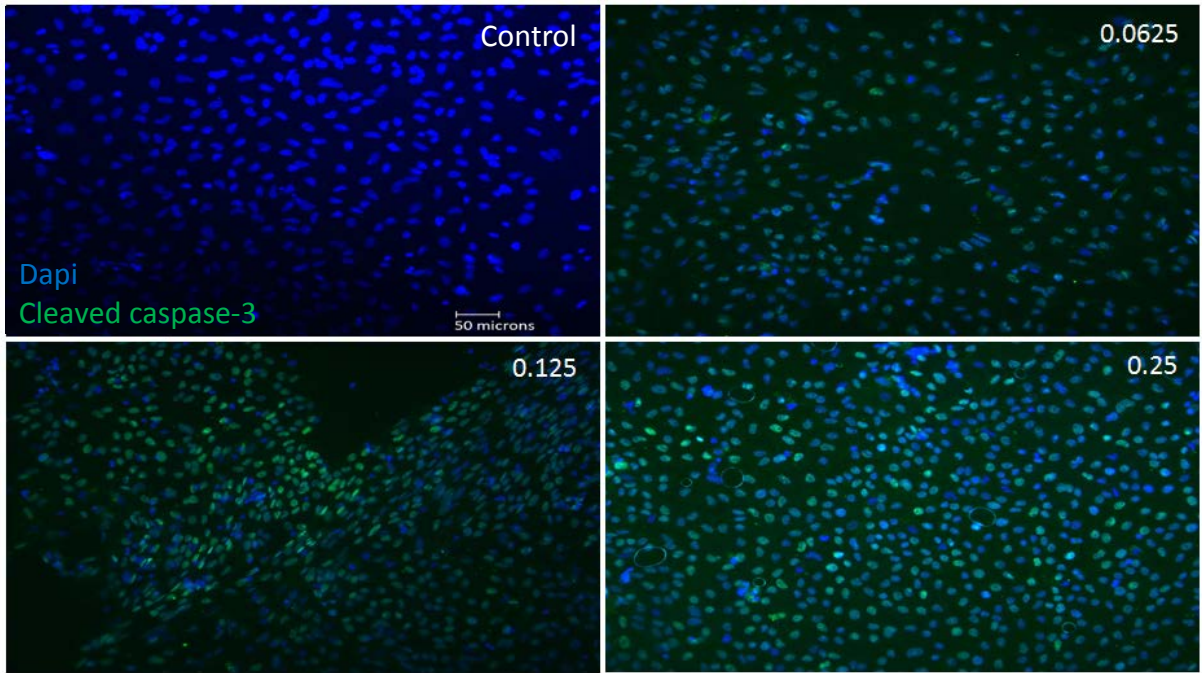


Figure 4.10. Apoptotic cell death upon exposure to different concentrations of ranibizumab following 72 hours post treatment. Immunofluorescence staining for cleaved caspase-3 (green) and nuclei (blue) in the mixed retinal cell culture under different ranibizumab concentrations for 72 hours corresponded with the 48 hour results. There was increased apoptotic cell death observed at half the clinical (0.0625 mg/mL), clinical (0.125 mg/mL), and double (0.25 mg/mL) the clinical doses compared to untreated control (0 mg/mL). Magnification x20. Scale bar: 50 μ m.

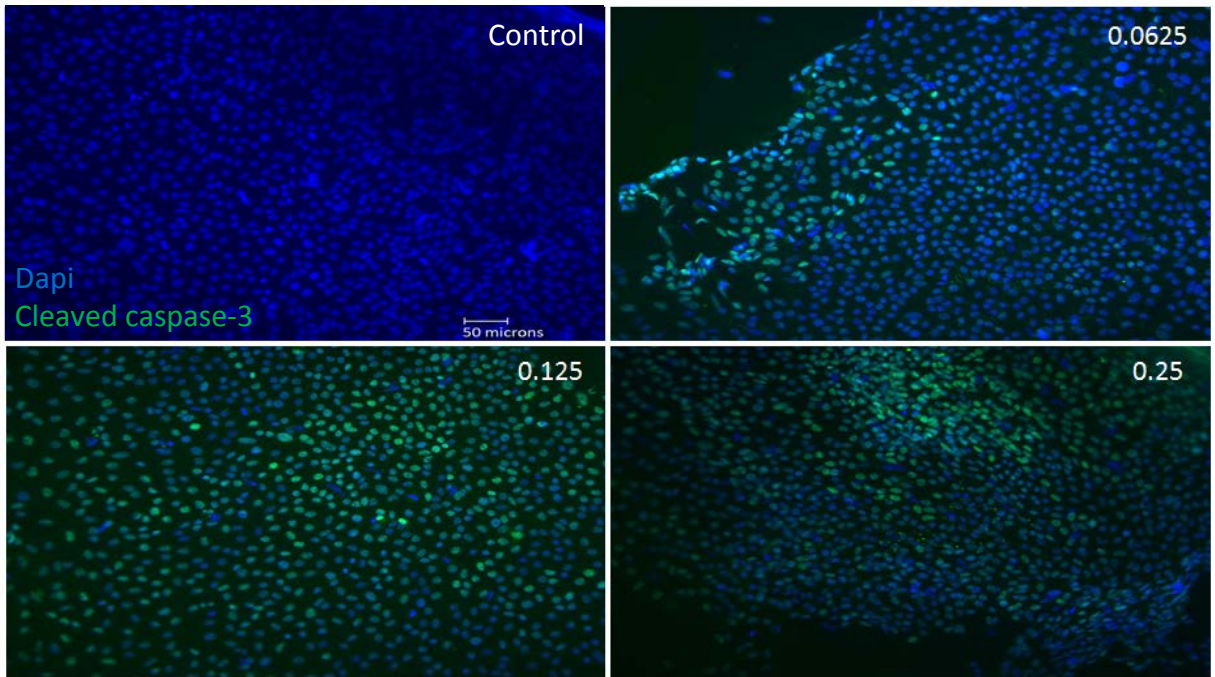


Figure 4.11. Apoptotic cell death of support cells surrounding RGCs.

Performing double-labeling studies of class III β -Tubulin (red) and cleaved caspase-3 (green) indicated that RGCs began to die from apoptosis at double the clinical dose (0.25 mg/mL) (arrowhead). At all doses, it was the surrounding supporting cells around the RGCs that were dying off through apoptosis. Images are shown with DAPI staining the nuclei in blue. Magnification x60. Scale bar: 20 μ m.

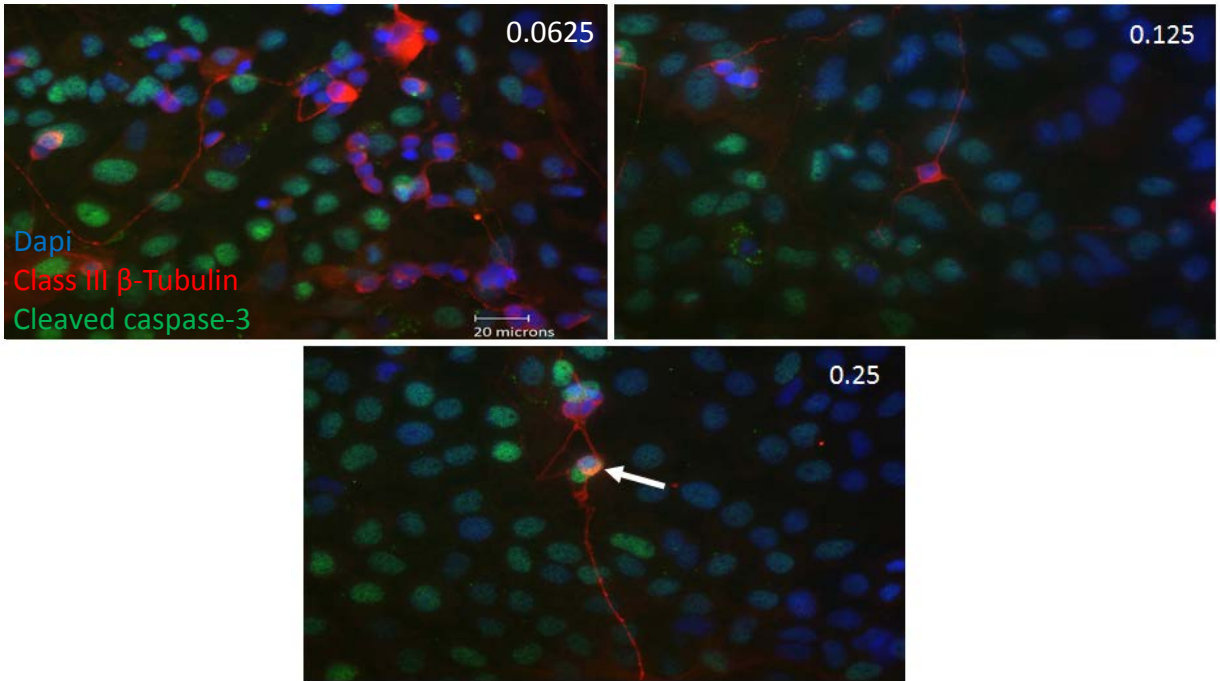
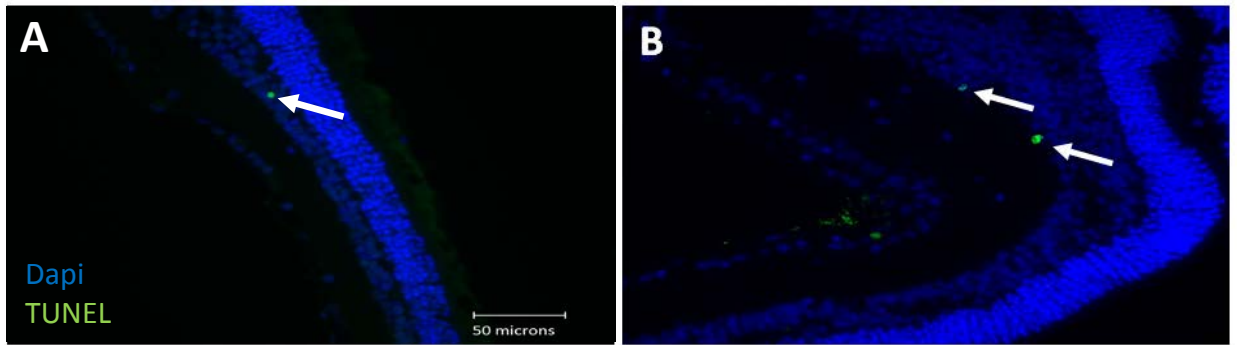


Figure 4.12. Apoptosis in the INL following TUNEL staining. TUNEL analysis of retinal sections showed apoptosis in the INL (arrowhead) as well for both the control (**A**) and diabetic (**B**) rats. Blue represents DAPI-stained nuclei and green represents TUNEL staining. INL, inner nuclear layer. Magnification x40. Scale bar: 50 μm .



decreased at half the clinical dose by 2.37% (0.0625mg/mL; 69.87 ± 8.20 %, $p=0.14$), significantly decreased at the clinical (0.125 mg/mL; 68.18 ± 6.00 %, $p=0.003$) and double the clinical doses (69.74 ± 4.50 %, $p=0.04$) by 4.06% and 2.5% respectively compared to untreated control (0 mg/mL; 72.24 ± 7.18 %) (Figure 4.13A). At 72 hours, the cellular metabolic activity further decreased and displayed the same trend as cells at 48 hours. Compared to the untreated control (67.15 ± 3.34), the cellular metabolic activity decreased at half the clinical dose by 0.56% (0.0625mg/mL; 66.59 ± 4.07 %, $p=0.57$), and significantly decreased at the clinical (0.125 mg/mL; 63.51 ± 4.70 %, $p=0.002$) and double the clinical dose (62.52 ± 5.04 %, $p<0.0001$) by 3.64% and 4.63% respectively (Figure 4.13B).

4.3.8 Increasing ranibizumab concentrations result in increased necrosis

Cells were treated for 48 hours with different concentrations of ranibizumab and necrosis was measured using a LDH assay. Necrosis increased by 14% at half the clinical dose (0.0625 mg/mL; 114.40 ± 43.48 %, $p=0.33$), significantly increased by 30.2% at the clinical dose (0.125mg/mL; 130.60 ± 44.31 %, $p=0.04$) and by 32.5% at double the clinical dose (0.25 mg/mL; 132.90 ± 29.44 %, $p=0.005$) compared to untreated control (0 mg/mL; 100.4 ± 21.27) (Figure 4.14A). During 72 hours, there was less necrosis compared to 48 hours but the same trend was observed. At 72 hours, necrosis increased by 10.6% at half the clinical dose (0.0625mg/mL; 109.00 ± 22.62 %, $p=0.19$), significantly increased by 27.7% at the clinical dose (0.125 mg/mL; 126.10 ± 22.57 %, $p=0.002$) and 22.1% at double the clinical dose (0.25 mg/mL; 120.5 ± 28.35 ,

Figure 4.13. Cellular metabolic activity following different concentrations of ranibizumab. Cellular metabolic activity, as measured using the MTT assay, was significantly decreased at the clinical dose (0.125 mg/mL) and double the clinical dose (0.25 mg/mL) of ranibizumab for both 48 (**A**) and 72 (**B**) hours. The cellular metabolic activity was further decreased at 72 hours. Data is expressed as means \pm SD. n=4. *p < 0.04, **p<0.003, ***p<0.0001 compared with controls.

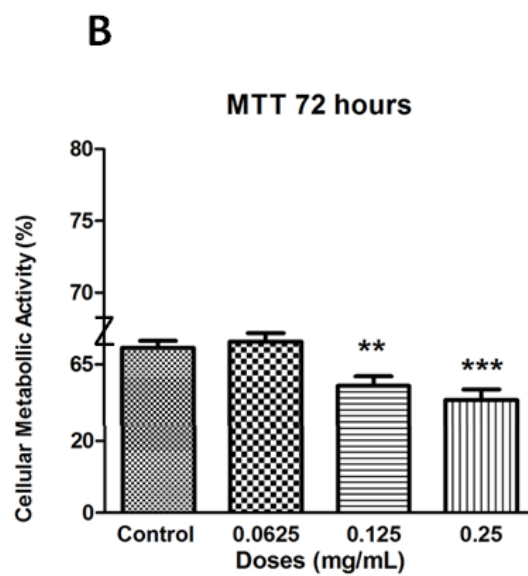
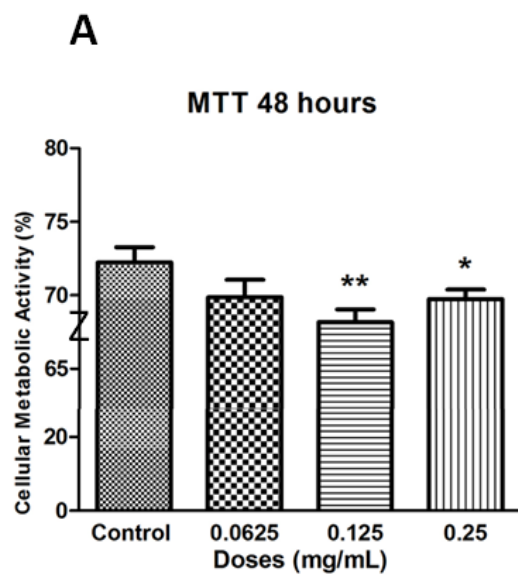
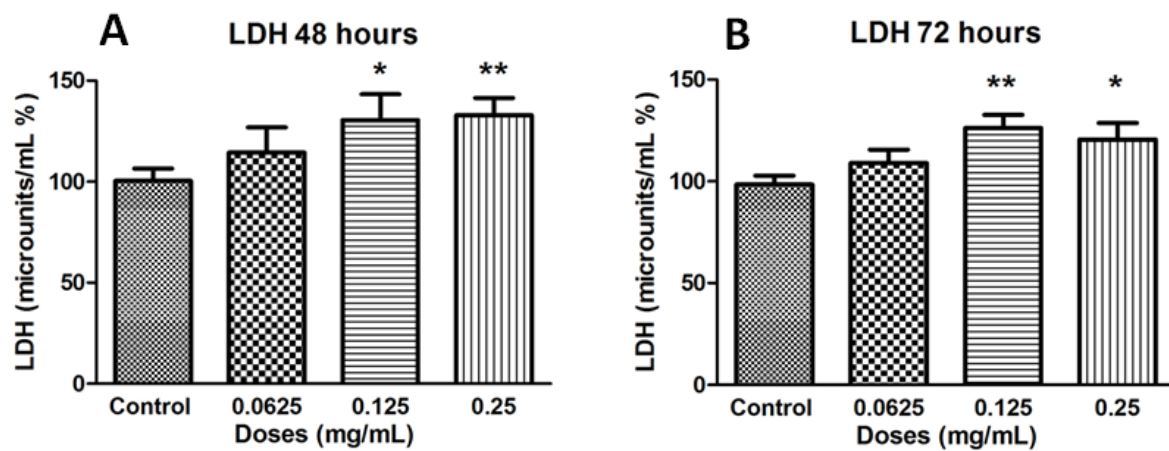


Figure 4.14. Necrosis following different concentrations of ranibizumab.

Necrosis, as measured using the LDH assay, was significantly increased at the clinical dose (0.125 mg/mL) and double the clinical dose (0.25 mg/mL) of ranibizumab for both 48 (**A**) and 72 (**B**) hours. There was less necrosis activity present at 72 hours compared to 48 hours. Data is expressed as means \pm SD. n=4. *p < 0.04, **p<0.005 compared to the controls.



p=0.03) when compared to the untreated control ($98.40 \pm 15.25\%$) (Figure 4.14B).

4.3.9 Increased apoptosis with increasing ranibizumab concentrations

Cells were treated for 48 hours with different concentrations of ranibizumab, and apoptosis was measured using the cell death detection ELISA assay. Apoptosis significantly increased at half the clinical dose (0.0625 mg/mL; $131.9 \pm 43.94\%$, p=0.02), the clinical dose (0.125 mg/mL; $124.00 \pm 22.79\%$, p=0.005), and double the clinical dose (0.25 mg/mL; $137.20 \pm 61.77\%$, p=0.04) by 35.4%, 27.5%, 40.7% respectively when compared to untreated controls ($96.50 \pm 19.34\%$) (Figure 4.15A). Cells displayed increased apoptosis when treated for 72 hours and showed the same trends as in 48 hours. There was a significant increase in apoptotic cells at half the clinical dose (0.0625 mg/mL; $142.3 \pm 55.20\%$, p=0.01), the clinical dose (0.125 mg/mL; $137.9 \pm 31.51\%$, p=0.001), and double the clinical dose (0.25 mg/mL; $142.70 \pm 39.79\%$, p=0.002) by 47.7%, 43.3%, 48.1% respectively when compared to untreated controls ($94.60 \pm 24.72\%$) (Figure 4.15B).

4.3.10 Increased apoptosis and necrosis with rat anti-VEGF concentrations

Different concentrations of rat-anti-VEGF at 48 hours had a significant increase in necrosis at half the clinical dose (0.0625 mg/mL; $134.8 \pm 30.61\%$, p=0.01), the clinical dose (0.125 mg/mL; $143.00 \pm 33.29\%$, p=0.003), and double the clinical dose (0.25 mg/mL; $172.50 \pm 48.52\%$, p=0.0002) by 29.8%, 38%,

67.5% respectively when compared to untreated controls ($105.00 \pm 21.46\%$) (Figure 4.16A). The cell death detection ELISA assay after 48 hours for different rat anti-VEGF concentrations showed increased apoptosis at half the clinical dose (0.0625 mg/mL; $139.80 \pm 29.90\%$, $p=0.001$), the clinical dose (0.125 mg/mL; $143.10 \pm 33.29\%$, $p=0.002$), and double the clinical dose (0.25 mg/mL; $152.40 \pm 33.46\%$, $p=0.0002$) by 41.9%, 45.2%, 54.5% respectively when compared to untreated controls ($97.88 \pm 25.41\%$) (Figure 4.16B).

Figure 4.15. Apoptosis following treatments with different concentrations of ranibizumab. Apoptosis, as measured using the cell death detection ELISA assay, was significantly increased at half the clinical (0.0625 mg/mL), clinical (0.125 mg/mL), and double the clinical dose (0.25 mg/mL) of ranibizumab for both 48 (**A**) and 72 (**B**) hours. There was increased apoptosis present at 72 hours compared to 48 hours. Data is expressed as means \pm SD. n=4. *p < 0.04, **p<0.005 compared to the controls.

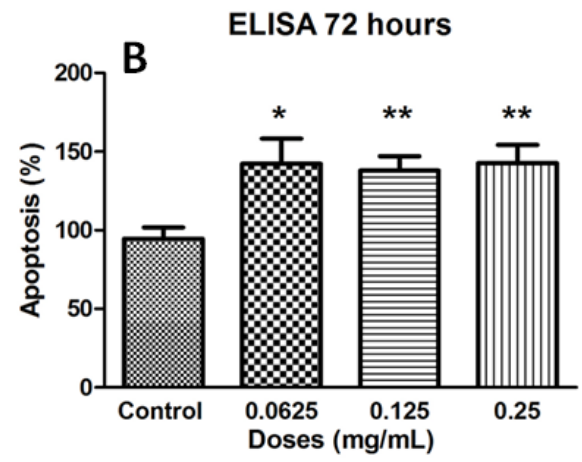
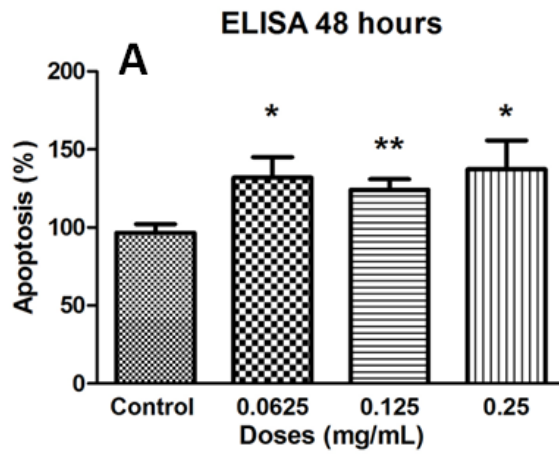
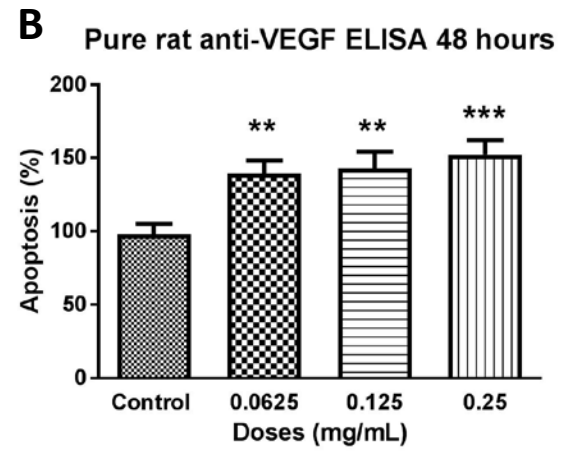
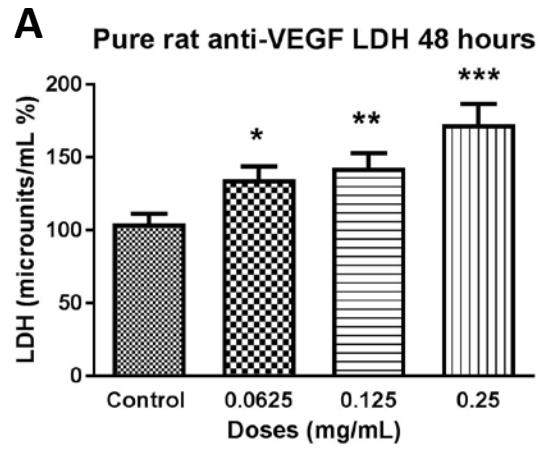


Figure 4.16. Necrosis and apoptosis following treatments with different concentrations of rat anti-VEGF. Necrosis **(A)** and apoptosis **(B)** at 48 hours was significantly increased at half the clinical (0.0625 mg/mL), clinical (0.125 mg/mL), and double the clinical dose (0.25 mg/mL) of rat anti-VEGF measured using the LDH assay and cell death detection ELISA assay respectively. Data is expressed as means \pm SD. n=4. *p < 0.01, **p<0.003, p<0.0002 compared to the controls.



4.4 Discussion

The aim of this study was to obtain *in vitro* and animal model mechanistic data to correlate with *in vivo* clinical observations. The first consideration was determination of the appropriate anti-VEGF concentrations. The values from the calculations of ranibizumab dilutions in the human vitreous were correlated to the rat vitreous, and based on the concentrations used in past studies, 0.125 mg/mL was used as the clinical dose^{15, 16}. The clinical intravitreal dose of ranibizumab is 0.5 mg, resulting in a concentration of 0.125 mg/ml in the vitreum of human patients. As such, 0.125 mg/ml was the final vitreous and medium concentration used for the *in vitro* and *in vivo* experiments^{16, 17}. Using 0.125 mg/mL as the final clinical concentration, half the clinical dose (0.0625 mg/mL) was also tested, as well as double the clinical dose (0.25 mg/mL) which is also the clinically relevant concentration of bevacizumab, another anti-VEGF clinically used for DME.

In relation to the frequency of injections, patients typically receive an anti-VEGF injection once a month for 3 months and are clinically assessed on month 4. They are then treated on an as needed basis until they are clinically stable according to their OCT tests and clinical assessments¹⁸. To simulate the treatment regime with rats, the rodents were injected once a week for 3 weeks and sacrificed on week 4.

Compared to normal controls, the diabetic rats were more sensitive to different concentrations of anti-VEGF injections. Compared to untreated diabetic controls, diabetic rats showed increased apoptotic deaths at half the clinical, clinical, and double the clinical doses whereas, non-diabetic control rats showed

increased apoptotic death at only double the clinical dose. The results were expected given the nature of the disease since diabetics are more sensitive to ocular changes compared to non-diabetics. The apoptotic death centered around the GCL and INL which correlates with a previous study¹⁹. While anti-VEGF therapy improves vascular changes, past studies have also indicated that VEGF is involved in neuroprotection by protecting retinal cells against damaging insults like hypoxia, glutamate excitotoxicity and deprivation of serum^{3-10, 19}. To ensure survival, retinal neurons have been shown to provide continuous trophic support. Under ischemic conditions in the retina, VEGF expression in neurons is increased^{19, 20, 21}. By eliminating VEGF through intravitreal anti-VEGF injections, neuronal cells that rely on VEGF for survival, such as bipolar, amacrine and glial cells, are put at risk of dying¹⁹.

When comparing the clinical dose of ranibizumab and the clinical dose of rat anti-VEGF, although there was no significant difference between the two, rat anti-VEGF showed an increased number of apoptotic cells when compared to ranibizumab. The non-diabetic rats were not significantly different from the untreated control. For the diabetic rats, both clinical ranibizumab and rat anti-VEGF had increased number of apoptotic cells compared to the untreated diabetic control. The results were unexpected since ranibizumab is humanized and species-specific. None the less, ranibizumab may have some cross over effect in blocking rat VEGF and causing apoptotic cell death.

In regards to the frequency of injections and number of apoptotic cells, non-diabetic and diabetic rats who received a single injection versus three

injections showed no significant difference. Despite showing no significance, rats that were injected three times showed higher numbers of apoptotic deaths. For the non-diabetic rats, the results from single injections versus three injections were not significantly different compared to the untreated control. For the diabetic rats, having an injection, either once or three times, resulted in increased apoptotic death compared to untreated diabetic control. Multiple injections lead to increased apoptotic cell death due to greater reduction of VEGF and less neuroprotection in the eye.

Most of the apoptotic death observed *in vivo* animal experiments occurred in the ganglion cell layer. As such, for the *in vitro* experiments it was important for the mixed retinal cell culture to contain RGCs. To test for the presence of RGCs, cells were stained for Class III β -tubulin (TUJ-1) which is a constituent of neuronal microtubules and frequently expressed on RGCs, as well as Brn3a and Thy 1 which are also RGC-specific markers²². Thy1 is a glycosylphosphatidylinositol anchored cell surface protein of the immunoglobulin superfamily which has been shown to be specifically expressed on RGCs^{23, 24, 25}. The expression of Thy 1 in the mixed retinal cell culture was at a level similar to past studies^{23, 26, 27}. Brn3a is a class IV POU domain transcription factor that has an important role in differentiation, survival, and axonal elongation during the development of RGCs²⁸. Brn3a has been determined to be a reliable marker of RGCs in past studies^{23, 24, 29, 30}. The mixed retinal cell culture used for the study had expression of all 3 markers as well as had signs of outgrowth and elongation, indicating the presence of RGCs.

Exposure to increasing concentrations of ranibizumab for 48 and 72 hours lead to a decrease in RGC's as detected by TUJ-1 staining. In regards to morphology, fewer contacts between RGCs and fewer outgrowths were observed. Staining for cleaved caspase-3 revealed that half the clinical, clinical, and double the clinical dose of ranibizumab resulted in increased apoptotic death compared to untreated control. Co-staining with TUJ-1 showed that RGCs remained relatively healthy and, in fact, the support cells around RGCs were the ones dying off. The observation correlates with the animal results since apoptotic death was also observed in the INL. No detrimental effects to RGCs as the result of ranibizumab treatments have been detected until administering double the clinical dose. Ranibizumab affects the supporting cells surrounding RGCs which in turn affect the morphology of RGCs as has been previously observed in the study. The damage to the supporting cells may affect the morphology of the optic nerve by causing a decrease in the ganglion cell layer and an increase in the cup/disk ratio as shown in our previous clinical study. The results correlate with past studies that have shown that treatments with anti-VEGF decrease the number of cells in INL but have no effect on the number of cells in GCL.¹⁹ Tests of anti-VEGF concentrations on pure RGC cell lines have also shown no significant changes³¹. Previous studies have noted that anti-VEGF alone is not cytotoxic to RGCs but when the cells are exposed to oxidative stress, the protective effect of VEGF is eliminated^{32, 33, 34}. Through the use of a mixed retinal cell culture, which is the closest cell based *in vitro* model to the composition of an *in vivo* retina, we have verified that RGC's are not being directly affected by

different anti-VEGF concentrations. The anti-VEGF treatments eliminate VEGFs neuroprotective functions, and potentially other unknown roles, causing the surrounding supporting cells to become cytotoxic and die thereby affecting RGC morphology.

The immunofluorescence results were supported by colorimetric assays, which suggest that as the concentration of ranibizumab increased, a significant decrease in cellular metabolic activity and an increase in cytotoxicity through necrosis and apoptosis at both 48 and 72 hours occurred. In accordance with the cleaved caspase-3 results, both half the clinical, clinical and double the clinical dose all showed significant increase in apoptotic death when tested using the cell death detection ELISA. Rat anti-VEGF was tested using the established concentrations to determine whether the antibody or the anti-VEGFs vehicle increased cell death. According to results, the antibody alone was more cytotoxic. Results from the LDH assay demonstrated that even at half the clinical dose, as well as at clinical and double the clinical doses, increased necrosis occurred. The cell death detection ELISA showed further apoptotic death under all 3 concentrations.

This is the first study to utilize a mixed retinal cell culture and conduct *in vitro* and *in vivo* experiments that mimic clinical conditions. The benchtop approach was a complementary addition to the overall study aimed at determining potential mechanisms to explain the clinical observation that repeated anti-VEGF injections may be detrimental to the optic nerve by decreasing RNFL thickness, increasing cup volume and increasing vertical

cup/disk ratio over time. For the aforementioned reason, the current study sought to obtain comprehensive results by the conduct of animal and mixed retinal cell culture experiments to determine whether different doses of anti-VEGF result in any changes to the retina.

In conclusion, repeated anti-VEGF injections may be detrimental to the retina by decreasing cellular metabolic activity and increasing cytotoxicity of retinal cells through necrosis and apoptosis. The cytotoxicity of the support cells affects RGC morphology which may explain why clinically anti-VEGF treatment results in decreased RNFL thickness, increased cup volume and increased cup/disk ratio. In contrast to current recommendations, the results provide a cautionary note to monitor both the retina and optic nerve status in patients undergoing frequent anti-VEGF injections.

4.5 References

1. Kaur C, Foulds W, Ling E. Blood-retinal barrier in hypoxic ischaemic conditions: basic concepts, clinical features and management. *Progress In Retinal And Eye Research* 2008;27(6):622-647.
2. Holt RIG, Cockram CS, Flyvbjerg A, Goldstein BJ. *Textbook of diabetes*. 4th ed. Chichester, West Sussex, UK: Wiley Blackwell; 2010.
3. D'Amore PA. Vascular endothelial cell growth factor-A: not just for endothelial cells anymore. *Am J Pathol* 2007;171:14-18.
4. Beazley-Long N, Hua J, Jehle T, Hulse RP, Dersch R, Lehring C et al. VEGF-A165b is an endogenous neuroprotective splice isoform of vascular endothelial growth factor A in vivo and in vitro. *Am J Pathol* 2013;183:918-929.
5. Miguel NC, Matsuda M, Portes AL, Allodi S, Mendez-Otero R, Puntar T et al. In vitro effects of bevacizumab treatment on newborn rat retinal cell proliferation, death, and differentiation. *Invest Ophthalmol Vis Sci* 2012;53:7904-7911.
6. Kim I, Ryan AM, Rohan R, Amano S, Agular S, Miller JW et al. Constitutive expression of VEGF, VEGFR-1, and VEGFR-2 in normal eyes. *Invest Ophthalmol Vis Sci* 1999;40:2115-2121.

7. Jin KL, Mao XO, Greenberg DA. Vascular endothelial growth factor: direct neuroprotective effect in in vitro ischemia. *Proc Natl Acad Sci USA* 2000;97:10242-10247.
8. Gomes E, Papa L, Hao T, Rockwell P. The VEGFR2 and PKA pathways converge at MEK/ERK1/2 to promote survival in serum deprived neuronal cells. *Mol Cell Biochem* 2007;305:179-190.
9. Tolosa L, Mir M, Asensio VJ, Olmos G, Llado J. Vascular endothelial growth factor protects spinal cord motoneurons against glutamate-induced excitotoxicity via phosphatidylinositol 3-kinase. *J Neurochem* 2008;105:1080-1090.
10. Mizutani M, Kern TS, Lorenzi M. Accelerated death of retinal microvascular cells in human and experimental diabetic retinopathy. *J Clin Invest* 1996;97:2883-2890.
11. Diabetes and Your Eyesight. Diabetes and Your Eyesight | Glaucoma Research Foundation. <http://www.glaucoma.org/glaucoma/diabetes-and-your-eyesight.php>. Accessed May 28, 2017.
12. Gajdosík A, Gajdosíková A, Stefek M, Navarová J, Hozová R. Streptozotocin-induced experimental diabetes in male Wistar rats. *Gen Physiol Biophys* 1999;18:54-62.

13. Chen S, Evans T, Deng D, Cukiernik M, Chakrabarti S. Hyperhexosemia induced functional and structural changes in the kidneys: role of endothelins. *Nephron* 2002;90:86-94.
14. Cai L, Chen S, Evans T, Cherian MG, Chakrabarti S. Endothelin-1-mediated alteration of metallothionein and trace metals in the liver and kidneys of chronically diabetic rats. *Int J Exp Diabetes Res* 2002;3:193-198.
15. Klettner A, Roider J. Comparison of Bevacizumab, Ranibizumab, and Pegaptanib In Vitro: Efficiency and Possible Additional Pathways. *Invest Ophthalmol Vis Sci* 2008;49(10):4523-4527.
16. Costa R, Carneiro AN, Rocha A, Pirraco A, Falcão M, Vasques L et al. Bevacizumab and ranibizumab on microvascular endothelial cells: A comparative study. *J Cell Biochem* 2009;108(6):1410-1417.
17. Hussain N, Ghanekar Y, Kaur I. The future implications and indications of anti-vascular endothelial growth factor therapy in ophthalmic practice. *Indian J Ophthalmol* 2007;55:445–450.
18. Lanzetta P, Loewenstein A. Fundamental principles of an anti-VEGF treatment regimen: optimal application of intravitreal anti-vascular endothelial growth factor therapy of macular diseases. *Graefes Arch Clin Exp Ophthalmol* 2017;255(7):1259-1273.

19. Park H-YL, Kim JH, Park CK. Neuronal Cell Death in the Inner Retina and the Influence of Vascular Endothelial Growth Factor Inhibition in a Diabetic Rat Model. *Am J Pathol* 2014;184(6):1752-1762.
20. Famiglietti EV, Stopa EG, McGookin ED, Song P, LeBlanc V, Streeten BW. Immunocytochemical localization of vascular endothelial growth factor in neurons and glial cells of human retina. *Brain Res* 2003;969:195-204.
21. Shima DT, Gougos A, Miller JW, Tolentino M, Robinson G, Adamis AP et al. Cloning and mRNA expression of vascular endothelial growth factor in ischemic retinas of *Macaca fascicularis*. *Invest Ophthalmol Vis Sci* 1996;37:1334-1340.
22. Sharma RK, Netland PA. Early born lineage of retinal neurons express class III β -tubulin isotype. *Brain Res* 2007;1176:11-17.
23. Zhang XM, Li Liu DT, Chiang SW, Choy KW, Pang CP, Lam DS et al. Immunopanning purification and long-term culture of human retinal ganglion cells. *Mol Vis* 2010;16:2867-2872.
24. Barnstable CJ, Drager UC. Thy-1 antigen: a ganglion cell specific marker in rodent retina. *Neuroscience* 1984;11:847-55.
25. Xu Z, Jiang F, Zeng Y, Alkhodari HT, Chen F. Culture of rat retinal ganglion cells. *J Huazhong Univ Sci Technolog Med Sci* 2011;31(3):400-403.

26. Leifer D, Lipton SA, Barnstable CJ, Masland RH. Monoclonal antibody to Thy-1 enhances regeneration of processes by rat retinal ganglion cells in culture. *Science* 1984;224:303-6.
27. Snow RL, Robson JA. Ganglion cell neurogenesis, migration and early differentiation in the chick retina. *Neuroscience* 1994;58:399-409.
28. Nadal-Nicolás FM, Jiménez-Lopez M, Sobrado-Calvo P, Nieto-Lopez L, Cañovas-Martínez I, Salinas-Navarro M et al. Brn3a as a Marker of Retinal Ganglion Cells: Qualitative and Quantitative Time Course Studies in Naïve and Optic Nerve–Injured Retinas. *Invest Ophthalmol Vis Sci* . 2009;50(8):3860-3868.
29. Liu W, Khare SL, Liang X, Peters MA, Liu X, Cepko CL et al. All Brn3 genes can promote retinal ganglion cell differentiation in the chick. *Development* 2000;127:3237-3247.
30. Quina LA, Pak W, Lanier J, Banwait P, Gratwick K, Liu Y et al. Brn3a expressing retinal ganglion cells project specifically to thalamocortical and collicular visual pathways. *J Neurosci* 2005; 25:11595-11604.
31. Schnichels S, Hagemann U, Januschowski K, Hofmann J, Bartz-Schmidt K-U, Szurman P et al. Comparative toxicity and proliferation testing of aflibercept, bevacizumab and ranibizumab on different ocular cells. *Br J Ophthalmol* 2013;97(7):917-923.

32. Thaler S, Fiedorowicz M, Choragiewicz TJ, Bolz S, Tura A, Henke-Fahle S et al. Toxicity testing of the VEGF inhibitors bevacizumab, ranibizumab and pegaptanib in rats both with and without prior retinal ganglion cell damage. *Acta Ophthalmol* 2008;88(5):e170-176.
33. Brar VS, Sharma RK, Murthy RK, Chalam KV. Bevacizumab neutralizes the protective effect of vascular endothelial growth factor on retinal ganglion cells. *Mol Vis* 2010;16:1848-1853.
34. Brar VS, Sharma RK, Murthy RK, Chalam KV. Evaluation of Differential Toxicity of Varying Doses of Bevacizumab on Retinal Ganglion Cells, Retinal Pigment Epithelial Cells, and Vascular Endothelial Growth Factor–Enriched Choroidal Endothelial Cells. *J Ocul Pharmacol Ther* 2009;25(6):507-512.

Chapter 5

5 General Discussion, Limitations, and Future Direction

5.1 Summary of Discussion

DR is the most common microvascular complication of diabetes and the leading cause of blindness among adults^{1, 2}. The goal of this thesis was to examine two common clinically-relevant treatments for DR and to determine whether they have an iatrogenic effect on the retina and the optic nerve. Numerous studies have been published on argon, and to a lesser extent PASCAL, panretinal photocoagulation (PRP) for PDR and the use of anti-VEGFs for DME. However, none of the studies have examined the effects of anti-VEGF treatments on the optic nerve and peripheral vision. This is especially alarming considering that over the past decade, with newer lasers being introduced into the market and higher affinity anti-VEGFs being developed, there have been an increasing number of reports indicating that diabetic patient's post-PRP or receiving anti-VEGFs developing signs of optic neuropathy and glaucoma.

In order to analyze the effects of PRP laser on the retina and optic nerve, the primary objective was to use clinical structural (OCT, HRT) and functional (visual field, visual acuity) diagnostic tests to monitor the retina and optic nerve. Secondly, the intent was to observe whether PRP was beneficial and improved diabetic ischemia. The results suggest that overall, PRP did not cause any significant changes to the macula or RNFL thickness over a 24-month time period. There was a slight thickening of the macula and RNFL at 6 months but this finding was likely due to intraretinal inflammation from the treatment^{3, 4, 5}. By 24 months, the thickness returned to baseline levels. Using the structural OCT

and HRT diagnostic tests to analyze the optic nerve revealed that overall, the morphology of the optic nerve appeared unchanged. There was a significant improvement in peripheral perfusion at 12 and 24 months post laser, thus improving the degree of ischemia in these diabetic patients. Despite the improvement, there was no change in central vision and a progressive significant decline in peripheral vision at 12 and 24 months post-laser was observed. The likely cause of peripheral deterioration was the destruction of peripheral retinal tissue by photocoagulation^{6, 7, 8}. When glaucoma specialists who were masked to the study were asked to grade the optic nerve photos of patients that received PRP laser, grading of the optic nerve was much more unreliable following PRP when compared to control eyes. Grader 1 indicated that there was a significant increase in the cup/disk ratio at 6 and 12 months followed by a further increase at 24 months. Grader 2 indicated that there was a non-significant increase that was happening to the optic nerve. Despite no observed morphological changes to the optic nerve, as determined by the OCT and HRT, the optic nerve became more difficult to grade due to non-morphological colouration changes that affected the optic nerve post-PRP.

The following is a pilot study that assesses the effects of PRP on the optic nerve. The results from the study highlight the importance of laser treatments in improving the overall diabetes by increasing perfusion of blood vessels and improving diabetic ischemia. This is the first study to correlate unreliable grading of the optic nerve and progressive visual field loss in patients post-PRP. The findings may explain why some diabetic patient's post-PRP laser treatments are

misdiagnosed with having normal-tension glaucoma. The misdiagnosed patients are treated with preventative glaucoma topical medications, have a number of health related quality of life issues related to side effects and cost. The study highlights the need for a more objective optic nerve analysis to assist clinicians in diagnosing normal tension glaucoma in diabetic patients who have received prior PRP.

In order to assess the effects of anti-VEGF therapy, the first objective was to recruit treatment naïve DR patients with underlying DME in order to analyze the effects of anti-VEGF injections and the frequency of injections on the retina and optic nerve using *in vivo* clinical pathological analysis. The second objective was to utilize an animal model to determine whether anti-VEGF therapy has any effects on the retina and neuronal cells of STZ-induced diabetic rats. The third objective was to generate a mixed retinal cell culture to examine whether different doses of anti-VEGF alter retinal cell metabolic activity or induce toxicity through the use of various colorimetric assays and immunofluorescence.

The macular thickness in anti-VEGF treated patients significantly decreased and central vision significantly improved from baseline over a 24-month time period. The results were expected as previous clinical trials and studies suggested likewise⁹⁻¹⁶. The anti-VEGF therapy was also beneficial in significantly improving perfusion of the diabetic eye, likely through the stabilization of blood vessels. Analysis of the optic nerve indicated that anti-VEGF therapy may be detrimental to the optic nerve by significantly decreasing RNFL thickness, increasing cup volume and increasing vertical cup/disk ratio as

measured on the OCT over a 24-month time period. As a secondary measure, to eliminate the possibility of the findings being due to scanning error or the repeatability or reproducibility of OCT, glaucoma specialists, who were masked to the study, were asked to grade the optic nerve photos of patients that underwent anti-VEGF therapy. Verifying the OCT data, both graders indicated a significant increase in the vertical cup/disk ratio of patients receiving anti-VEGF injections, whereas control patients showed no change. Data from monitoring IOP of the patients over a 24 month period showed consistent pressure values with no significant increase. In combination with OCT, the data suggested that morphological changes occurred to the optic nerve in DME patients undergoing anti-VEGF therapy for which glaucoma is not the primary cause. Of note are the differences in the OCT data of patients with different number of anti-VEGF injections. Patients that received less than 10 injections had no significant change in the cup/disk ratio whereas, patients that had more than 10 injections had a significant increase in the cup/disk ratio. Despite the findings that the patients that had more than 10 injections had a greater baseline vertical cup/disk ratio than patients that had less than 10 injections, baseline vertical cup/disk ratio between the two groups was not significantly different. In accordance, when analyzing peripheral visual fields, although a decline in the peripheral visual fields was observed from 6 to 24 months, it was not significant.

The overall results from using an *in vivo* animal model to explain retinal changes during anti-VEGF therapy revealed that diabetic rats are much more sensitive to anti-VEGF than non-diabetic rats. Diabetic rats had a significant

increase in apoptotic cell deaths at half the clinical, clinical, and double the clinical doses. In comparison, non-diabetic rats only showed significant apoptotic cell death for double the clinical dose when compared to untreated controls. Apoptotic death was centered around GCL and INL in both the non-diabetic and diabetic rats, corresponding with previously published results¹⁷. VEGF has been shown to play a neuroprotective role for retinal neurons, bipolar, amacrine and glial cells, protecting against damaging insults like hypoxia, glutamate excitotoxicity and deprivation of serum¹⁷⁻²⁵. Eliminating VEGF through intravitreal anti-VEGF injections increases the risk of cell death. Comparing the effects of ranibizumab to rat anti-VEGF, rat anti-VEGF resulted in more apoptotic death but the difference was not significant. Compared to untreated controls, no significance in the number of apoptotic cells for the controls rats was detected. However, both ranibizumab and rat-VEGF had significantly increased apoptotic cells compared to untreated diabetic control rats. Though ranibizumab is humanized and species-specific, it still appears to have some cross over effect by blocking rat VEGF and causing apoptotic death. In regards to the frequency of injections, a single injection resulted in less apoptotic death as compared to having three injections of clinical doses though the difference was not significant. Increased frequency of injections presumably resulted in increased apoptotic cell death due to greater reduction of VEGF and less neuroprotection in the eye. In the control rats, one or three injections resulted in no significant difference in the amount of apoptotic cells compared to untreated controls. For the diabetic rats,

having one injection or three injections resulted in a significant higher amount of apoptotic death compared to untreated diabetic control.

A mixed retinal cell culture was developed for the study and verified for the presence of RGC by the immunofluorescence of TUJ-1, Brn3a and Thy 1, all of which are RGC-specific markers. When cells were dosed with half the clinical, clinical, and double the clinical doses of ranibizumab, as the concentration increased, RGC's decreased in number, had fewer contacts between cells and fewer outgrowths were observed. When stained with cleaved caspase-3, the number of apoptotic deaths increased at half the clinical, clinical, and double the clinical doses. The co-staining of caspase-3 and RGC's revealed that ranibizumab was likely not detrimental to RGCs unless at double the clinical dose. For all doses, supporting cells around RGCs were dying through apoptosis, thus affecting the morphology of the RGCs as previously described. It is likely that anti-VEGFs eliminate VEGFs neuroprotective function, and potentially other unknown roles, causing the surrounding supporting cells to become cytotoxic and die thereby affecting RGC morphology. The results correlate with animal findings since apoptotic death was also observed in INL. The finding is consistent with clinically observed results. The dying of support cells affects RGC morphology, which in turn could affect the morphology of the optic nerve by causing a decrease in the ganglion cell layer and an increase in the cup/disk ratio as shown previously. Since structural changes happen prior to functional changes, the changes affecting the optic nerve could explain a decline in peripheral vision in DME patients undergoing anti-VEGF therapy at 6 months.

The results of the immunofluorescence were further supported by the colorimetric assays which indicated that, as the concentration of ranibizumab increased, there was a significant decrease in cellular metabolic activity and an increase in cytotoxicity through necrosis and apoptosis at both 48 and 72 hours. The cell death detection ELISA, in accordance with the caspase-3 results, showed a significant increase in apoptotic cell death at half the clinical, clinical, and double the clinical doses. Rat anti-VEGF was also tested under the same concentrations as ranibizumab to determine whether the antibody or the anti-VEGFs vehicle was causing increased cell death in retina. Findings have established that the rat anti-VEGF was more cytotoxic than ranibizumab. Through the LDH assay, it was observed that even half the clinical dose caused increased necrosis as well as the clinical and double the clinical doses. The cell death detection ELISA showed further apoptotic death with all 3 concentrations.

This is the first long-term study analyzing the effects of anti-VEGF therapy on the optic nerve. The valuable conclusion from my study is that anti-VEGF treatments are detrimental to the optic nerve despite improvements in central vision based on *in-vivo* clinical and *in-vitro* studies. The finding is especially alarming since anti-VEGFs are becoming more commonly used as the first line of treatment due to the ease, simplicity and speed of the treatment. Recent studies suggest eliminating the use of panretinal photocoagulation in favour of anti-VEGFs for proliferative diabetic retinopathy treatments^{26, 27}. In western Canada, instead of administering anti-VEGFs once a month for 3 months, clinicians are treating patients with anti-VEGF injections on the weekly basis. Currently, there

are novel anti-VEGFs in development, such as Aflibercept (Eylea®), which are VEGF traps and have a much higher binding affinity for VEGF, as well as longer duration of action as compared to ranibizumab (Lucentis). Despite short-term improvements, the possibility of long-term damage to the optic nerve and creating another form of blindness is especially important to address and provide a cautionary note to monitor both the retina and optic nerve status in patients undergoing frequent anti-VEGF injections.

5.2 Limitations

A limitation of chapter 2 when examining the effects of the PRP laser is the low number of participants in the study. Despite meeting power number calculations for the treatment group, at least 16 control patients in the study would have been preferred. Although the number of participants for the control group did not meet the limit, the control group did not show any significant difference in any of the testing and showed stable trends.

A limitation for chapter 3 is the limited 24 month time period for the clinical analysis of the patients. A longer duration of the study would have been preferred to observe continued changes to the retina. Despite changes to the RNFL thickness, increase in cup/disk ratio and slight deterioration of peripheral vision, it is still uncertain whether or not the changes are progressive and will continue to get worse or reach steady state over time.

The main limitation for chapter 4 is the use of rat animal models as surrogates for humans. A rat model was used for the *in vivo* work and *in vitro* work by generating a rat mixed retinal cell culture. Even though rodents and humans share a large percentage of DNA, there are major differences. In regards to diabetes, humans develop T1DM and T2DM. T1DM is associated with absolute insulin deficiency due to autoimmune destruction of pancreatic beta cells whereas T2DM is caused by a combination of insulin resistance and insulin deficiency^{28, 29}. The rats were made diabetic by pharmacological induction which targeted and destroyed the beta-cells. Furthermore, there is no established diabetic animal model to demonstrate all of the vascular and neural

complications associated with advanced proliferative DR which the study focused on³⁰. Even though the study mimicked *in vitro* and *in vivo* clinical conditions as closely as possible, the differences should be considered when translating these types of studies to humans.

5.3 Future Direction

Clinical reports of DR patients being diagnosed with having glaucoma and optic neuropathy show that the patients have often undergone PRP laser treatment multiple years ago. As both glaucoma and the effects of PRP on RNFL and optic disk are often progressive, it would be enticing to extend the follow up period beyond 2 years to increase the ability to discern small, yet progressive changes. The extended study period would potentially allow to determine predictive factors that affect the progress and rate of the retinal changes.

Regarding the study presented in chapter 3, it is well established that structural changes precede functional changes. Monitoring patients over 24 month time period might have not been sufficient. To determine whether or not the effects of anti-VEGF therapy as observed on the RNFL, the optic disk and ultimately peripheral vision are indeed progressive and cause optic neuropathy, it would be enticing to extend the follow up period beyond 2 years. The next step would be to conduct a multi-center study analyzing not just ranibizumab but other anti-VEGF medications such as bevacizumab and aflibercept. These commonly used anti-VEGFs all have different molecular characteristics, which cause differences in potency, systemic clearance, and systemic VEGF inhibition^{31, 32}. It would be of interest to determine whether higher affinity anti-VEGFs result in greater changes to the optic nerve as well as if there are any predictive factors that affect progress and rate of the treatments.

Future studies for chapter 4 should focus on identifying the supporting cells that became apoptotic under different doses of anti-VEGF. Additionally, the

study should be repeated using different clinical anti-VEGFs rather than ranibizumab alone to determine whether higher affinity anti-VEGFs result in greater amounts of apoptotic cellular death when visualized under immunofluorescence and with colorimetric assays.

5.4 References

1. Kennedy L, Idris I, Gazis A. Problem solving in diabetes. Oxford: Clinical Publishing; 2006.
2. Lechner J, O'Leary OE, Stitt AW. The pathology associated with diabetic retinopathy. *Vision Res.* 2017.
3. Muqit MMK, Marcellino GR, Henson DB, Fenerty CH, Stanga PE. Randomized Clinical Trial To Evaluate The Effects Of Pascal Panretinal Photocoagulation On Macular Nerve Fiber Layer. *Retina.* 2011;31(8):1699-1707.
4. Shimura M, Yasuda K, Nakazawa T, Kano T, Ohta S, Tamai M. Quantifying alterations of macular thickness before and after panretinal photocoagulation in patients with severe diabetic retinopathy and good vision. *Ophthalmology.* 2003;110(12):2386-2394.
5. Mitsch C, Pemp B, Kriechbaum K, Bolz M, Scholda C, Schmidt-Erfurth U. Retinal Morphometry Changes Measured With Spectral Domain-Optical Coherence Tomography After Pan-Retinal Photocoagulation In Patients With Proliferative Diabetic Retinopathy. *Retina.* 2016;36(6):1162-1169.
6. Frank RN. Visual Fields and Electroretinography Following Extensive Photocoagulation. *Arch Ophthalmol* 1975;93(8):591-598.

7. Hudson C, Flanagan JG, Turner GS, Chen HC, Young LB, Mcleod D. Influence of laser photocoagulation for clinically significant diabetic macular oedema (DMO) on short-wavelength and conventional automated perimetry. *Diabetologia* 1998;41(11):1283-1292.
8. Subash M, Comyn O, Samy A, et al. The Effect of Multispot Laser Panretinal Photocoagulation on Retinal Sensitivity and Driving Eligibility in Patients With Diabetic Retinopathy. *JAMA Ophthalmol* 2016;134(6):666-671.
9. Nguyen QD, Shah SM, Heier JS, Do DV, Lim J, Boyer D et al. Primary End Point (Six Months) Results of the Ranibizumab for Edema of the mAcula in Diabetes (READ-2) Study. *Ophthalmology* 2009;116(11):2175-2181.
10. Nguyen QD, Shah SM, Khwaja AA, Channa R, Hatef E, Do DV et al. Two-Year Outcomes of the Ranibizumab for Edema of the mAcula in Diabetes (READ-2) Study. *Ophthalmology* 2010;117(11):2146-2151.
11. Do DV, Nguyen QD, Khwaja AA, Channa R, Sepah YJ, Sophie R et al. Ranibizumab for Edema of the Macula in Diabetes Study. *JAMA Ophthalmol* 2013;131(2):139-145.
12. Do DV, Sepah YJ, Boyer D, Callanan D, Gallemore R, Bennett M et al. Month-6 primary outcomes of the READ-3 study (Ranibizumab for Edema

- of the mAcula in Diabetes-Protocol 3 with high dose). *Eye (Lond)* 2015;29(12):1538-1544.
13. Massin P, Bandello F, Garweg JG, Hansen LL, Harding SP, Larsen M et al. Safety and Efficacy of Ranibizumab in Diabetic Macular Edema (RESOLVE Study): A 12-month, randomized, controlled, double-masked, multicenter phase II study. *Diabetes Care* 2010;33(11):2399-2405.
 14. Mitchell P1, Bandello F, Schmidt-Erfurth U, Lang GE, Massin P, Schlingemann RO et al. The RESTORE study: ranibizumab monotherapy or combined with laser versus laser monotherapy for diabetic macular edema. *Ophthalmology* 2011;118(4):615-625.
 15. Ishibashi T, Li X, Koh A, Lai TY, Lee FL, Lee WK et al. The REVEAL Study: Ranibizumab Monotherapy or Combined with Laser versus Laser Monotherapy in Asian Patients with Diabetic Macular Edema. *Ophthalmology* 2015;122(7):1402-1415.
 16. Brown DM, Nguyen QD, Marcus DM, Boyer DS, Patel S, Feiner L et al. Long-term Outcomes of Ranibizumab Therapy for Diabetic Macular Edema: The 36-Month Results from Two Phase III Trials. *Ophthalmology* 2013;120(10):2013-2022.
 17. Park H-YL, Kim JH, Park CK. Neuronal Cell Death in the Inner Retina and the Influence of Vascular Endothelial Growth Factor Inhibition in a Diabetic Rat Model. *Am J Pathol* 2014;184(6):1752-1762.

18. D'Amore PA. Vascular endothelial cell growth factor-A: not just for endothelial cells anymore. *Am J Pathol* 2007;171:14-18.
19. Beazley-Long N, Hua J, Jehle T, Hulse RP, Dersch R, Lehring C et al. VEGF-A165b is an endogenous neuroprotective splice isoform of vascular endothelial growth factor A in vivo and in vitro. *Am J Pathol* 2013;183:918-929.
20. Miguel NC, Matsuda M, Portes AL, Allodi S, Mendez-Otero R, Puntar T et al. In vitro effects of bevacizumab treatment on newborn rat retinal cell proliferation, death, and differentiation. *Invest Ophthalmol Vis Sci* 2012;53:7904-7911.
21. Kim I, Ryan AM, Rohan R, Amano S, Aguilar S, Miller JW et al. Constitutive expression of VEGF, VEGFR-1, and VEGFR-2 in normal eyes. *Invest Ophthalmol Vis Sci* 1999;40:2115-2121.
22. Jin KL, Mao XO, Greenberg DA. Vascular endothelial growth factor: direct neuroprotective effect in in vitro ischemia. *Proc Natl Acad Sci USA* 2000;97:10242-10247.
23. Gomes E, Papa L, Hao T, Rockwell P. The VEGFR2 and PKA pathways converge at MEK/ERK1/2 to promote survival in serum deprived neuronal cells. *Mol Cell Biochem* 2007;305:179-190.
24. Tolosa L, Mir M, Asensio VJ, Olmos G, Llado J. Vascular endothelial growth factor protects spinal cord motoneurons against glutamate induced

- excitotoxicity via phosphatidylinositol 3-kinase. *J Neurochem* 2008;105:1080-1090.
25. Mizutani M, Kern TS, Lorenzi M. Accelerated death of retinal microvascular cells in human and experimental diabetic retinopathy. *J Clin Invest* 1996;97:2883-2890.
 26. Li X, Zarbin MA, Bhagat N. Anti-Vascular Endothelial Growth Factor Injections: The New Standard of Care in Proliferative Diabetic Retinopathy? *Dev Ophthalmol* 2017:131-142.
 27. Bressler SB, Liu D, Glassman AR, Blodi BA, Castellarin AA, Jampol LM et al. Change in Diabetic Retinopathy Through 2 Years. *JAMA Ophthalmol* 2017;135(6):558-568.
 28. Zand H, Morshedzadeh N, Naghashian F. Signaling pathways linking inflammation to insulin resistance. *Diab Met Syndr: Clin Res Rev* 2017;712:1-3.
 29. Holt RIG, Cockram CS, Flyvbjerg A, Goldstein BJ. *Textbook of diabetes*. 4th ed. Chichester, West Sussex, UK: Wiley Blackwell; 2010.
 30. Robinson R, Barathi VA, Chaurasia SS, Wong TY, Kern TS. Update on animal models of diabetic retinopathy: from molecular approaches to mice and higher mammals. *Dis Model Mech* 2012;5(4):444-456.

31. Spaide RF, Fisher YL. Intravitreal bevacizumab (Avastin) treatment of proliferative diabetic retinopathy complicated by vitreous hemorrhage. *Retina* 2006;26:275-278.
32. Chun DW, Heier JS, Topping TM, Duker JS, Bankert JM. A pilot study of multiple intravitreal injections of ranibizumab in patients with center-involving clinically significant diabetic macular edema. *Ophthalmology* 2006;113:1706-1712.

6 Appendices

6.1 Approved use of human participants undergoing PRP treatment



**Western
Research**

Research Ethics

Use of Human Participants - Revision Ethics Approval Notice

Principal Investigator: Dr. Cindy Hutnik
File Number:103197
Review Level:Delegated
Protocol Title:A 12-Month Cohort Study Assessing the Nature and the Time Course of Structural and Functional Changes to the Retina Following Either Conventional Panretinal Photocoagulation or PASCAL Photocoagulation in Severe Proliferative or Proliferative Diabetic Retinopathy Patients
Department & Institution:Schulich School of Medicine and Dentistry/Ophthalmology,Western University
Sponsor:
Ethics Approval Date:December 20, 2013 **Expiry Date:**August 31, 2014
Documents Reviewed & Approved & Documents Received for Information:

Document Name	Comments	Version Date
Revised Letter of Information & Consent	Revised consent form changes highlighted	
Protocol	Revised protocol changes highlighted (including OPTOS, the new instrument used).	

This is to notify you that The University of Western Ontario Research Ethics Board for Health Sciences Research Involving Human Subjects (HSREB) which is organized and operates according to the Tri-Council Policy Statement: Ethical Conduct of Research Involving Humans and the Health Canada/CH Good Clinical Practice Practices: Consolidated Guidelines; and the applicable laws and regulations of Ontario has reviewed and granted approval to the above referenced revision(s) or amendment(s) on the approval date noted above. The membership of this REB also complies with the membership requirements for REB's as defined in Division 5 of the Food and Drug Regulations.

The ethics approval for this study shall remain valid until the expiry date noted above assuming timely and acceptable responses to the HSREB's periodic requests for surveillance and monitoring information. If you require an updated approval notice prior to that time you must request it using the University of Western Ontario Updated Approval Request Form.

Members of the HSREB who are named as investigators in research studies, or declare a conflict of interest, do not participate in discussion related to, nor vote on, such studies when they are presented to the HSREB.

The Chair of the HSREB is Dr. Joseph Gilbert. The HSREB is registered with the U.S. Department of Health & Human Services under the IRB registration number IRB 0000940.

Signature _____

Ethics Officer to Contact for Further Information

<input type="checkbox"/> Erika Basile	<input checked="" type="checkbox"/> Grace Kelly	<input type="checkbox"/> Mina Mekhail	<input type="checkbox"/> Vikki Tran
---------------------------------------	---	---------------------------------------	-------------------------------------

This is an official document. Please retain the original in your files.

6.2 Approved use of human participants undergoing anti-VEGF treatment



Research Ethics

Western University Health Science Research Ethics Board HSREB Delegated Initial Approval Notice

Principal Investigator: Dr. Cindy Hutnik
Department & Institution: Schulich School of Medicine and Dentistry\Ophthalmology, Western University

HSREB File Number: 105570
Study Title: Two year Analysis of Changes in Optic Nerve Structure in Diabetic Macular Edema Patients Receiving Multiple Ranibizumab Injections
Sponsor:

HSREB Initial Approval Date: August 29, 2014
HSREB Expiry Date: August 31, 2016

Documents Approved and/or Received for Information:

Document Name	Comments	Version Date
Other	Letter to patient for appointment reminder	2014/07/18
Letter of Information & Consent	PDF Letter of Information	2014/08/25
Sponsor Protocol	Protocol (Received for information only)	2014/08/25
Other	Patient appointment reminder letter	2014/08/25


The Western University Health Science Research Ethics Board (HSREB) has reviewed and approved the above named study, as of the HSREB Initial Approval Dated noted above.

HSREB approval for this study remains valid until the HSREB Expiry Date noted above, conditional to timely submission and acceptance of HSREB Continuing Ethics Review. If an Updated Approval Notice is required prior to the HSREB Expiry Date, the Principal Investigator is responsible for completing and submitting an HSREB Updated Approval Form in a timely fashion.

The Western University HSREB operates in compliance with the Tri-Council Policy Statement Ethical Conduct for Research Involving Humans (TCPS2), the International Conference on Harmonization of Technical Requirements for Registration of Pharmaceuticals for Human Use Guideline for Good Clinical Practice Practices (ICH E6 R1), the Ontario Personal Health Information Protection Act (PHIPA, 2004), Part 4 of the Natural Health Product Regulations, Health Canada Medical Device Regulations and Part C, Division 5, of the Food and Drug Regulations of Health Canada.

Members of the HSREB who are named as Investigators in research studies do not participate in discussions related to, nor vote on such studies when they are presented to the REB.

The HSREB is registered with the U.S. Department of Health & Human Services under the IRB registration number IRB 00000940.

 Ethics Officer, on behalf of Dr. Joseph Gilbert, HSREB Chair

Ethics Officer to Contact for Further Information

<input type="checkbox"/> Erika Basile	<input checked="" type="checkbox"/> Grace Kelly	<input type="checkbox"/> Mina Mekhail	<input type="checkbox"/> Vikki Tran
---------------------------------------	---	---------------------------------------	-------------------------------------

This is an official document. Please retain the original in your files.

6.3 Approved animal use protocol

>>> eSiriusWebServer

2015/03/05 4:15 PM >>>



AUP Number: 2010-001

PI Name: Chakrabarti, Subrata

AUP Title: Pathogenesis of Diabetic Retinopathy

Official Notification of AUS Approval: A MODIFICATION to Animal Use Protocol 2010-001 has been approved.

The holder of this Animal Use Protocol is responsible to ensure that all associated safety components (biosafety, radiation safety, general laboratory safety) comply with institutional safety standards and have received all necessary approvals. Please consult directly with your institutional safety officers.

Submitted by: Kinchlea, Will D
on behalf of the Animal Use Subcommittee

The University of Western Ontario
Animal Use Subcommittee / University Council on Animal Care
Health Sciences Centre, • London, Ontario • CANADA – N6A 5C1
PH: 519-661-2111 ext. 86768 • FL 519-661-2028
Email: auspc@uwo.ca • <http://www.uwo.ca/animal/website/>

6.4 Copyright permission

LICENCE TO PUBLISH



Manuscript Number: EYE-16-1307R	Journal Name: EYE	(the "Journal")
Proposed Title of the Contribution: Structural and Functional Changes to the Retina and Optic Nerve Following Panretinal Photocoagulation over a 2 Year Time Period		(the "Contribution")
Author(s): Richard Filek, Phil Hooper, Tom Shekdar, John Gonder, Devesh K Varma, Lisa Heckler, William Hodge, Subrata Chakrabarti, Cindy ML Hutnk		(the "Author(s)")

To: *The Royal College of Ophthalmologists* (the "Society")

- In consideration of the Society evaluating the Contribution for publication (and publishing the Contribution if the Society so decides) the Author(s) grant to the Society for the full term of copyright and any extensions thereto, subject to clause 2 below, the exclusive right and irrevocable licence:
 - to edit, adapt, publish, reproduce, distribute, display and store the Contribution in all forms, formats and media whether now known or hereafter developed (including without limitation in print, digital and electronic form) throughout the world;
 - to translate the Contribution into other languages, create adaptations, summaries or extracts of the Contribution or other derivative works based on the Contribution and exercise all of the rights set forth in (a) above in such translations, adaptations, summaries, extracts and derivative works;
 - to license others to do any or all of the above; and
 - to re-license article metadata without restriction (including but not limited to author name, title, abstract, citation, references, keywords and any additional information, as determined by the Society).
 - Ownership of copyright remains with the Author(s), and provided that, when reproducing the Contribution or extracts from it or the Supplementary Information (defined below), the Author(s) acknowledge first and reference publication in the Journal, the Author(s) retain only the following non-exclusive rights:
 - to reproduce the Contribution in whole or in part in any printed volume (book or thesis) of which they are the Author(s);
 - they and any academic institution where they work may reproduce the Contribution for the purpose of course teaching;
 - to post a copy of the Contribution as accepted for publication after peer review (in a locked word processing file, or a PDF version thereof) on the Author(s)' own web sites, or institutional repositories, or the Author(s)' funding body(s)' archive, six months after publication of the printed or online edition of the Journal, provided that they also link to the Contribution on the Society's web site; and
 - to reuse figures or tables created by the Author(s) and contained in the Contribution in oral presentations and other works created by them.
 - The Author(s) grant to the Society for the full term of copyright and any extensions thereto the same rights that have been granted in respect of the Contribution as set out in clause 1 above, in and to all supplementary material in any form (including without limitation images, videos, tables and/or graphs) submitted by the Author(s) to the Society with or in connection with the Contribution ("Supplementary Information") but on a non-exclusive basis.
 - The Society acknowledges that an earlier version of the Contribution and/or Supplementary Information may have been submitted to a pre-print service (in accordance with that service's standard licence terms).
 - The Author(s) jointly and severally warrant and represent to the Society and Nature Publishing Group, a division of Macmillan Publishers Ltd ("NPG") that:
 - the Author(s) are the sole Author(s) of and sole owners of the copyright
- in the Contribution and the Supplementary Information and the Contribution and the Supplementary Information is the original work of the Author(s) and not copied (in whole or part) from another work. If however the Contribution or the Supplementary Information includes materials from other sources, the Author(s) warrant they have obtained the permission of the owners of the copyright in all such materials to enable them to grant the rights contained herein. Copies of all such permissions are attached to this licence:
- all of the facts contained in the Contribution and the Supplementary Information are true and accurate;
 - the signatory (the Author or the employer) who has signed this Agreement below has full right, power and authority to enter into this Agreement and grant the rights herein on behalf of all of the Authors;
 - nothing in the Contribution or the Supplementary Information is obscene, defamatory, libellous, violates any right of privacy or publicity, infringes any intellectual property rights (including without limitation copyright, patent, database or trademark rights) or any other human, personal or other rights of any person or entity or is otherwise unlawful; and
 - nothing in the Contribution or the Supplementary Information infringes any duty of confidentiality which any of the Author(s) may owe to anyone else or violates any contract, express or implied, of any of the Author(s), and all of the institutions in which work recorded in the Contribution or the Supplementary Information was created or carried out, have authorised such publication.
- The Author(s) authorise the Society to take such steps as it considers necessary at its own expense in the Author(s) name and on their behalf if the Society believes that a third party is infringing or is likely to infringe copyright in the Contribution and/or Supplementary Information including but not limited to initiating legal proceedings.
 - The Author(s) hereby waive or agree not to assert (where such waiver is not possible at law) any and all moral rights they may now or in the future hold in connection with the Contribution and the Supplementary Information.
 - The Author(s) shall cooperate fully with the Society in relation to any legal action that might arise from the publication of the Contribution and/or Supplementary Information and the Author(s) shall give the Society access at reasonable times to any relevant accounts, documents and records within the power or control of the Author(s).
 - The Author(s) agree that NPG is intended to have the benefit of and shall have the right under the Contracts (Rights of Third Parties) Act 1999 to enforce the terms of this Agreement.
 - If the Contribution is rejected by the Society and not published, all rights under this licence shall revert to the Author(s).
 - This Agreement shall be governed by and construed in accordance with the laws of England and Wales. The parties irrevocably agree that the courts of England and Wales shall have exclusive jurisdiction to settle any dispute or claim that arises out of or in connection with this Agreement or its subject matter or formation.

Signed for and on behalf of the Author(s): 	Print name: Richard Filek	Date: March 16, 2017
Address: 		

**ELSEVIER LICENSE
TERMS AND CONDITIONS**

Oct 19, 2017

This Agreement between Richard Filek ("You") and Elsevier ("Elsevier") consists of your license details and the terms and conditions provided by Elsevier and Copyright Clearance Center.

License Number	4203280479888
License date	Oct 06, 2017
Licensed Content Publisher	Elsevier
Licensed Content Publication	Progress in Retinal and Eye Research
Licensed Content Title	Blood-retinal barrier in hypoxic ischaemic conditions: Basic concepts, clinical features and management
Licensed Content Author	C. Kaur,W.S. Foulds,E.A. Ling
Licensed Content Date	Nov 1, 2008
Licensed Content Volume	27
Licensed Content Issue	6
Licensed Content Pages	26
Start Page	622
End Page	647
Type of Use	reuse in a thesis/dissertation
Intended publisher of new work	other
Portion	figures/tables/illustrations
Number of figures/tables/illustrations	1
Format	electronic
Are you the author of this Elsevier article?	No
Will you be translating?	No
Original figure numbers	Figure 1
Title of your thesis/dissertation	A CLINICO-PATHOLOGICAL STUDY OF THE STRUCTURAL AND FUNCTIONAL CHANGES IN THE RETINA AND OPTIC NERVE FOLLOWING DIABETIC RETINOPATHY TREATMENTS
Expected completion date	Oct 2017
Estimated size (number of pages)	294
Requestor Location	Richard Filek
Total	0.00 CAD

**WOLTERS KLUWER HEALTH LICENSE
TERMS AND CONDITIONS**

Oct 19, 2017

This Agreement between Richard Filek ("You") and Wolters Kluwer Health ("Wolters Kluwer Health") consists of your license details and the terms and conditions provided by Wolters Kluwer Health and Copyright Clearance Center.

License Number	4207231262553
License date	Oct 13, 2017
Licensed Content Publisher	Wolters Kluwer Health
Licensed Content Publication	WK Health Book
Licensed Content Title	Eye Pathology
Licensed Content Author	Ralph C. Eagle MD
Licensed Content Date	Jan 1, 2016
Type of Use	Dissertation/Thesis
Requestor type	individual
Format	print and electronic
Portion	figures/tables/illustrations
Number of figures/tables/illustrations	2
The ID numbers of the figures/tables/illustrations are...	Figure 9-11 and Figure 9-27
Will you be translating?	no
Reusing current or a previous edition	previous edition
Previous edition being used...	Second edition
Circulation/distribution	50
Order reference number	
Title of your thesis / dissertation	A CLINICO-PATHOLOGICAL STUDY OF THE STRUCTURAL AND FUNCTIONAL CHANGES IN THE RETINA AND OPTIC NERVE FOLLOWING DIABETIC RETINOPATHY TREATMENTS
Expected completion date	Oct 2017
Estimated size (number of pages)	294
Requestor Location	Richard Filek

Billing Type
Billing Address

Total 0.00 CAD

RE: Permission to use images for PhD dissertaion

Caroline Bozell

Mon 10/9/2017 2:07 PM

To: Richard Filek

Hi Richie,

Thank you so much for your interest in the Retina Image Bank! All images on the site can be used for educational purposes as long as they include the following customized copyright statement alongside each:

"This image was originally published in the Retina Image Bank® website. Author. Photographer. Title. Retina Image Bank. Year; Image Number. © the American Society of Retina Specialists."

I hope this helps. If you have any questions or need anything else please let us know.

Thanks,
Caroline

Caroline Bozell
Director, Retina Image Bank and Member Sections

RE: NON RIGHTSLINK- Permission to use images for PhD dissertation

Wiley Global Permissions

Wed 10/18/2017 7:01 AM

To: Richard Filek

Dear Richie,

Thank you for your email.

Permission is granted for you to use the material requested for your thesis/dissertation subject to the usual acknowledgements (author, title of material, title of book/journal, ourselves as publisher) and on the understanding that you will reapply for permission if you wish to distribute or publish your thesis/dissertation commercially.

You should also duplicate the copyright notice that appears in the Wiley publication in your use of the Material. Permission is granted solely for use in conjunction with the thesis, and the material may not be posted online separately.

Any third party material is expressly excluded from this permission. If any material appears within the article with credit to another source, authorisation from that source must be obtained.

Best wishes

Kelly Hoff
Permissions Coordinator
Copyright & Permissions

WILEY

**Touch Medical Media LICENSE
TERMS AND CONDITIONS**

Oct 19, 2017

This is a License Agreement between Richard Filek ("You") and Touch Medical Media ("Touch Medical Media") provided by Copyright Clearance Center ("CCC"). The license consists of your order details, the terms and conditions provided by Touch Medical Media, and the payment terms and conditions.

All payments must be made in full to CCC. For payment instructions, please see information listed at the bottom of this form.

License Number	4212620689330
License date	Oct 06, 2017
Licensed content publisher	Touch Medical Media
Licensed content title	European ophthalmic review (Online)
Licensed content date	Jan 1, 2007
Type of Use	Thesis/Dissertation
Requestor type	Academic institution
Format	Electronic
Portion	image/photo
Number of images/photos requested	3
Title or numeric reference of the portion(s)	Figure 1, Figure 2, and Figure 3
Title of the article or chapter the portion is from	The Mechanism of Retinal Photocoagulation – How Does the Laser Work?
Editor of portion(s)	N/A
Author of portion(s)	Einar Stefánsson
Volume of serial or monograph.	N/A
Page range of the portion	76-77
Publication date of portion	February 10, 2011
Rights for	Main product
Duration of use	Current edition and up to 5 years
Creation of copies for the disabled	no
With minor editing privileges	no
For distribution to	Canada
In the following language(s)	Original language of publication
With incidental promotional use	no
The lifetime unit quantity of new product	Up to 499
Made available in the following markets	
The requesting person/organization is:	Richard Filek
Order reference number	
Author/Editor	
Title of New Work	
Publisher of New Work	
Expected publication date	Oct 2017
Estimated size (pages)	
Total (may include CCC user fee)	0.00 USD

6.5 Antibodies used for experiments

Primary antibody	Dilution	Company, Location
Mouse CD90/Thy 1.1	1:200	Abcam; Toronto, Ont, Canada
Chicken Class III β -Tubulin antibody/TUJ-1	1:400	Abcam; Toronto, Ont, Canada
Rabbit Brn3a	1:100	Abcam; Toronto, Ont, Canada
Rabbit cleaved caspase-3	1:400	Cell Signaling Technology Inc., Boston, Massachusetts, USA

6.6 Curriculum vitae

Richard Filek

EDUCATION

Western University *London, Ontario*
HONOURS BACHELORS OF MEDICAL SCIENCE HONORS **SEPTEMBER 2008 – APRIL 2012**

Western University *London, Ontario*
DOCTOR OF PHILOSOPHY– PATHOLOGY **AUGUST 2012-PRESENT**
AND LABORATORY MEDICINE

SCHOLARSHIPS/AWARDS

Western University *London, Ontario*
WESTERN SCHOLARS **SEPTEMBER 2008-APRIL 2009**

Western University *London, Ontario*
DEAN'S HONOR ROLL **SEPTEMBER 2010-APRIL 2011**
SEPTEMBER 2011-APRIL 2012

Western University *London, Ontario*
WESTERN GRADUATE RESEARCH SCHOLARSHIP **SEPTEMBER 2012 – PRESENT**

Western University *London, Ontario*
SCHULICH GRADUATE SCHOLARSHIP **SEPTEMBER 2014 - PRESENT**

Lawson Health Research Institute *London, Ontario*
STUDENTSHIP AWARD- SPRING 2015 INTERNAL RESEARCH **JULY 2015- JULY 2016**
FUND COMPETITION - AWARDED \$15,000

Department of Ophthalmology- Ophthalmology Research Day 2016 *London, Ont*
OUTSTANDING RESEARCH DAY PRESENTATION BY A GRADUATE STUDENT
NOVEMBER 2016
- AWARDED \$1,000

Department of Ophthalmology, Western University *London, Ontario*
McGRATH RESEARCH SCHOLARSHIP (2016/17) **JANUARY 2017**
- AWARDED \$8,000

Department of Pathology and Laboratory Medicine, *London, Ontario*
Western University
THE CAMERON WALLACE GRADUATE STUDENT AWARD IN PATHOLOGY **MARCH 2017**

The award recognizes a graduate student's achievement in both Pathology research and course work. This award is given in recognition of Dr. Cameron Wallace who was head of the Department of Pathology from 1965-1974

-AWARDED \$1400

ABSTRACTS AND OTHER PRESENTATIONS

Ivey Eye Institute

2013 OPHTHALMOLOGY RESEARCH DAY

▪Platform presentation; "Investigating the structural and functional changes to the retina following PRP in diabetic retinopathy patients"

London, Ontario

NOVEMBER 1, 2013

St. Joseph's Health Care London

4th ANNUAL DIABETES RESEARCH DAY

▪Poster presentation; "Investigating the structural and functional changes to the retina following PRP in diabetic retinopathy patients"

London, Ontario

NOVEMBER 12, 2013

Western University

2013 ANNUAL PATHOLOGY RESEARCH DAY

2014 ANNUAL PATHOLOGY RESEARCH DAY

2015 PATHOLOGY AND LABORATORY MEDICINE RESEARCH DAY

PATHOLOGY AND LABORATORY MEDICINE RESEARCH DAY 2016

PATHOLOGY AND LABORATORY MEDICINE RESEARCH DAY 2017

▪Poster presentation; "Structural and functional changes to the retina following anti-VEGF treatments in diabetic retinopathy patients"

London, Ontario

APRIL 26, 2013

MARCH 28, 2014

MARCH 30, 2015

APRIL 7, 2016

MARCH 30, 2017

Pan-American Association of Ophthalmology

2015 PAN-AMERICAN RESEARCH DAY

▪Poster presentation; "Visual Field Indices as the Primary outcome for New Glaucoma Drug Testing: A Systematic Review"

Denver, Colorado, USA

MAY 2, 2015

The Association for Research in Vision and Ophthalmology

2015 ARVO ANNUAL MEETING, DENVER COLORADO, USA

▪Poster presenter; "Visual Field Indices as the Primary outcome for New Glaucoma Drug Testing: A Systematic Review"

MAY 3-7, 2015

ARVO 2016 ANNUAL MEETING, SEATTLE WASHINGTON, USA

▪Poster presenter; "Investigating the Structural and Functional Changes to the Retina Following PRP in Diabetic Retinopathy Patients"

MAY 1-5, 2016

ARVO 2017 ANNUAL MEETING, BALTIMORE, MARYLAND, USA

▪Platform presentation; "A Clinico-Pathological Study of the Structural and Functional Changes to the Retina and Optic Nerve following anti-VEGF Treatments for Diabetic Macular Edema"

MAY 7-11, 2017

- Selected by the Annual Meeting Program Committee as a "Hot Topic"
- Representing the newest and most innovative research being conducted in various specialties
- This distinction is awarded to just over 2% of all 2017 Annual Meeting abstracts

Canadian Ophthalmological Society

2016 COS ANNUAL MEETING & EXHIBITION, OTTAWA CANADA

▪Platform presentation; "Investigating the structural and functional changes to the retina following PRP in diabetic retinopathy patients"

JUNE 17-20, 2016

2017 COS ANNUAL MEETING & EXHIBITION, MONTREAL CANADA

▪Platform presentation; "A Clinico-Pathological Study of the Structural and Functional Changes to the Retina and Optic Nerve following anti-VEGF Treatments for Diabetic Macular Edema"

JUNE 15-18, 2017

Ivey Eye Institute
OPHTHALMOLOGY RESEARCH DAY 2016

London, Ontario
NOVEMBER 4, 2016

▪Platform presentation; “Investigating the Structural and Functional Changes to the Retina Following PRP in Diabetic Retinopathy Patients”

PUBLICATIONS

Journal Articles

London, Ontario

Malvankar-Mehta MS, Filek R, Iqbal M, Shakir A, Mao A, Si F, Malvankar M.G, Mehta SS, Hodge WG. Immediately sequential bilateral cataract surgery-a cost-effective procedure. Can J Ophthalmol. 2013;48:482–488

- Published
- Co-first author; set up the search strategy, screening of the publications, data extraction and writing of the manuscript

Bali S, Filek R, Si F, Hodge WG. Systemic immunosuppression in high risk penetrating keratoplasty: a systematic review. J Clin Med Res. 2016 Apr;8(4):269-76.

- Published
- Secondary author; set up the search strategy, screening of the publications, and data extraction

Filek R, Hooper P, Sheidow T, Gonder J, Varma D, Heckler L, Hodge W, Chakrabarti S, Hutnik CML. Structural and functional changes to the retina and optic nerve following panretinal photocoagulation over a 2-year time period. Eye (Lond). 2017 Apr 28. doi: 10.1038/eye.2017.66. [Epub ahead of print]

- Published
- As first author, I devised the protocol, ethics approval, grant, recruited patients, scheduling, diagnostic testing, data analysis, wrote and submitted the manuscript

Lin T, Filek R et al. Impression Cytology Implicates Cell Autophagy in Aqueous Deficiency Dry Eye. Clin. Ophthalmol. 2017;11:773-779

- Published
- As co-first author, I conducted experiments and wrote the manuscript for publication

Filek R, Hooper P, Sheidow T, Gonder J, Varma D, Heckler L, Chakrabarti S, Hutnik CML. Two-year analysis of structural and functional changes to the retina and optic nerve following anti-VEGF treatments for diabetic macular edema patients.

- Submitted for publication to Ophthalmology®, the journal of the American Academy of Ophthalmology
- As first author, I devised the protocol, ethics approval, grant, recruited patients, scheduling, diagnostic testing, data analysis, wrote and submitted the manuscript

Filek R, Hooper P, Sheidow T, Chakrabarti S, Hutnik CML. Retinal cell death following anti-VEGF treatment in a diabetic rat model and retinal cell culture.

- Submitted for publication to Progress in Retinal and Eye Research
- As first author, I devised the protocol, created a mixed retinal cell culture, worked with rats, intravitreal animal injections, colorimetric assays, immunofluorescence, data analysis, wrote and submitted the manuscript

DEPARTMENTAL AND COMMUNITY ACTIVITIES

St. Joseph's Health Care London *London, Ontario*
Physiotherapy and Ophthalmology Departments

VOLUNTEER

MAY 2010- PRESENT

- Contributed 239.43 total volunteer hours
- Assist patients in registration for their appointments

Youth Science London

London, Ontario

43rd ANNUAL LONDON DISTRICT SCIENCE FAIR-JUDGE

APRIL 9, 2013

THE 30TH LONDON DISTRICT SCIENCE OLYMPICS-VOLUNTEER

MAY 23, 2013

44th ANNUAL LONDON DISTRICT SCIENCE FAIR

APRIL 5, 2014

2015 THAMES VALLEY SCIENCE & ENGINEERING FAIR

MARCH 28, 2015

- Judged and determined for awards the best junior and senior physical science projects
- Volunteered and taught secondary school students. Created scientific activity schedule (Experiments, games, sports)

Pathology Research Based Graduate Education Committee *London, Ontario*
PATHOLOGY GRADUATE STUDENT REPRESENTATIVE **AUGUST 2014- PRESENT**

- Elected by the Pathology & Laboratory Medicine Graduate Students to be their student representative
- Listen to questions and concerns that the graduate students may have, express these issues to the Pathology Research Based Graduate Education Committee and resolve those issues

Schulich Graduate Student Council, Western University *London, Ontario*
PATHOLOGY AND LABORATORY MEDICINE REPRESENTATIVE **AUGUST 2014-PRESENT**

- Represent the Pathology Department on the Schulich Graduate Student Council
- Communicate with the Pathology Department and its graduate students Schulich events, workshops, socials, academic information nights, and fundraisers
- Work in collaboration with the other departmental reps to create and organize Schulich wide academic, professional, and social events

Western Pathology Association, Western University *London, Ontario*
RESEARCH REPRESENTATIVE **OCTOBER 31, 2014- SEPTEMBER 1, 2016**

- Promote student and faculty interactions within the Department of Pathology and Laboratory Medicine through academic, professional and social events
- Advance the Department's vision, aims and goals by enhancing team work, collaborations, and intellectual exchange

Proctor exams, Western University

Path 2420a

Path 3240a/9240a

Path 3245b/9245b

Path 2420a

Path 3240a/9240a

London, Ontario

DECEMBER 8, 2014

DECEMBER 15, 2014

FEBRUARY 25, 2015

DECEMBER 18, 2015

DECEMBER 20, 2015

Executive Council Student Representative, Western University *London, Ontario*
REPRESENTATIVE **MAY 2015-PRESENT**

▪ Represent the voice of the graduate student body by sitting in on Schulich Executive Committee meetings with all departmental chairs of the Schulich School of Medicine & Dentistry